THE DEVELOPMENT OF THEORETICAL AND EMPIRICAL MATRIX AND INTER-ELEMENT CORRECTION COEFFICIENTS AND APPLICATION IN THE X-RAY SPECTROCHEMICAL ANALYSIS OF SEVERAL METAL AND MINERAL MULTI-COMPONENT SYSTEMS

Robert DiFruscia

A Thesis

in

The Department

of

Chemistry

Presented in Partial Fulfillment of the Requirements
for the Degree of Doctor of Philosophy at
Concordia University
Montréal, Québec, Canada

February 1981

ABSTRACT

THE DEVELOPMENT OF THEORETICAL AND EMPIRICAL MATRIX AND INTER-ELEMENT CORRECTION COEFFICIENTS AND APPLICATION IN THE X-RAY SPECTROCHEMICAL ANALYSIS OF SEVERAL METAL AND MINERAL MULTI-COMPONENT SYSTEMS

Robert DiFruscia, Ph.D.
Concordia University, 1981

The objective of this thesis is to develop a modified Lachance-Traill approach in the x-ray fluorescent spectrochemical analysis of multi-component systems.

The study involves the experimental determination of matrix and inter-element correction coefficients from aqueous solution media using binary element systems. Theoretical α-coefficients are also evaluated using intensities calculated from the fundamental XRF intensity equations. Correlations between the experimental and the theoretical coefficients are then established to show the validity and effectiveness of the approach. A data base of α-coefficients is thus established for use in the analysis of multi-component systems.

The method is then applied to the study of several metal and mineral systems. The effectiveness of the procedure in the analysis of complex systems is shown.

Cette thèse
est dédiée à
mes trés chères
parents.

ACKNOWLEDGEMENT

I wish to express my sincere appreciation to Professor J.G. Dick for his valuable guidance and direction throughout the investigation.

I am particularly grateful to Chi Chung Wan for the many helpful and encouraging discussions on some of the more difficult experiments conducted over the years we worked together.

TABLE OF CONTENTS

LIST OF TABLES

LIST OF FIGURES

1. INTRODUCTION

1.1 General

The increasing need for routine analysis of multicomponent systems, such as alloys, minerals, etc., in analytical chemistry has preferred the use of instrumental techniques over the classical wet chemical procedures. Instruments with the capabilities of analyzing numerous elements either sequentially or simultaneously allow a large number of samples to be processed in the minimum amount of time with very little loss in precision and accuracy.

One of the most powerful tools of the analytical chemist is x-ray fluorescence spectrometry because of the wide range of elements that can be determined and the fact that for almost any type of sample both liquid or solid specimens can be used with a minimum of preparation. The major disadvantage, however, is the existence of certain absorption-enhancement contributions which complicate the analyte intensity-concentration relationship. The measured x-ray intensities, because of these effects are usually found to vary with the concentration of the analyte element in a non-linear fashion. This can be attributed to the fact that the intensities of the fluorescent x-rays produced within the

specimen depend on the mass fractions of the elements in the specimen and the relationship of their mass absorption coefficients for the primary radiation. Similarly, absorption of fluorescent radiation within the specimen depends on the mass absorption coefficients for the fluorescent radiation (1). The various types of effects which can occur are shown in Figure 1. If the absorption coefficients of the specimen for the primary and fluorescent x-rays are nearly constant over the same range of concentration, a linear relationship exists as shown by curve (a). If absorption by the specimen, of either the primary or the fluorescent radiation, or both, is greater than that of the analyte, the measured relative intensity is below that given by the linear relationship and is shown by curve (b). This effect is referred to as positive absorption. If the specimen absorbs the primary or the fluorescent radiation or both less than does the analyte element, an absorption effect in the opposite sense usually occurs as indicated by curve (c). This is referred to as negative absorption. Finally, there is the possibility of fluorescence following the absorption by the analyte element of a characteristic x-ray radiation from one of the other elements present in the specimen. This possibility, indicated by curve (d) is associated with an enhancement effect. Accordingly, there are

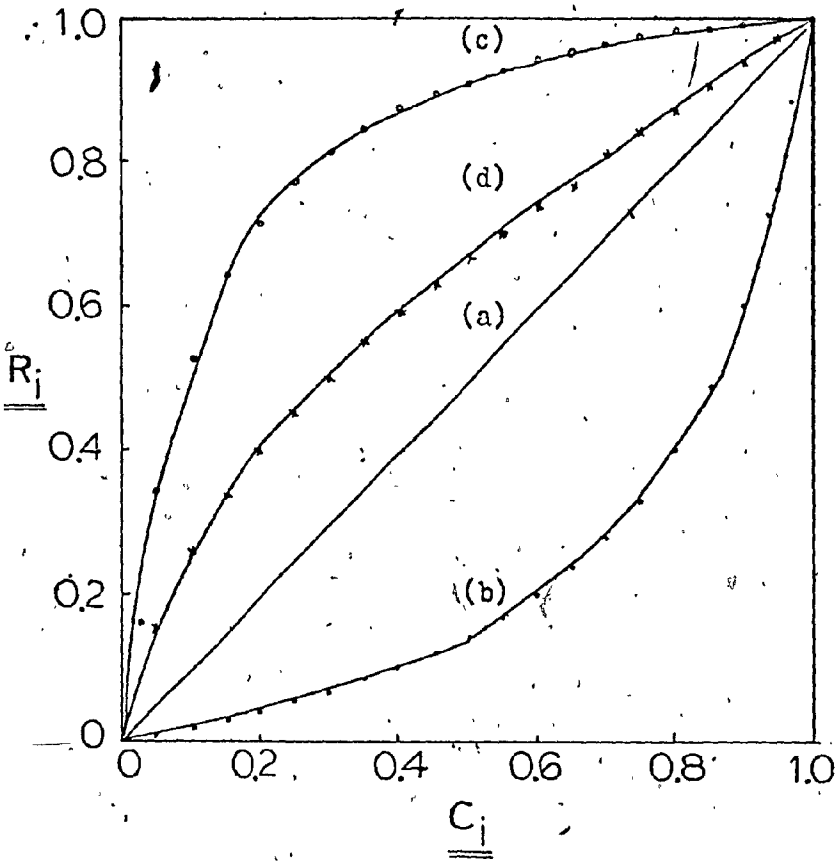

Figure 1* :- INTER-ELEMENT EFFECT SYSTEMS

(a) Linear Calibration Curve
(b) Positive Absorption
(c) Negative Absorption
(d) Enhancement Effect

* (ref. 93)

two major contributors which are responsible for inter-element effects: firstly, absorption and secondly, enhancement. If a specimen consists of two elements, A and B, in which A is the analyte and B a coexisting interfering element, a "pure" absorption will occur if the absorption edge of B is on the long wavelength side of the absorption edge of A. In contrast, enhancement will occur if the absorption edge of B lies on the short wavelength side of the absorption edge of A, and as such the x-ray lines of B, in addition to the primary incident x-rays, can also excite the analyte lines under certain conditions provided the absorption edge of A is greater than the x-ray lines of B being considered. However, in the case of enhancement, an absorption effect coexists in varying degrees (2).

1.2 Theoretical

1.2.1 Theoretical derivations of the Intensity-Concentration relationship

Extensive studies have been carried out on the derivation of theoretical relationships for the calculation of fluorescent x-ray intensities (3,4,5,6,8). In all cases, equations have been presented for the primary fluorescent x-ray intensity which arises from the excitation of elements present due to absorption of the incident x-radiation, and

the secondary fluorescent x-ray intensity which is due to the enhancement effect observed when element(s) can be excited by the fluorescent x-rays emitted from coexisting element(s). Sherman (4,5) and Fujino and Shiraiwa (6) consider a further effect, the tertiary fluorescent x-ray intensity, which is due to the secondary fluorescent x-rays.

It has been shown that the primary and secondary fluorescent x-ray intensities contribute the major part of the overall intensity (6). Accordingly, the tertiary fluorescent intensity contribution becomes negligible. In view of this, discussion will be restricted to the primary and secondary fluorescent x-ray intensity equations, using the formulations of Fujino and Shiraiwa (6) with some modifications in notation.

The primary fluorescent x-ray intensity for an analyte element A can be represented as Equation 1, and the secondary fluorescent x-ray intensity produced by other elements present capable of enhancing the analyte A, can be represented by Equation 2.

Two important parameters appearing in Equations 1 and 2 involved in the calculation of the efficiency of the fluorescent x-ray production from an element are the fluorescent yield (ω) and the absorption-edge jump ratio (r).

EQUATION 1

Primary Fluorescent x-ray Intensity :

$$I_1(A) = \frac{C_A}{\sin(\Psi)} \int_{\lambda_o}^{\lambda_{edge}^A} \frac{\mu_A(\lambda)\, I_o(\lambda) \left(K_A \omega_A R_P^A\right) \cdot d\lambda}{\mu_m(\lambda)\csc(\phi) + \mu_m(\lambda_A)\csc(\Psi)}$$

where :

λ_{edge}^A	:	wavelength of absorption edge of the analyte element A
λ_o	:	minimum wavelength of the incident primary beam
ϕ	:	angle of incidence of primary beam
Ψ	:	angle of emergence of emitted x-rays
$I_o(\lambda)$	:	intensity of incident x-rays of continuum
$I_1(A)$	:	intensity of primary fluorescent x-rays of analyte
C_A	:	weight fraction of element A
ω_A	:	fluorescent yield of element A
K_A	:	absorption jump of element A
R_P^A	:	Intensity fraction of P-line, in the characteristic x-ray series which P-line belongs to
$\mu_A(\lambda)$	:	mass absorption coefficient of element A at wavelength λ
$\mu_A(\lambda_A)$	:	mac of element A at analyte wavelength λ_A
$\mu_m(\lambda) = \sum_i C_i \mu_i(\lambda_i)$		which represents the mac for the specimen at the wavelength λ

EQUATION 2

Secondary Fluorescent x-ray Intensity :

$$I_2(A) = \frac{1}{2\sin(\Psi)} \sum_k \int_{\lambda_o}^{\lambda^B_{edge}} \frac{\left(\mu_B(\lambda_B)\, C_K\, \omega_B\, R^B_P\right)\left(\mu_A(\lambda_K)\, C_K\, \omega_A\, R^A_P\right)}{\mu_m(\lambda)\csc(\phi) + \mu_m(\lambda_A)\csc(\Psi)} \cdot$$

$$I_o(\lambda)\, S_N \cdot d\lambda$$

where :

$$S_N = \left\{ \frac{1}{\mu_m(\lambda_A)\csc(\Psi)} \left[\ln\left(1 + \frac{\mu_m(\lambda_A)\csc(\Psi)}{\mu_m(\lambda_k)}\right)\right] + \right.$$

$$\left. \frac{1}{\mu_m(\lambda)\csc(\phi)} \left[\ln\left(1 + \frac{\mu_m(\lambda)\csc(\phi)}{\mu_m(\lambda_k)}\right)\right]\right\}$$

The fluorescent yield represents the probability of the excited state to result in the emission of fluorescent radiation. The absorption-edge jump ratio represents a measure of that portion of the total absorbed x-radiation that is absorbed by a specified atomic energy level (9,10). Diagrams of these values versus the atomic number of the analyte element are shown in Figures 2 and 3 (9). It can be concluded from these that the fluorescent yield is a major limitation of sensitivity.

These equations have been derived under certain assumptions regarding the geometry of the x-ray beams, specimen, and physical constants (3,4,6). It is assumed that the specimen is homogeneous in nature, with a flat surface and of infinite thickness. Since the penetrating distance of x-rays in a sample is usually less than about 0.1 mm, this criteria can be easily met. Regarding the geometry of the incident and emergent x-ray beams, an assumption that the incident x-rays are parallel is also made.

Another factor which has been considered negligible is scattering absorption. Ebel et al. (11,12,13,14) have shown through theoretical calculations that, for bulk samples, less than 1% of the total fluorescent x-ray intensity is due to scattering, whereas for thin film samples, as much

Figure 2 (ref. 9)

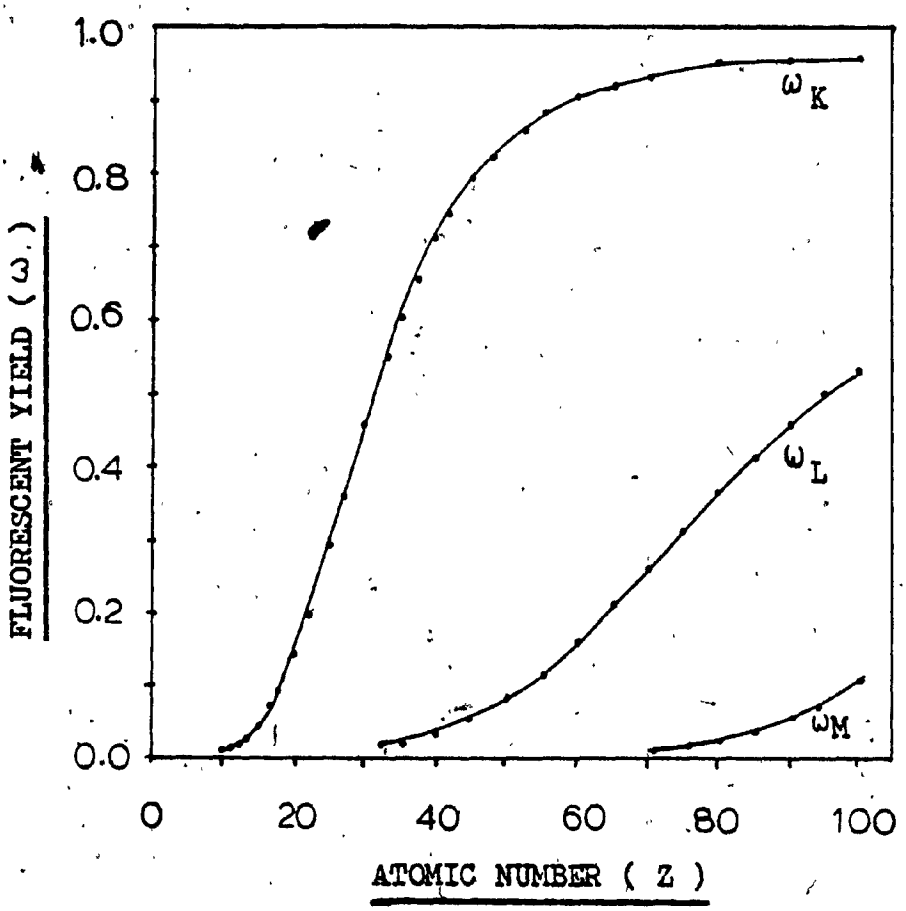

The fluorescent yield (ω) varies with the atomic number and the particular series of x-ray lines.

Figure 3 (ref. 9)

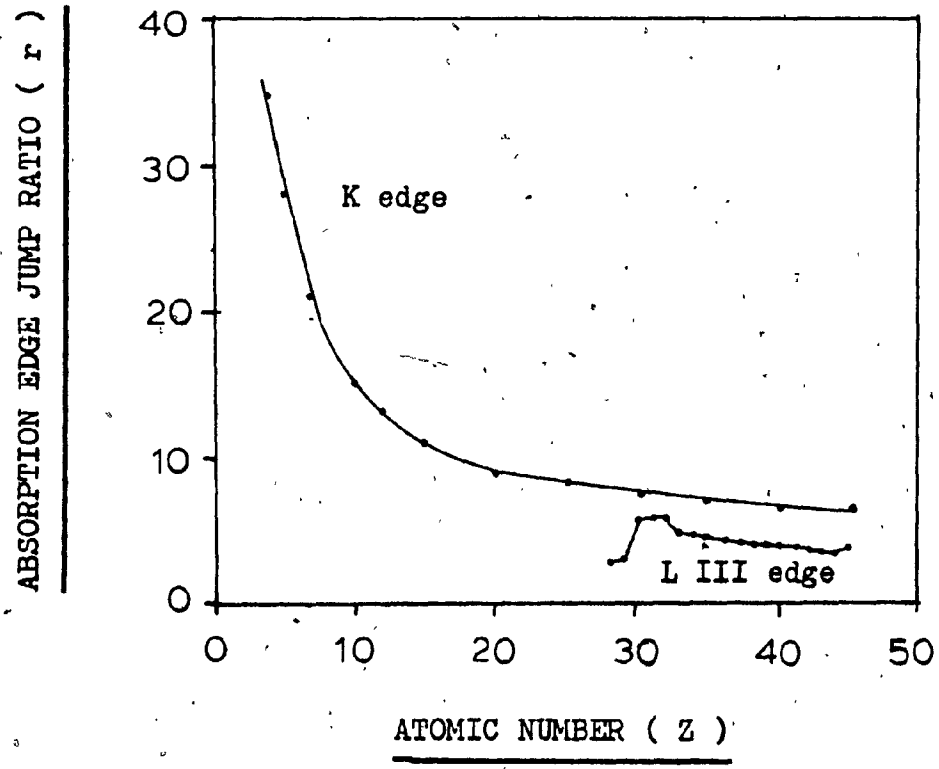

The absorption edge jump ratio (r) varies with the atomic number and the series of x-ray lines.

as a 30% contribution occurs. Accordingly, for bulk samples, the assumption would yield little error. Scatter, however, can be significant, especially for the lighter elements.

The derived equations for the primary and secondary x-ray intensities are in agreement with other authors. However, they differ from Sherman's derivation by a normalizing factor (6).

1.2.2 Application of the theoretical equations to the calculation of x-ray intensities

The validity of these derived equations has been shown by comparison of measured experimental intensities with those theoretically calculated. Gillam and Heal (3), using molybdenum Kα monochromatic x-rays for the incident beam and an alloy consisting of 80% iron and 20% nickel, found that the secondary fluorescent x-ray intensity contribution for iron was as much as 10% of the total intensity. Sherman (5) under the assumption of a monochromatic beam has compared intensities for binary and tertiary systems of various oxide mixtures, and found good agreement with the experimental results. Fujino and Shiraiwa (6) acknowledge the simplification used by Sherman (5) but question the existence of such a wavelength. They perform their calculation using a polychromatic incident x-ray beam where the intensity

distribution of the continuous x-rays emitted from a massive target is theoretically calculated using Kramer's formulae (6). Extensive calculations were performed on nickel-iron, iron-chromium binary alloys and nickel-iron-chromium alloys over a wide range of concentrations. Errors ranging less than 1% between experimental and theoretical data have been attributed to inaccuracies of the physical constants and the intensity distribution of the x-ray continuum. Another source of error could be attributed to the effect of neglecting the minor components present in the true samples (ie. Cu, Mn, C, Si) in their calculations (6,7). Their rigorous treatment also included calculations for the tertiary fluorescent effects present, which proved to be insignificant compared to the primary and secondary intensity contributions. Tertian (15) has commented on the fact that numerous authors have used the nickel-iron-chromium alloys extensively as examples for comparison. These alloys are dense and comparatively restricted in nature as far as atomic number and concentration ranges are concerned, so that such examples tend to give a particular and not a general picture of the situation. Tertian (15,16) performed calculations on binary mixtures of rare earth oxides using the basic equations for the primary and secondary fluorescent x-ray intensities, and using both monochromatic and

polychromatic incident x-rays. Müller (8) calculated the intensities for several two-component mixtures of rare earth oxides as functions of the concentration without taking into account inter-element excitation and compared the results with experimental data in order to establish the magnitude of the secondary fluorescent x-ray intensity. The magnitude of the inter-element excitation depended upon the wavelength of the radiation of the associated elements in relationship to the absorption edge of the element that was being excited. Inter-element excitation was found to be negligible when the radiation of the associated element was far away from the absorption edge. When the radiation is close to the absorption edge, however, the associated element may cause an increase in the fluorescent intensity of the other element of as much as 10% to 30%. The major portion of the fluorescent radiation is produced by the primary incident x-radiation. Inter-elemental excitation is sometimes of minor importance so that the absorption coefficients allow one to estimate the magnitude of fluorescence caused by the associated element. Müller (17) also brings up the question of an effective wavelength referred to as a weighted average wavelength and its usefulness in simplifying calculations with Equation 1. Mention is also made of the variation of this wavelength with the concentration of the analyte in the

specimen.

Both Müller (8,17) and Tertian (15,16) use data for the spectral distribution of the primary x-ray continuum which have been published (18,20) or experimental data collected in their laboratories.

1.2.3 The concept of an effective wavelength

The existence of an effective wavelength has caused much confusion in the literature as to its validity and particularly its usefulness.

The true effective wavelength was firstly recognized by Kalman and Heller (21) who applied the mean value theorem of integral calculus. The theorem states that for a function $y = f(x)$, which is continuous over the closed interval $a \leq x \leq b$ and possesses an anti-derivative in the open interval $a < x < b$ for each x, there exists at least one number c between a and b such that:

$$\int_a^b f(x) \cdot dx = (b - a) f(c) \qquad (3)$$

where f(c) is the average value of the integrand (22). This concept was subsequently used by Pluchery (23), Fujino and Shiraiwa (6), Ebel et al. (24,25), Müller (8,17) and Sherman

(5).

In Sherman's original calculations (4), it was suggested that a wavelength corresponding to the wavelength of the characteristic peaks of the x-ray tube target, usually Kα or Lα, would contribute the greatest amount to the excitation, and that the monochromatic wavelength satisfying the effective wavelength concept should lie in this region. In a later publication (5) the author acknowledges the existence of a mean wavelength derived from the mean value theorem, and states that it should vary with the composition of the specimen and the incident radiation.

Leroux, Mahmud and Davey (26) undertook studies to show the existence of an effective wavelength through experiment. They applied the mean value theorem to derive an average wavelength (λ-ave) for which the weight distribution is equal on either side of the ordinate, which coincides with the average wavelength of the idealized primary beam converted into fluorescent radiation. However, the spectral distribution of any primary beam is more complex, and the authors show that the most effective wavelength might be quite different in value from λ-ave as calculated for an idealized primary beam. These calculations show that the most effective wavelength for the individual elements

varies from 6% to 21% for elements of atomic number 50 and 23 respectively. The significant effects of the excitation potential of the tungsten anode and the modification of the quality of the original primary beam by filtering out the L lines using nickel foils are also shown. In the latter case no agreement between the two were found.

The study also points out the fact that the weighted average wavelength is appreciably shorter than the absorption edge of the fluorescent element, although the fluorescence is most effectively produced by wavelengths near the absorption edge.

Since the average wavelength in the study is derived from the mass absorption coefficients of a particular element as a function of wavelength, and the effective wavelength is derived from knowledge of the primary beam as well as the mass absorption coefficients for the element of interest, a possible source of error accounting for the found differences may thus be explained.

Fujino and Shiraiwa (6) also studied the existence of this true effective wavelength by performing a series of rigorous calculations with their theoretical model for different binary systems of varying compositions. The authors also included treatment of secondary fluorescence which

others have omitted. They arrived at the conclusion that the true effective wavelength tends to vary significantly with the composition of the specimen. However, it can be shown that if the relative intensities of two alloys of differing composition are taken, one can obtain an apparent effective wavelength which differs from the effective wavelength and has less physical meaning. Their conclusions show that since the primary and secondary fluorescent x-ray contributions cannot be distinguished experimentally, the effective wavelength concept should be used for simplification purposes in derivations and not for direct estimation of the total fluorescent x-ray intensity. The approximation becomes poorer by inclusion of the secondary fluorescent effects.

Tertian (15,16) in a series of papers has also performed these calculations and introduced several different concepts for this effective wavelength. The author took into account both primary and secondary effects and concluded that the effective wavelength notion is unfounded and that selection of this wavelength is arbitrary. In certain cases the existence of more than one wavelength can also be shown. The author further states that the choice of this wavelength should be made solely on physical grounds and not mathematical ones. Subsequently Tertian defines two other wavelengths

which can be used. These appear in Figure 4 along with a λmean which corresponds to the mean value of the fluorescent intensity distribution. In Figure 4, λ max corresponds to a maximum value on the curve which is the most effective wavelength in the spectrum with respect to its intensity in the distribution, and λmed corresponds to the one that leaves equal areas on both sides of the ordinate (15,27).

Tertian also agrees with other authors as to the variation of the effective wavelength with sample composition under fixed excitation conditions. As such, this concept offers little interest for analytical applications. Accordingly, by using fused diluted samples to overcome the matrix effects, he shows the existence of an effective wavelength which would give the fluorescent intensity proportional to the actual experimental measurements, and which he terms the analytically equivalent wavelength (15).

Stephenson (22) criticizes Tertian's (15) approach, noting his reluctance to recognize the work of other authors by defining his own terminology and his denial of any physical significance for this wavelength. The author stresses the fact that the equations are derived on physical grounds and not pure mathematics. Tertian (15) has also claimed that the works of several authors (6,7,25) tend to give a partic-

Figure 4 (ref. 27)

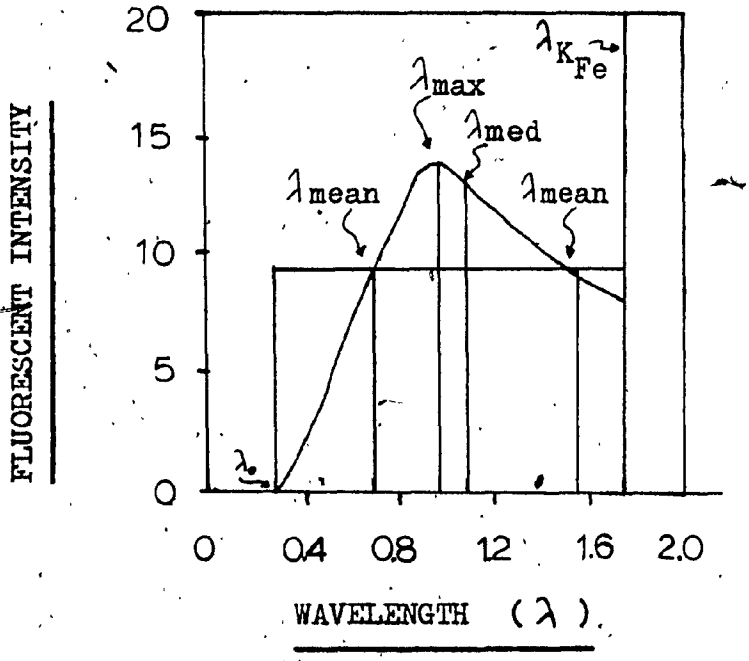

Several proposed effective wavelengths as related to the fluorescent integrated intensity.

ular not general situation and were influenced by a lack of precise data about the spectral intensity distribution. However, Tertian's (15,16) examples are no improvement, especially since the parameters used in these calculations are even more inaccurate since they involve measurements in a spectral region where authors decline to give values for data because of the tremendous uncertainties involved. A last point is stressed which considers the possible existence of more than one such an effective wavelength and Tertian's (15,16) reluctance to mention this situation in the chosen examples. Tertian (28) retaliates in a subsequent paper with the derivation of several different approaches to solving the mean value theorem.

In a more recent paper (27), the authors have repeated the work of Fujino and Shiraiwa (6,7) using binary mixtures of iron, chromium and nickel as dilute solid solutions to show the existence and applications of an equivalent wavelength notion. Included are variations with composition, instrument geometry and derivations for the effects on influence coefficients used in inter-element corrections.

Jenkins (29,30) gives a general procedure for the evaluation of the effective wavelength and has concluded that, in practice, where the contributions from the characteristic

source lines are insignificant, it can be represented roughly as two-thirds of the analyte absorption edge wavelength (ie. the two-thirds rule (31)). However, if the characteristic lines are significant these should be chosen.

Mencik (32) has taken a totally different approach to this problem by suggesting the use of an effective mass absorption coefficient. The author shows that this concept gives a better agreement than the value defined by the two-thirds rule (25), because it can take into account the detailed distribution of the values of the mass absorption coefficient as a function of the wavelength of the primary x-radiation, including the absorption edges if there are several.

In summary, the effective wavelength concept is useful since it allows a reduction of the integral equations for the fluorescent x-ray intensities, allowing simplifications which can be easily adapted in studies of inter-element effects. However, it must be stressed that confusion in the literature is ever present, and that a distinction between the use of this concept for intensity calculation purposes, or validity in simplification of Equations 1 and 2, should be made.

1.3 Matrix and Inter-Element Correction Methods

Correction for the non-linearity which occurs in Intensity-Concentration curves can be achieved by several techniques comprising either an experimental or a mathematical approach.

1.3.1 The experimental approach

In the experimental methods a linear relation is obtained by adjustment of the specimen composition. This can be achieved by succesive dilution of the specimen with an inert matrix, which has the result of decreasing the matrix effects. The method of standard additions can then be used. In this case incremental additions of the element of interest are made in order to obtain a calibration curve. The method proves useful for samples where little or inadequate information as to the matrix composition exists. Accordingly, no standard reference materials are required, and would be of little value due to the unknown nature of the specimen.

The technique is especially effective in minor constituent analysis where the concentrations are of the order of less than 5% to 10%, and where the Intensity-Concentration relationship is likely to remain linear in the region of additions for the analyte element.

Another method utilizes calibration standards. In this method, it is important that the standards used be of similar composition to the samples to be analyzed. The physical nature of the standards and unknowns must also be similar.

Linear calibration curves will usually be obtained for thin films, minor and trace analytes in low atomic number matrices and fusion discs. However, if non-linear curves are obtained an increase in the number of calibration standards can be used to obtain a more reliable set of data over the range of concentrations expected.

Another of the methods most often used is the internal standard technique. In this case, an internal standard element is added to the specimen which has excitation and absorption-enhancement characteristics similar to that of the analyte in that particular matrix. The advantages are that it compensates for the absorption effects and instrumental drift. When considering powders or briquets, partial compensation for variations in density also occur. The disadvantages, however, limit the usefulness of the technique, since such samples as bulk solids, foils and metal parts can not be subjected to this method. Such considerations as mixing and specimen homogeneity, limit the use to liquid specimens and specimens which can be dissolved in acid or other solvents,

or fused. This subsequent increase in sample preparation time, as well as limitations as to the analyte concentrations possible, must also be considered. Although the method is easily applied to one analyte in a multi-component system, it becomes impractical to use for multiple analytes.

1.3.2 The mathematical approach

The mathematical approach to the correction of matrix and inter-element effects consists of using the basic theoretical equations to develop simpler algorithms which can be applied to experimental data. The established relations thus developed depend on the use of empirical correction factors which must be evaluated from reference standards prior to analysis of the unknowns.

Two of the methods used in the mathematical approach are the fundamental parameters method and the empirical coefficients method.

1.3.2.1 The fundamental parameters approach

Criss and Birks (19) were the first to introduce their novel approach by simplifying the existing theoretical equations (4,6) relating intensity to concentration through the use of the experimentally-determined spectral distribution for a variety of x-ray tube targets (20). Since both Equ-

ations 1 and 2 involve integral terms, their approach was to divide the spectral distribution of the incident x-ray beam into a number of wavelength intervals ($\Delta\lambda$) with corresponding intensities I(λ). Figure 5 illustrates the technique using a tungsten target tube. As such, the integral terms can be replaced by summations which simplify the calculation (19). Equations 1 and 2 can then be represented as Equation 4. Suitable parameters are found in the literature and the calculation is performed with reference to a pure standard.

As noted by Sherman (4) inversion of the formulae to show concentration as explicit functions of the intensities or intensity ratios is clearly impossible. Accordingly, Criss and Birks (19) use an alternative method employing an iterative procedure to determine the mass fractions. This involves making successively better estimates of the mass fractions until the corresponding calculated relative intensity agrees with the measured relative intensity.

In a recent paper, the authors (33) have pointed out that the fundamental parameters expression has essentially no restriction on the range of composition which can be considered and requires only pure element standards. The disadvantages of these approaches are that rather large com-

Figure 5 (73)

a) Intensity Distribution of Primary x-ray Beam:

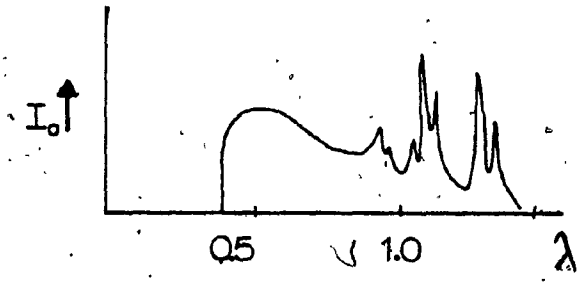

b) Graphical Integration:

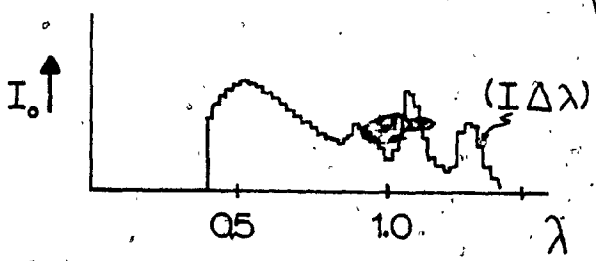

EQUATION 4[20]

$$\underline{\text{Primary}} + \underline{\text{Secondary}} = g_i C_i \sum_k \left(\frac{D_i(\lambda_k)\,\mu_i(\lambda_k)\,I(\lambda_k)\,\Delta\lambda_k}{\mu_m(\lambda_k)\csc(\epsilon) + \mu_m(\lambda_i)\csc(\Psi)} \right.$$

$$\left\{ 1 + \frac{1}{2\mu_i(\lambda_k)} \sum_j D_j(\lambda_k) C_j K_j \mu_i(\lambda_j) \mu_j(\lambda_k) \cdot \left[\frac{1}{\mu_m(\lambda_k)\csc(\epsilon)} \cdot \right. \right.$$

$$\ln\left(1 + \frac{\mu_m(\lambda_k)\csc(\epsilon)}{\mu_m(\lambda_j)}\right) + \frac{1}{\mu_m(\lambda_i)\csc(\Psi)} \cdot \ln\left(1 + \right.$$

$$\left.\left.\left.\left. \frac{\mu_m(\lambda_i)\csc(\Psi)}{\mu_m(\lambda_j)} \right) \right] \right\} \right)$$

where :

$$\mu_m(\lambda) = \sum_{i=1}^{n} C_i \mu_i(\lambda)$$

$$K_j = \left(1 - \frac{1}{J}\right)\omega$$

puter facilities are required which may not be at the disposal of every laboratory. Other factors which have severely limited the utilization of the fundamental parameters approach are the inaccuracies in the absorption coefficients, fluorescent yields and primary spectral distributions, and the attempts to eliminate all but pure element standards, which has resulted in biased calculated compositions (33).

Criss and Birks (19) have applied the method to the analysis of stainless steels and iron- and nickel-base alloys with a 2% deviation from the wet chemical analysis. By using a different approach, employing a multi-component standard, the authors (33) have obtained results for NBS stainless steel standards and iron-nickel alloys that have an average deviation of 1.2% relative for the major constituents (ie. $>$ 2.5% by weight) and for minor constituents (ie. 0.5% to 2.5% by weight) an average deviation of 1.6% relative, except for silicon which showed deviations as large as 70% relative. The use of a pure element standard gives an average bias of 3% relative for chromium and 2% relative for nickel. This illustrates the unsuitability of using pure element standards. The use of empirical methods would require at least 10 to 30 well-characterized multi-component standards (1), depending on the range of compositions expected and the form of the empirical coefficient

equations.

Gould and Bates (34) have used the Criss and Birks (19) fundamental parameters approach and describe in detail a program set up for analysis using this technique.

Palme and Jagoutz (35) have used the method for the determination of major and minor elements on fused geological samples using calibration constants obtained from the ratio of intensities from measured standards to those theoretically calculated. Their results agree strongly with published data for these rock standards (36).

Stephenson (37) has modified the approach by deriving a system that accounts for absorption and enhancement effects, is independent of the spectral distribution of the x-ray source and requires only one multi-component standard. This was achieved through the use of the most efficient incident excitation energy for the element under consideration. This energy, according to the authors, is slightly greater than the energy of the absorption edge associated with the measured x-ray line. The weight fractions of each element in an unknown is then iteratively adjusted until convergence occurs. Any discrepancies between calculated and accepted values have been attributed to the assumed value of the most efficient excitation energy for each element. The authors

performed analyses on certain glasses, rocks and metal alloys with acceptable results.

Ciccarelli (38) developed a program for quantitative analysis by modifying Stephenson's approach (37) in order to allow general use on smaller computer systems. The effective wavelength was chosen as the one wavelength which is less than the absorption edge of the measured line and capable of maximum excitation of that particular line. Data is presented for three NBS standards.

Laguitton and Mantler (39) have developed a very flexible algorithm which provides the user with a choice of different types of specimen to be analyzed (ie. bulk or thin films) as well as a choice of data output for the required task performed. A major disadvantage lies in the necessity of using a large computer system. However, the authors have analyzed thirty-six NBS standard reference materials comprising iron-nickel, iron-chromium, nickel-chromium and iron-nickel-chromium alloys with excellent agreement with the accepted results.

Englund (40) has extended the technique to cover the tertiary effects and has tested this on a variety of stainless steels, tool steels and nickel base alloys. The author demonstrates the possibility of calibrating on materials

different from the samples to be analyzed. In this study, the importance of the tertiary effects are stressed, in contrast to other authors.

Hawthorne and Gardner (41,42,43) in a series of articles have developed a Monte Carlo Simulation of the x-ray fluorescence process. The method was verified for the nickel-iron-chromium systems of NBS standards. It was found that when tertiary effects are not accounted for, the analyses results obtained contain more than 1% relative error in twelve of fifteen determinations. When accounted for, the analyses results contained more than 1% relative error in only four of fifteen determinations. However, in their study a ^{109}Cd source was used instead of the usual x-ray tubes. This can therefore account for the contribution of the tertiary effects which are as high as 5% in certain cases.

1.3.2.2 The empirical approach

In general, empirical methods appearing in the literature are derived on the following assumptions:

a) The specimen is homogeneous, flat and infinitely thick

b) The primary x-radiation is monochromatic or a monochromatic beam has the same effects as the actual polychromatic primary spectrum for all specimen compositions of interest.

c) The enhancement effects have the same effect as

low matrix absorption and can be regarded as a negative absorption.

Rasberry and Heinrich (1) have examined twelve formulae which have appeared in the literature which are quite different in appearance. However, they have shown that most of these are equivalent to several distinct forms which can be obtained by mathematical transformation based on certain basic assumptions about the systems under examination. Such factors as equalling the sums of the mass fractions present to unity and modification of the correction terms to a particular standard method of representation have been considered. Individual derivations of most of the empirical formulations appearing in the literature have been summarized in texts by Müller (10), Bertin (9), Jenkins (30), Birks (18) and Liebhavsky (44).

Beattie and Brissey (45) developed regression equations which can be represented by Equation 5 of Table 1. The main difference is their derivation of the ratio, R_A, which is the inverse of the notation used in Table 1.

Equation 5 has been used to evaluate correction coefficients from experimental data on binary mixtures. The corresponding correction coefficients appear as the term α_{AB} which represents the effect of element B on the analyte A.

TABLE 1

a) General Regression : (reference 45)

$$C_A / R_A = \sum \alpha_{AB} C_B \qquad (5)$$

b) Lachance-Traill : (references 48,50,51)

$$C_A / R_A = 1 + \sum_{B \neq A} \alpha_{AB} C_B \qquad (6)$$

c) Claisse-Quintin : (reference 53)

$$C_A / R_A = 1 + \sum_{B \neq A} \alpha_{AB} C_B + \sum_{B \neq A} \alpha_{ABB} C_B^2 + \sum_{B,C \neq A} \alpha_{ABC} C_B C_C \qquad (7)$$

d) Rasberry-Heinrich : (reference 1)

$$C_A / R_A = 1 + \sum_{B \neq A} \alpha_{AB} C_B + \sum_{B \neq A} \left(\frac{\beta_{AB} C_B}{1 + C_A} \right) \qquad (8)$$

e) Tertian : (references 57,58,59,60,61)

$$C_A / R_A = \left[1 + \sum_{B \neq A} \alpha_{AB} C_B + \sum_{B \neq A} \beta_{AB} C_A C_B \right] \cdot \left(\frac{1}{1 + \epsilon_A} \right) \qquad (9)$$

Sherman used a similar approach (46) and obtained a set of linear equations from his earlier theoretical equations.

Burnham, Hower and Jones (47) have elaborated regression equations for a three-component system based on Sherman's equations (46). The correction coefficient α_{AB} was calculated from a series of simultaneous equations for each analyte using the regression Equation 5 set up for several calibration reference standards. Once the coefficients have been determined an unknown sample can be analyzed by the following form of Equation 5:

$$\begin{aligned}
(R_A\alpha_{AA}-1)C_A + R_A\alpha_{AB}C_B + R_A\alpha_{AC}C_C &= 0 \\
R_B\alpha_{BA}C_A + (R_B\alpha_{BB}-1)C_B + R_B\alpha_{BC}C_C &= 0 \\
R_C\alpha_{CA}C_A + R_C\alpha_{CB}C_B + (R_C\alpha_{CC}-1)C_C &= 0 \\
C_A + C_B + C_C &= 1
\end{aligned} \qquad (5a)$$

where R_i represents the ratio of the measured analyte i intensity to that of the pure element i standard, C_i represents the weight fraction of the element i present and α_{ii} the correction coefficient.

When the system is used as an approximation, (ie. when residual or additional elements are present or the incident beam is polychromatic), it becomes over-determined and there

is a choice of which equation to omit (47). Beattie and Brissey (45) and Lachance and Traill (48) have concluded that the most desirable solution can be obtained by eliminating the equation that contained the most abundant element.

Burnham et al. went one step further and used an iterative procedure to obtain more reliable results. The authors also developed a much simpler graphical method of analysis for the three-component system which eliminates the problem encountered in the regression equations (47).

Marti (49), Birks (19) and Müller (17) applied similar methods in analyzing stainless steels. Marti (49) uses standards to establish calibration curves. The equations assume the following form:

$$
\begin{aligned}
I'_A &= aC_A + U_A = I_A (\alpha_{AA}C_A + \alpha_{AB}C_B + \alpha_{AC}C_C + \ldots) \\
I'_B &= bC_B + U_B = I_B (\alpha_{BA}C_A + \alpha_{BB}C_B + \alpha_{BC}C_C + \ldots) \\
I'_C &= cC_C + U_C = I_C (\alpha_{CA}C_A + \alpha_{CB}C_B + \alpha_{CC}C_C + \ldots) \\
1 &= C_A + C_B + C_C + \ldots)
\end{aligned}
\qquad (5b)
$$

where I_i and I'_i refer to the measured and corrected intensities respectively; a,b,c are the coefficients of the slope for the corrected calibration curves; U_i refers to the background of the corrected calibration curves; α_{ii} represents

the influence coefficients and C_i the weight fractions of the element i in the specimen. The author further simplifies the system by assuming that the influence of iron on the individual elements present is unity. The influence coefficients are determined and correlations between the coefficients and atomic number of the interfering element, as well as the mass absorption, are noted. However, a lack of correlation is evident.

Lachance and Traill (48,50,51) introduced a new approach which differs from previous ones by eliminating the analyte concentration term which appeared in the denominator formerly. The new equation takes the form of Equation 6 in Table 1. The advantages are not apparent for binary systems but, as noted by Beattie and Brissey (45), when using multi-component systems there are n^2 ways to solve the equations (ie. n refers to the number of elements present in the sample), each giving a different set of solutions, since the equations are based on a rough assumption and the coefficients are empirical. The result is a set of inconsistent equations. One solution previously suggested was to omit the equation for the most abundant element. These limitations are not present in Equation 6 which allows a complete and unique solution for the unknowns in a set of linear equations (48).

The authors compare numerous equations found in the literature and derive the corresponding α_{AB} term for each system for comparison purposes.

The authors (52) have applied Equation 6 in the analysis of multi-component systems consisting of at least nine elements and have shown the advantages of the method. Influence coefficients are given and a strong correlation between the coefficients and theory exists indicating a physical significance unlike those previously determined.

Claisse and Quintin (53) have modified Equation 6 to compensate for inadequate assumptions made in the derivation. When α-factors are determined by regression analysis of data from standard samples it is found that the expression may not adequately compensate for the enhancement and third element effects where a wide range of concentrations are covered.

The assumption of a polychromatic beam behaving as a monochromatic one introduces other uncertainties such as that the α-coefficients should be constant. Equation 7 of Table 1 is similar to the original Equation 6 except for the higher terms and the cross-products.

A major disadvantage of this method lies in the difficulty in obtaining the correction coefficients experimentally

because the required number of standards required becomes very large.

The authors (54) develop a method of theoretically evaluating the α-coefficients from binary and ternary component systems. This is the simplest and most practical approach since for a binary system there are only two unknowns:

$$C_A = R_A (1 + \alpha_{AB} C_B + \alpha_{ABB} C_B^2) \quad (7a)$$

and in the case of a ternary system there are five coefficients to be determined:

$$C_A = R_A (1 + \alpha_{AB} C_B + \alpha_{AC} C_C + \alpha_{ABB} C_B^2 + \alpha_{ACC} C_C^2 + \alpha_{ABC} C_B C_C) \quad (7b)$$

They have also concluded that only the binary coefficients α_{AB} and α_{ABB} are necessary and that most of the α_{ABC} coefficients are negligible. Accordingly, this simplification reduces the minimum required standards to 2(n-1).

Lachance (55) has investigated the Claisse-Quintin relation and has concluded that the error to be expected using a single coefficient is often negligible while the error using the first and second order coefficients is less than the precision and accuracy of analytical measurements encountered in normal laboratory practice.

Rasberry and Heinrich (1) propose a different type of correction equation to take enhancement effects into consideration (Equation 8). The coefficients α_{AB} are used when the significant effect of the element B on the analyte A is absorption, in which case the corresponding β_{AB} is equal to zero. In this case, the equation is of the Lachance-Traill form. When the predominant effect of element B on the analyte A is enhancement the β_{AB} coefficients are used with the corresponding α_{AB} equal to zero. In some cases where a combination of effects occurs the use of both the α and β coefficients may be required to adequately treat the inter-element effects. However, the authors have never observed such a case.

In contrast to the Lachance-Traill model, the proposed algorithm for the secondary effects has no theoretical basis and was derived from a best-fit to experimental data. This factor was also observed by Andrews (56).

The α and β -coefficients can be determined by two methods. One method uses a graphical approach where a plot of (C_A/R_A) versus C_A is constructed. The coefficient is determined as the intercept as C_A approaches zero. The second method uses a series of simultaneous equations set up from (n-1) calibration standards. In solving for unknowns

these equations do not permit a simple, explicit solution for the weight fractions and an iterative technique is necessary.

Tertian (57,58,59,60,61) has developed a formulation, Equation 9, which makes allowances for variations in coefficients and enhancement effects. The former represented by the term ($\alpha_{AB} + \beta_{AB} C_A$) in the equation for the individual coefficients, and the latter by the term ϵ_A for the overall crossed-product effects which can be negligible in many cases when considering diluted systems.

Emphasis is laid on the experimental determination of correction coefficients and cross-product effects. However, due to its form, application to multi-component systems must be very difficult.

Recent work on inter-element corrections involves modifications to the existing methods.

Rasberry and Heinrich (62) proposed a delta adaptation to their previous model. This involves calibration around a single standard reference specimen.

They have found this technique useful in applications where the samples are in a limited concentration range and less sensitive to errors in correction coefficients than the

general procedure.

The new system can easily be developed as follows:

$$\triangle (C_i/R_i) = (C_i/R_i)_s - (C_i/R_i)_u \qquad (10)$$

where the subscripts s and u denote standard and unknown respectively. Equation 8 can then be represented as:

$$\triangle (C_i/R_i) = \sum_{k \neq i} \alpha_{ik} \triangle (C_k) + \sum_{k \neq i} \beta_{ik} \triangle \left(\frac{C_k}{1 + C_i} \right) \qquad (11)$$

where the $\triangle$ in the summation terms indicate differences between the standard and the unknowns.

Claisse et al. (63,64) have also developed a differential delta method in which Equation 7 is compared to one reference standard. The unknown samples in this technique are considered as the standard with a slight change in composition. Accordingly, the difference in x-ray intensity between the sample and the reference standard for any element is related to the small difference in concentration of the element and to a small difference in matrix effects.

Application of the above to Equation 7, and defining an additional term for the apparent concentration of A as follows:

$$C_A^{app} = \frac{I_A}{I_A^*} (C_A^*) \qquad (12)$$

where * refers to the reference standard. Equation 7 can be represented in the following form:

$$C_A = C_A^{app} \left(1 + \sum \delta_i \Delta C_i \right) \qquad (13)$$

where

$$\Delta C_i = C_i - C_i^* \qquad (14)$$

and

$$\delta_{AB} = \frac{\alpha_{AB} + \alpha_{ABB} C_B}{1 + \sum \alpha_{AB} C_B^* + \sum \alpha_{ABB} C_B^{*2}} \qquad (15)$$

It can be seen that the δ -coefficient is dependent on the composition of the standard as well as the α -coefficients. As such, when a different standard is used the δ -coefficients are calculated from the same set of α -coefficients and there is no need to redetermine these.

The δ -modification of the Claisse-Quintin, Lachance-Traill and Rasberry-Heinrich relationships are also evaluated.

Weight fractions in unknowns are solved through an iterative procedure.

Inter-element corrections can also be solved by means of multiple regression employing first, second and higher order polynomials to obtain a best-fit to the calibration curves. This technique was applied by Alley and Meyers (65) and Mitchell and Hopper (66). Such systems require a very large number of calibration standards and are useful in a limited concentration range. Whereas, in the previous systems, the correction coefficients have a physical significance, these do not. Coefficients obtained through the use of these polynomial equations do not represent the effects of one element on the other.

All of the presented models involved concentration correction methods, in which the chemical composition is expressed in terms of emitted x-ray intensity corrected for matrix or inter-element effects. A different category includes the intensity correction procedures developed by Lucas-Tooth and Price (67) and Lucas-Tooth and Pyne (68). Both models employ interfering-element intensities for correction purposes rather than interfering-element concentrations. This model can be represented by Equation 16.

$$C_A = a + I_A \left(b + \alpha_{AA} I_A + \sum_{B \neq A} \alpha_{AB} I_B \right) \quad (16)$$

Since the interfering element intensity is subject to matrix effects, the intensity correction method is applicable over a relatively small concentration range. The inter-element correction coefficients are almost impossible to calculate from first principles. Thiele (69) used a similar approach but corrected the intensities for background counts.

1.4 The Experimental Application of Matrix and Inter-Element Correction Methods

1.4.1 The choice of a mathematical model to apply

Discussion has been restricted to detailing the various methods available to the analyst. However, certain other factors must be explored before practical use is made of any of these techniques.

The empirical methods have an advantage in that any laboratory can easily apply these without the high cost of computers, especially if these are not readily available. Another advantage is that the analyst need not concern himself with various parameters necessary in the theoretical calculations which may be significantly different for the equipment under use. Although some of the parameters found

in the literature are reliable, not enough spectral data is available for the x-ray continuum if different operating potentials and x-ray tubes are used as is the case in most multi-component analyses.

Another important factor which must be mentioned concerns the specimen under analysis. No distinctions have been made concerning the physical nature of the specimen except that it should be flat, homogeneous and infinitely thick. Since perfect adhesion to these rules rarely occurs, a specimen-type error may occur when comparing experimental data to theoretical data, which is the basis of the fundamental parameters method. The use of empirical methods would most likely minimize the errors since they would include any of the experimental fluctuations which can occur, as well as those due to the nature of the specimen under analysis in a particular instrument.

It can also be noted that extensive work has been devoted to the analysis of stainless steels using the fundamental parameters method. Most authors have tested the method for three elements (ie. iron, nickel and chromium) which are present in considerable amounts in these alloys and have obtained excellent results, which may not be the case with other alloys especially those containing considerable amounts of low atomic numbered elements (ie. aluminum,

magnesium and silicon). It has also been shown, in certain cases, that high deviations do occur for the low atomic number elements present (33). Several authors (35,37) have applied the technique to geological samples with satisfactory results.

The empirical methods can prove more flexible in the long wavelength regions. Data can be collected over the full x-ray spectrum without the need of depending on uncertainties in parameters which may exist at the extreme ends of the wavelength span. However, other problems do occur which affect data results in both cases at these extremes.

As one goes towards the longer wavelengths, other factors such as absorption, scatter and low intensities are readily encountered, which cause lower sensitivities for these elements.

In the case of empirical methods, the physical nature of the specimen under analysis affects the intensities considerably at these longer wavelengths, so that homogeneity as well as surface finish and particle size becomes critical.

1.4.2 The choice of the Lachance-Traill approach for matrix and inter-element corrections

The criteria for choosing a correction model must consider the ease of application of the technique as well as the physical significance of the method with respect to the true inter-element effects.

Multiple regression has been extensively used. However, the correction coefficients obtained do not necessarily yield the true effects of one element on an other but a statistical best fit to the data is provided. Accordingly, the individual coefficients are useless for other systems except the one used to obtain them.

If the method under investigation does yield coefficients which do represent the true effects of one element on an other, a data base of correction coefficients could be established and used for a variety of analyses.

Any one of the previous techniques considered could be used, however, it can be seen that most of these have been derived as extensions of the Lachance-Traill approach (48, 50,51). In view of this, the Lachance-Traill model appears to be the simplest formulation to apply.

The argument which exists in the literature and accounts

for the various modifications arises from the inadequate assumptions used in the derivation of the equation. Since the primary x-ray beam is polychromatic and not monochromatic, the question arises if the method is capable of providing adequate correction for enhancement effects.

Although enhancement effects have been found not to be linearly additive in the same manner as absorption effects, Tertian (57) has nevertheless indicated that, under conditions of polychromatic excitation the two effects behave in a similar manner.

Both Tertian (57) and Lachance (55) have shown, as a consequence of the polychromatic nature of the primary x-ray beam, the correction coefficients are not constant as assumed, but tend to vary over a wide range of concentrations.

On the basis of these arguments, various authors have modified the approach to take the inadequate assumptions into consideration. Rasberry and Heinrich (1) have added an extra term to account for enhancement effects, whereas Claisse and Quintin (53) have taken the polychromatic nature of the primary incident x-radiation into consideration by using higher order coefficients. However, the evaluation of these models becomes more complex because of the larger

number of standards required.

Accordingly, the simpler Lachance-Traill model could be satisfactorily used if several assumptions are considered:

a) If the concentration range is restricted to a particular level, the correction coefficients can be considered constant.

b) The correction coefficients should be determined experimentally under such conditions.

c) The enhancement effect is additive and therefore the experimental data should take this into consideration, as well as the absorption effects.

1.4.3 The availability of correction coefficients

Correction coefficients are affected by various factors such as instrumental geometry and type of x-ray tube target used. Although Lachance (55) has found the effects of instrumental geometry to be minimal for the case of higher atomic number elements, Tertian (27) has arrived at different conclusions using a variety of high and low atomic number elements in binary mixtures.

The choice of x-ray tube target also affects the coefficients, since the elements present in the specimen are excited by different x-ray continuum composed of the characteristic x-ray lines of the target element which are responsible for the greater part of the excitation process, de-

pending on the analyte element.

Accordingly, data appearing in the literature must be carefully screened before use. Most often, too little data is available for general use, especially when different instrumentation and x-ray tubes have been employed. It can also be noted, in many cases, that the coefficients have been evaluated for a specific type of specimen considering only a few of the components present. The correction coefficients in the former case may not represent the true inter-element effects, but a summation of the effects present in a particular matrix.

In the case of geological materials, the use of synthetic mixtures of metal oxides to determine correction coefficients is significant. Gross errors may exist especially if pressed powder discs are used, since particle size and matrix composition are critical for the low atomic number elements (70). Although satisfactory results have been obtained using such a form, the coefficients are usually obtained through multiple regression equations using a minimum of standards. Accordingly, significant variations will occur when different coefficients are compared.

The theoretical models have also been used to determine correction coefficients (71,72).

In the literature, generally, the only significance attached to the coefficients is that satisfactory results are obtained in the analysis.

In summary, although literature data is often available it is either incomplete in the sense that certain coefficients required are lacking. In this case, these must be determined and may not necessarily be consistent with the others. Accordingly, evaluation of a large number of coefficients should exist, where these have been derived from an experimental model under strict rules.

1.4.4 Purposes and approach to the investigation

The purpose of the investigation is to apply the Lachance-Traill correction equation in a general analytical approach. The fundamental approach used in this study is that it is more fruitful to initially examine certain preliminary data in detail before attempting the direct development of a specific analytical technique. This approach was confirmed by subsequent findings, reported herein. The direct approach to the development of applications might yield results more rapidly, but it can also lead to an erroneous or a restricted view of the system, as demonstrated by various analytical schemes developed in the literature for specific sample types.

The work described in this thesis is divided into four main divisions:

1) The determination of Lachance-Traill α-correction coefficients through an improved experimental technique and data analysis.

2) The correlation of experimental coefficients with theoretically-derived coefficients obtained through several methods.

3) The application of these coefficients in the general chemical analysis of multi-component systems using an approach which would minimize any interferences.

4) A theoretical study of various multi-component systems and the results of a Lachance-Traill type method of analysis.

The experimental techniques used to date involve mainly solids, compressed powders or fused powders, with the coefficients determined using similar media.

In the case of specimens involving metals or metallic alloys, these generally have surfaces prepared for x-ray fluorescence examination, by either machining and/or grinding and polishing. Such methods of preparation imply some degree of roughness for the final surface, the degree depending on the finishing technique and the care exerted therein. It can be shown (73,74) that the longer the wavelength to be detected in the x-ray fluorescence analytical process the less the tolerance to surface roughness.

In addition to this problem, it should be noted that, for

the abrasives used in any final process of surface finishing, the grinding and polishing technique must be such as to avoid interfering effects based on abrasive embedment at the surface of the specimen (eg. silicon carbide, aluminum oxide, etc.).

Where solid specimens are concerned, of the type involving metals or alloys, heterogeneity of component distribution at the examined surface, and the smearing of certain components over the surface during preparation or finishing processes, can also contribute to the overall error (73,74,75).

The preparation of mineral substances and samples of geological materials for analysis usually involves the compacting under pressure, with or without binder additions, of the finely-divided mineral. The finely-divided state is obtained by crushing and grinding samples of the mineral matter of adequate size. The grinding operation may result in particles of powder of identical size. Where the particle size is sufficiently small, no interfering effects based on particle sizing are encountered. Where the particle size exceeds some critical value, based to a degree on the wavelength to be detected, interfering effects can be anticipated (76-82). On the other hand, the grinding process may

result in particles whose sizes vary as a result of the variations in the hardness, or response to the grinding action, of the various components present. Variations in particle sizing with composition of the particles can also lead to interfering effects (76-82).

The main concern is to develop an experimental technique under conditions which would eliminate the influences of perturbing factors such as particle size, grain composition, surface-finish and heterogeneity effects, and which would allow flexibility as to the relative amount of sample available, its physical nature and its general lack of homogeneity.

The aqueous solution technique has been applied by several investigators, among whom are Waterbury and Hakkila (83), Zimmerman and Ingles (84), Kang, Keel and Solomon (85) and Dwiggins (86). In such instances, the effects of absorption and enhancement were reduced to levels where they could be ignored, this being accomplished by the use of highly-dilute solutions of the analytes of interest. The total solids concentration in these cases rarely exceeded 2% by weight. At such low concentration levels, however, emission intensities were low, with associated poor relative accuracy and precision for the analytes determined.

With solid concentrations totalling approximately 10% by weight, absorption and enhancement effects cannot be ignored and the use of correction coefficients for such effects is mandatory. The higher emission intensities permit improved accuracy and precision. Work in this area has been carried out by Dick and Nguyen (87,88,89) and the initial reports indicate very good accuracy and precision with respect to the determination of a wide range of components in extensive ranges of concentration. Both synthetic solutions and solutions of commercial alloys have been analyzed. The α-correction coefficients required in such analytical programs were also determined relative to aqueous media.

The aqueous solution technique for the determination of α-correction coefficients and for use in the analysis of multi-component systems has the following advantages:

1) There are no heterogeneity effects based on component segregation effects.

2) There are no surface effects arising from grinding and polishing, thus eliminating smearing effects due to abrasives used.

3) There are no particle size effects present.

4) The quantity of sample required for a complete analysis can be as low as 1 gram in 100 grams of solution. This therefore easily accomodates very low sample requirements.

5) The method allows samples of unusual states, such as turnings, drillings, millings, etc., to be treated.

6) Heterogeneous samples of a physical nature similar to the above can also be treated.

On the other hand, the aqueous solutions do require careful sample cell preparation to avoid uncontrollable errors, (ie. gas bubbles, radiolysis effects and surface irregularities).

However, the advantages are far more consequential, since the use of an aqueous solution for both the analysis and α-coefficient determination eliminates any matrix difference problems. These usually occur due to the physical differences which exist between the standards used and the specimen under analysis.

2. THE DETERMINATION OF LACHANCE-TRAILL α-CORRECTION COEFFICIENTS

2.1 Introduction

Lachance and Traill (50-52)have shown that the theoretical Equation 4 can be modified to obtain their Equation 6 through certain assumptions previously stated.

In this study, since aqueous media are used both in the determination of correction coefficients and in analyses, an additional term representing the aqueous matrix which constitutes greater than 80% of the total weight fraction, is introduced into Equation 6. This modified equation is shown as:

$$c_i = R_i \left(1 + \alpha_{im} c_m + \sum_{\substack{j=1 \\ j \neq i}}^{n} \alpha_{ij} c_j \right) \qquad (17)$$

where: c_m is the weight fraction of the aqueous matrix (usually H_2O-HNO_3); α_{im} is the correction coefficient for the effect of aqueous matrix m on the analyte element i. The modification is based on the fact that the matrix is comprised of low absorbing elements (ie. H, O, N, Li and B) which can be grouped into one correction coefficient representing the net effect (84, 87-89).

When applying such a system both matrix and inter-element correction coefficients must be evaluated.

2.2 Different Algorithms

2.2.1 The aqueous matrix effects

When considering the aqueous matrix effect, we are dealing with the effect of the matrix m on an analyte i and thus the coefficient can be represented as α_{im}. The simplest method for evaluating the individual α_{im}'s is through the use of binary solution components. Two samples of differing concentrations of the analyte are prepared and, using Equation 16 for each sample, the following are obtained:

$$c_{i(1)} = R_{i(1)} \left(1 + \alpha_{im} \cdot c_{m(1)}\right) \qquad (17a)$$

$$c_{i(2)} = R_{i(2)} \left(1 + \alpha_{im} \cdot c_{m(2)}\right) \qquad (17b)$$

where the subscripts (1) and (2) indicate the different samples and i the analyte element of interest. By taking the ratio of Equation 17a and 17b, and rearranging the terms, the following is obtained:

$$\alpha_{im} = \frac{I_{i(1)}\, c_{i(2)} - I_{i(2)}\, c_{i(1)}}{I_{i(2)}\, c_{i(1)}\, c_{m(2)} - I_{i(1)}\, c_{i(2)}\, c_{m(1)}} \qquad (18)$$

where: I_i represents the net measured intensity for the

analyte i.

2.2.2 The inter-element effects

In addition to the matrix effects previously stated each element present in the sample exhibits to some degree an inter-element effect. Again the simplest method of solving such a system is to employ the minimum number of components in the sample. Accordingly, we can represent the inter-element correction coefficient as α_{ij} where i is the analyte and j the interfering element. In order to solve for inter-element effects the matrix-effects correction coefficient must be previously determined.

Similarly to the matrix effects, equations can be derived for the inter-element effects and the following obained:

$$\alpha_{ij} = \frac{I_{i(2)}c_{i(1)}(1+\alpha_{im}c_{m(2)}) - I_{i(1)}c_{i(2)}(1+\alpha_{im}c_{m(1)})}{I_{i(1)}c_{i(2)}c_{j(1)} - I_{i(2)}c_{i(1)}c_{j(2)}} \qquad (19)$$

2.2.3 The third-element effects

The situation in practice of complete dissolution of a specimen into a H_2O-HNO_3 matrix rarely occurs. In such cases the use of hydrochloric acid or perchloric acid may

be required. However, since our matrix modification accounts for the low absorbers (ie. H, O, N, Li and B) the effect of the chlorine must be determined separately due to its significant effect. Accordingly, we have a situation where the analyte, matrix and chlorine are present. The following Equation 20 can be used in these cases necessitating the "third-element effect" correction:

$$\alpha_{ij} = \frac{(I_{i(2)} - I_{i(1)}) + \alpha_{im}(I_{i(2)}c_{m(2)} - I_{i(1)}c_{m(1)})}{I_{i(1)}c_{j(1)} - I_{i(2)}c_{j(2)}} \qquad (20)$$

where j in this case would represent the effect of Cl on the analyte i.

2.3 The Validity of the Intensity Correction Algorithms

Verification of the correction capabilities of these coefficients on the net measured x-ray fluorescent intensity can be obtained by a simple calculation involving the appropriate form of the following:

$$I_{i(corr)} = I_{i(net)}\left(1 + \alpha_{im}c_m + \sum_{\substack{j=1 \\ j\neq i}}^{n} \alpha_{ij}c_j\right) \qquad (21)$$

where $I_{i(corr)}$ represents the corrected net intensity for

the analyte i radiation and $I_{i(net)}$ is the net measured intensity corrected for background.

The results show the correction for matrix and/or inter-element effects present in the system under investigation with $I_{i(corr)}$ as the net intensity free from these effects.

Another important calculation which can be used as a check, is the I^o (ie. intensity of 100% analyte element) which can be compared to the experimental value. Agreement within experimental error should occur. However, it has been noticed (90) that certain discrepancies, more severely with the light elements, does occur. This has been traced to the absorption power of the mylar film covering on the sample cell. The corrected intensity for this absorption effect is found to be of the following form (90):

$$I_{(corr\ mylar)} = I_i \cdot \exp(k_{mylar} \cdot x) \qquad (22)$$

where: I_i represents the net measured analyte intensity; k_{mylar} is the mylar absorption coefficient and x the thickness in inches of the mylar film used. The value of k_{mylar} can be obtained by using the following equation:

$$k_{mylar} = (13.5 \pm 0.4)\,\lambda^{(2.80 \pm 0.03)} \qquad (23)$$

Figure 6 shows the relationship of k_{mylar} to the emitted wavelength for the element under examination (90).

2.4 Experimental Determination of α-Correction Coefficients

2.4.1 Experimental solution preparation

In the determination of correction coefficients a series of solutions are prepared on a weight fraction basis using reagent grade chemicals, usually the metal nitrates or the pure metal dissolved in nitric acid. Solutions for the study of matrix effects are prepared on the basis of varying the analyte element concentration over a 10% to 20% range by weight. When dealing with inter-element effects, in order to keep the system simple as much as possible, as well as to make the degree of the effect quite evident, the analyte concentration is kept constant while the interfering element concentration is varied over a specific range. In all cases a H_2O-HNO_3 matrix is used with the addition of HCl if dissolution does not occur readily.

Sample cells consist of disposable SPEX (#3515) polypropylene x-ray liquid cells with a nominal capacity of approximately 10 ml of solution. The surface is carefully covered with a layer of mylar film (Spectro-film, Somar Laboratories Inc., 0.00025 inch or $> 6\mu m$) and secured by a

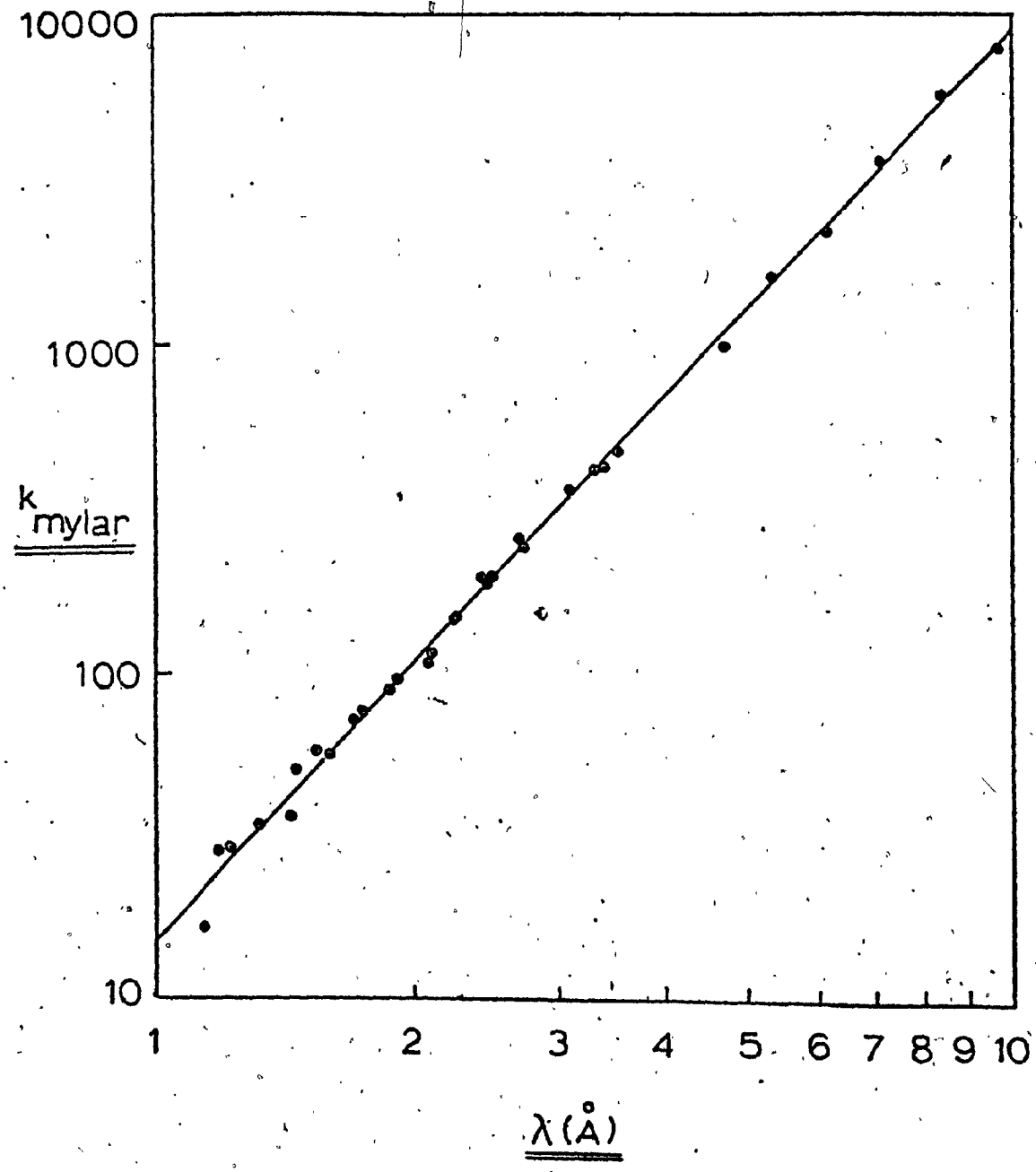

Figure 6 :- Relationship of k_{mylar} to Emitted Wavelength for Element Under Examination. (Log-log plot of k_{mylar} versus λ)

disposable plastic ring. Care must be exerted in the preparation of the sample cells to prevent any surface irregularities or inclusion of entrapped air bubbles.

When using aqueous solution media, certain problems may arise during irradiation of the sample which may cause significant effects. Chemical effects which arise through the unstability of the solution to irradiation can be very severe if it occurs. This rarely occurs except for a few elements (eg. silver). These usually take the form of a precipitation which causes a significant decrease in intensity with time due to losses of the analyte. Physical effects which can occur can easily be prevented if certain precautions are taken. The most severe of these is the release of dissolved gases in the solution under irradiation, which tend to exert a pressure on the mylar film covering, thereby distorting the surface. In order to avoid the release of any dissolved gases, the sample solutions are boiled and cooled before final bulking to the appropriate weight fraction. Under these conditions no noticeable bubble formation occurs and the sample can be repeatedly irradiated with no significant decrease in intensity. Another factor which may affect the solution is heating when under irradiation. This can be eliminated by making sure the irradiation time is quite short and the sample chamber is kept

cool.

2.4.2 Calculation methods

The purpose of the study was to obtain a mean value for the correction coefficients, with as close a proximity to the true value in each case. This could be realized only with a large population for the coefficient evaluation. Accordingly, a strict statistical data treatment algorithm was developed to obtain the maximum information from a series of data. Each system involved a triplicate determination to assure that no adverse effects are present as would be evidenced if fluctuations in the α-levels occurred. Previous investigators (87-89,91) have evaluated coefficients by averaging the ratios obtained using solutions of maximum concentration differences. However, biased data can be obtained in this manner since there is no statistical reason to follow such a technique of analysis. Other authors (72) have arrived at the coefficients through the use of a linear regression technique. It has been suggested that the linear regression technique should be used also as a criteria for the rejection of measurements which fall outside acceptable limits. At this point the measurement would be eliminated and the regression process repeated. In the case of inter-element effects multiple re-

gression could be used in the same manner. However, linear regression is derived on the basis that dependent and independent variables can be clearly identified. In the present model described it is impossible to separate these (ie. we have in effect two dependent variables) but they are not suitable for use with the present data. Accordingly, the choice of the most simple and flexible method, assuming a non-biased approach to the data analysis, is justified. Use of a linear regression technique as a tool for rejection, after which a better line is fitted, introduces a large degree of bias. This is especially true where the main point is to minimize the errors which may exist in a set of data points by producing the best straight line through them. The formulation eventually accepted considers the results obtained from all the ratios in a particular series (ie. if eight solutions are used, twenty-eight ratios for the coefficient can be evaluated). Since triplicate series are studied the population becomes significant. The total coefficients from the series are examined by calculating the mean and standard deviation. As a precaution, erroneous data is rejected according to an empirical $\pm 1s$ test (92). The $\pm 1s$ test was obtained by examination of different systems and establishing statistical tests which reject the least amount of data as well as preventing any bias from

being introduced into the technique. The acceptable results from each series were then averaged and the new standard deviation calculated. The same test to determine rejectable data was applied to other series and final acceptable values calculated.

Due to such a large volume of data, computer programs ALPHAMAT and INTERM1 were developed for the calculation of matrix and inter-element α-correction coefficients respectively (Appendix A).

Typical examples are shown in Tables 2 and 3 for the determination of α_{CrM} and α_{CrCa} respectively. The matrix and inter-element effects can be graphically shown as in Figures 7 and 8, for these same systems (92).

2.4.3 Results and Discussion

Experimental data throughout the study was collected using a Picker Nuclear spectro-diffractometer (45^{o} incident and take-off angles), a radiation analyzer and an ultra-stable two-tube generator. Operating conditions used in the evaluation of the α-correction coefficients are shown in Table 4.

The accumulated α_{ij} coefficients evaluated experimentally are shown in Table 5 (93-95). Each value is the

TABLE 2

EFFECT OF AQUEOUS MATRIX ON CHROMIUM

Solution	c_{Cr}	c_M	$I_{CrK\alpha}$*
1.	0.00978	0.99022	3701
2.	0.01955	0.98045	7246
3.	0.02932	0.97068	10538
4.	0.03910	0.96090	13260
5.	0.0587	0.9414	18471
6.	0.0782	0.9218	21494
7.	0.1173	0.8827	28450
8.	0.1564	0.8446	33290

* net intensity for CrKα line, cps. (W at 50 kV/20 mA, air path)

Combination of solution	α_{CrM}	Combination of solution	α_{CrM}	Combination of solution	α_{CrM}
1/2	-0.6925.. *	2/5	-0.8323..	4/5	-0.8228..
1/3	-0.7375..	2/6	-0.8705..	4/6	-0.8864..
1/4	-0.8030..	2/7	-0.8580..	4/7	-0.8641..
1/5	-0.8118..	2/8	-0.8593..	4/8	-0.8644...
1/6	-0.8536..	3/4	-0.8817..	5/6	-0.9299..
1/7	-0.8461..	3/5	-0.8486..	5/7	-0.8789..
1/8	-0.8494.. *	3/6	-0.8853..	5/8	-0.8748..
2/3	-0.7732..	3/7	-0.8671..	6/7	-0.8229..
2/4	-0.8397..	3/8	-0.8667..	6/8	-0.8426...
				7/8	-0.9611..

* rejects on first inspection

Acceptable data:

Average value α_{CrM} = -0.853

Std. devn. = $\pm$ 0.023

Series (1) $\alpha_{CrM} = -0.85^3 \pm 0.02^3$ (23 data)

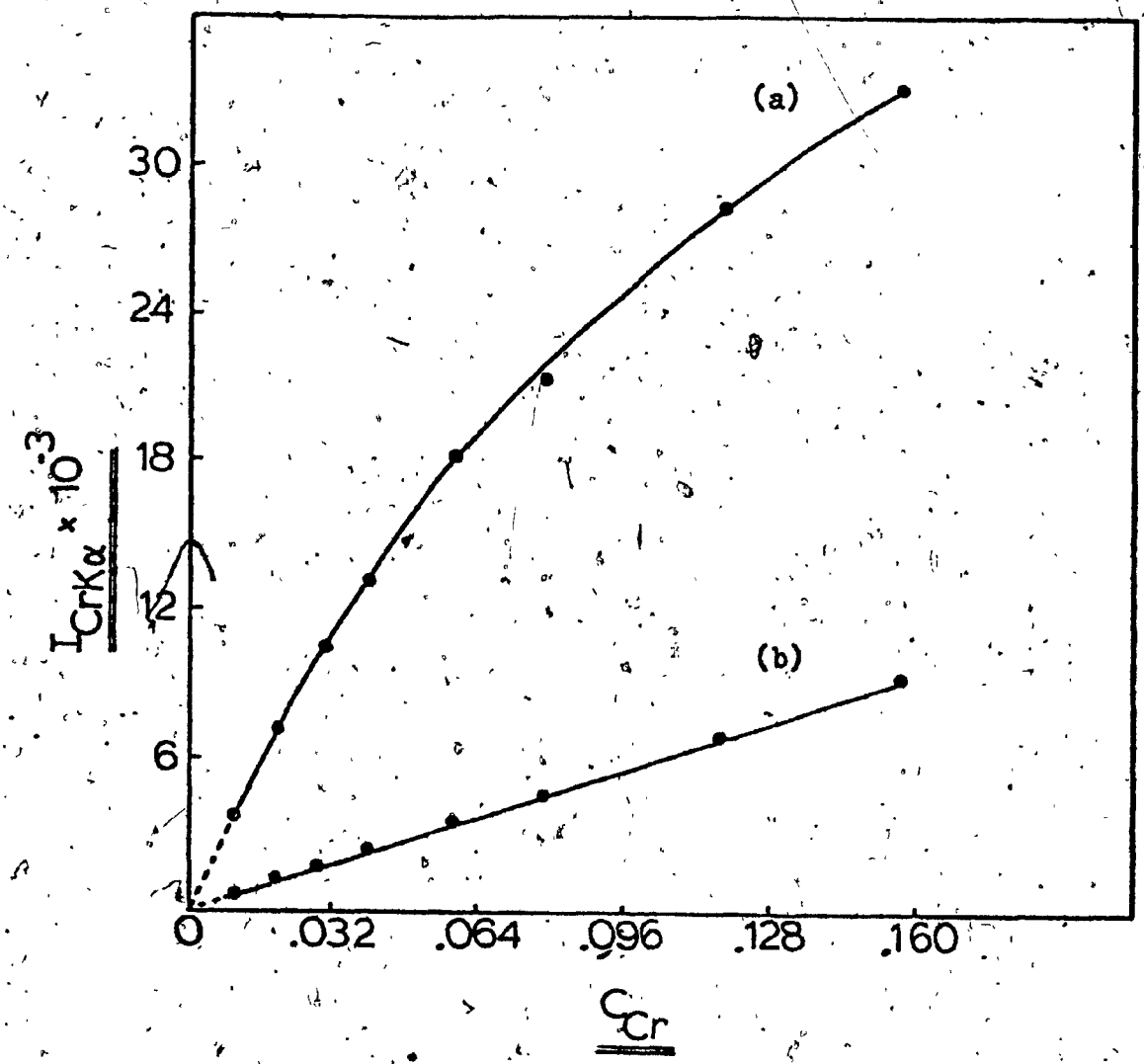

Figure 7 :- EFFECT OF AQUEOUS MATRIX ON CHROMIUM

(a) net measured Intensity vs C_{Cr}

(b) corrected Intensity vs C_{Cr}

TABLE 3

EFFECT OF CALCIUM ON CHROMIUM

Solution	c_{Cr}	c_{Ca}	c_M	$I_{CrK\alpha}$ *
1.	0.01000	0.0	0.99000	21342
2.	0.01000	0.01000	0.98000	18568
3.	0.01000	0.02000	0.97000	16666
4.	0.01000	0.03000	0.96000	15062
5.	0.01000	0.04000	0.95000	13418
6.	0.01000	0.05000	0.94000	12513
7.	0.01000	0.06000	0.93000	11559

* net intensity for CrKα line, cps. (W at 50 kV/20 mA, Helium path)

Combination of solution	α_{CrCa}	Combination of solution	α_{CrCa}	Combination of solution	α_{CrCa}
1/2	1.5179..	2/4	1.2377..	3/7	1.3971...
1/3	1.3735..	2/5	1.4753..	4/5	2.2206..
1/4	1.3529..	2/6	1.3313..	4/6	1.4747..
1/5	1.4903..	2/7	1.3375...	4/7	1.4474...
1/6	1.3867..	3/4	1.2947..	5/6	0.7630...
1/7	1.3858..	3/5	1.6810..	5/7	1.0289..
2/3	1.1919..	3/6	1.4017..	6/7	1.3773..

*rejects on first inspection

Acceptable data:

Average value α_{CrCa} = 1.3808

Std. devn. = ±0.0875

Series (1) $\alpha_{CrCa} = 1.38^{0} \pm 0.08^{7}$

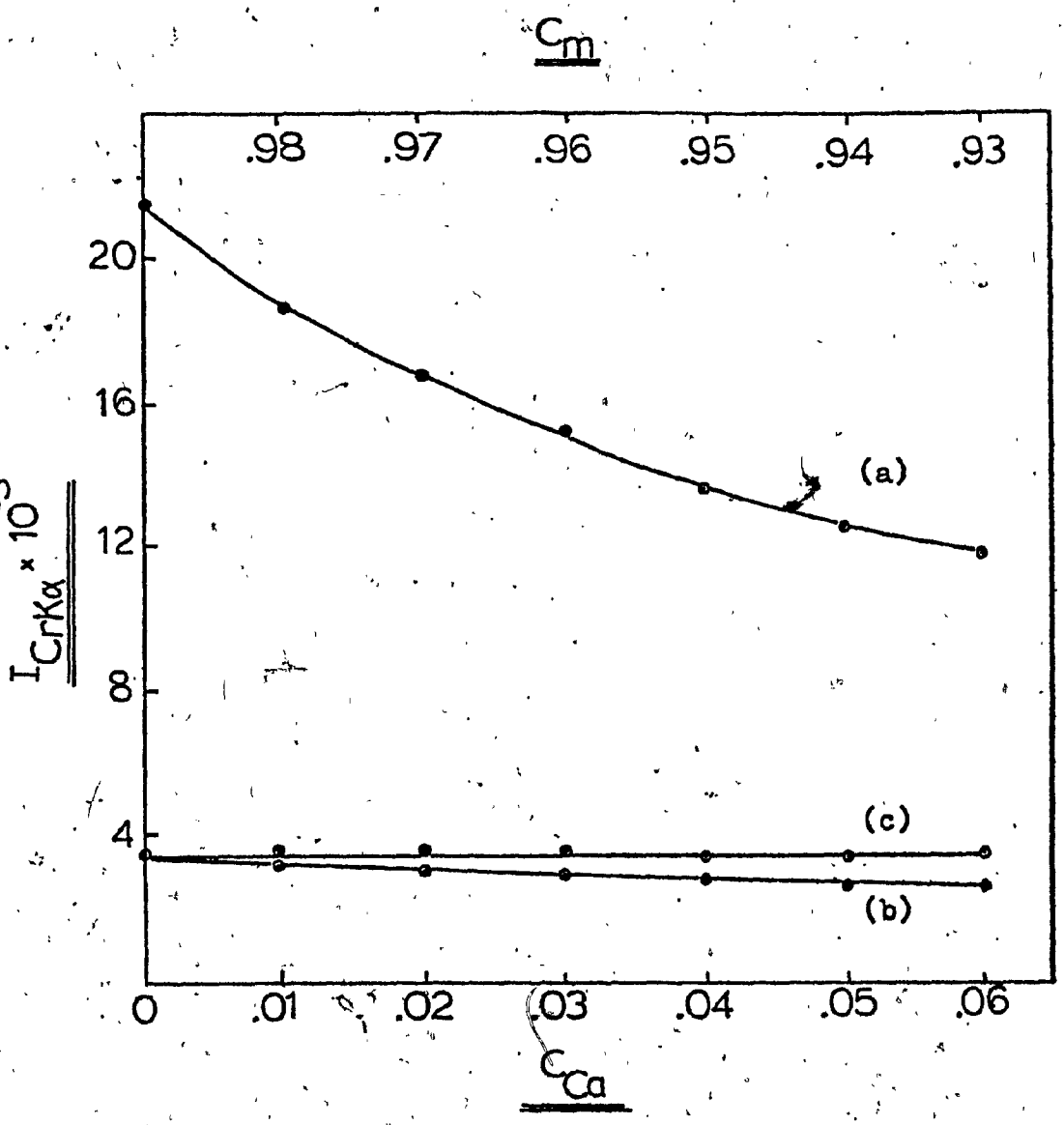

Figure 8 :- EFFECT OF AQUEOUS MATRIX AND CALCIUM ON CHROMIUM

(a) net measured Intensity vs C_M and C_{Ca}

(b) net measured Intensity corrected for aqueous matrix only vs C_{Ca}

(c) net measured Intensity corrected for matrix and calcium effects

TABLE 4

OPERATING CONDITIONS

Element	P	Cl	K	Ca	Cr	Mn	Fe	Co	Ni	Cu	Zn	Cd	Sn	Pb
Target	Cr	Cr	Cr	Cr	W	W	W	W	W	W	W	W	W	W
kV	50	50	50	44	50	50	50	50/46	50/40	50	50/40	50/46	50	50
Collimator	coarse	coarse	coarse	coarse	fine	fine	fine	fine	fine	fine	fine	fine	fine	fine
Crystal	PET	PET	PET	LiF	LiF	LiF	LiF	LiF	LiF	LiF	LiF	LiF	LiF	LiF
Counter	PF	PF	PF	Sc	Sc	Sc	Sc	Sc	Sc	Sc	Sc	Sc	Sc	Sc
Time *	20s	20s	10s	10s	10s	10s	10s	10s	10s	10s	10s	10s	10s	10s
Radiation	Kα	Kα	Kα	Kα	Kα	Kα	Kα	Kα	Kα	Kα	Kα	Kα	Kα	Lα
Path	He	He	He	He	air	air	air	air	air	air	air	air	air	air

* Fixed time counts — all determinations were average of 5 counting periods

TABLE 5

EXPERIMENTAL α_{ij} - COEFFICIENTS [4]

Elements j	Elements i: Al[1]	P	Cl	K	Ca	Cr	Mn	Fe	Co	Ni	Cu	Zn	Cd	Sn
M	1.3	-0.34	-0.39	-0.71	-0.79	-0.89	-0.86	-0.90	-0.91	-0.923	-0.924	-0.943	-0.962	-0.962
Na	nd	1.16	nd	-0.22	-0.39	-0.56	-0.60	-0.68	-0.72	-0.77	-0.78	-0.82	nd	nd
Mg	nd	1.5	1.6	0.11	-0.10	-0.35	-0.46	-0.57	-0.64	-0.69	-0.71	-0.79	-0.93	nd
Al		3.6	1.8	0.23	0.03	-0.22	-0.33	-0.49	-0.53	-0.63	-0.64	-0.70	-0.93	nd
P	nd		2.6	0.83	0.26	0.08	-0.01	-0.20	-0.26	-0.41	-0.40	-0.51	nd	nd
Cl	1.9	-0.4		1.36	0.77	0.52	0.36	0.07	0.03	-0.14	-0.16	-0.23	nd	-0.82
K	nd	-0.4	-0.15		1.54	1.01	0.86	0.39	0.40	0.16	0.15	-0.08	nd	nd
Ca	nd	0.2	-0.01	-0.35		1.37	1.19	0.83	0.64	0.38	0.38	0.11	nd	nd
Cr	nd	1.2	0.4	-0.31	-0.49		nd[2]	1.74	1.42	0.96	1.01	0.57	-0.54	-0.59
Mn	3.3	1.3	0.6	-0.16	-0.46	-0.18		-0.23	1.58	1.12	1.16	0.70	-0.50	-0.54
Fe	5.3	1.5	1.00	-0.12	-0.41	-0.58	0.00		-0.02	1.46	1.47	1.04	-0.45	-0.47
Co	nd	1.5	1.0	-0.03	-0.25	-0.60	-0.59	-0.03		-0.11	1.63	1.20	-0.42	-0.43
Ni	7.2	2.3	1.4	0.06	-0.17	-0.39	-0.52	-0.54	-0.05		-0.05	1.51	-0.27	-0.34
Cu	7.4	nd	1.5	0.24	-0.14	-0.39	-0.65	-0.58	-0.59	-0.34		-0.17	-0.22	-0.28
Zn	nd	3.0	1.6	0.38	0.05	-0.35	-0.42	-0.53	-0.53	-0.59	-0.10		-0.09	-0.17
Cd	nd	nd	1.0	nd	1.41	2.07	1.84	1.29	1.15	0.77	0.79	0.40		nd
Sn[1]	nd	nd	1.8	nd	nd	nd	nd	1.48	nd	nd	0.68	0.38	nd	
Pb	nd	nd	nd	nd	2.17	nd	1.66	1.09	1.09	0.67	0.71	0.40	1.3	nd

1. Initial approach -- low population results (ref. 87,94)
2. Kβ chromium interferes with manganese Kα . Manganese Kβ used but Table is primarily Kα .
3. Coefficients for lead are Lα line where $\alpha_{PbM} = -0.974$ and $\alpha_{PbSn} = -0.26$ (ref. 87,92)
4. ref. 93

result of an average of at least fifty acceptable data points. The validity of each was evaluated by comparing calculated pure analyte intensities after mylar film corrections and comparison to pure element standards. Graphical analysis of each series also revealed the degree of the particular effect and gave a good indication of the success of the correction applied.

From Table 5, it is evident that the precision for the coefficients varies with the element, giving poorer values for the lower atomic numbered elements. This is reasonable, since with the lighter elements the intensities are significantly lower so that even an increase in the counting period does not improve the coefficient statistics.

Since the Lachance-Traill equations used in α-correction coefficient determination are of a hyperbolic form, if we vary the intensity within the uncertainty limits (which on a relative basis generally become larger with decreasing atomic number of the analyte) and calculate the resulting coefficient, a curve similar to Figure 9 is obtained. In this instance only one arm of the hyperbola is shown since we are interested on that portion of the curve which yields coefficients with physical significance, (ie. $\alpha_{ij} > -1$). This curve can then be arbitrarily divided into

three sections as indicated. If the instantaneous slope of the curve is now considered we have the following:

$$\left(\frac{d\alpha}{dI}\right)_a < \left(\frac{d\alpha}{dI}\right)_b < \left(\frac{d\alpha}{dI}\right)_c \qquad (24)$$

where the subscripts refer to the sections of the curve in Figure 9. For a given ΔI, or uncertainty in the measurement of intensity, we have:

$$(\Delta\alpha)_a \leq (\Delta\alpha)_b < (\Delta\alpha)_c \qquad (25)$$

for any α in these regions. Indications are that the uncertainty in the measured intensity will most significantly affect the α-coefficient in section (c), less so than in section (b) and the least of all in section (a). Since most of the light elements will appear in the section (c) of the curve, their precisions will likely suffer the most. From this empirical formulation and the calculation of the maximum possible errors associated with the calculation of the α_{ij}'s, and the various manipulations, the coefficients can at best be represented to two significant figures and at most three for the more favoured elements.

Table 6 gives some indication of the deviations which occur in these experimental systems.

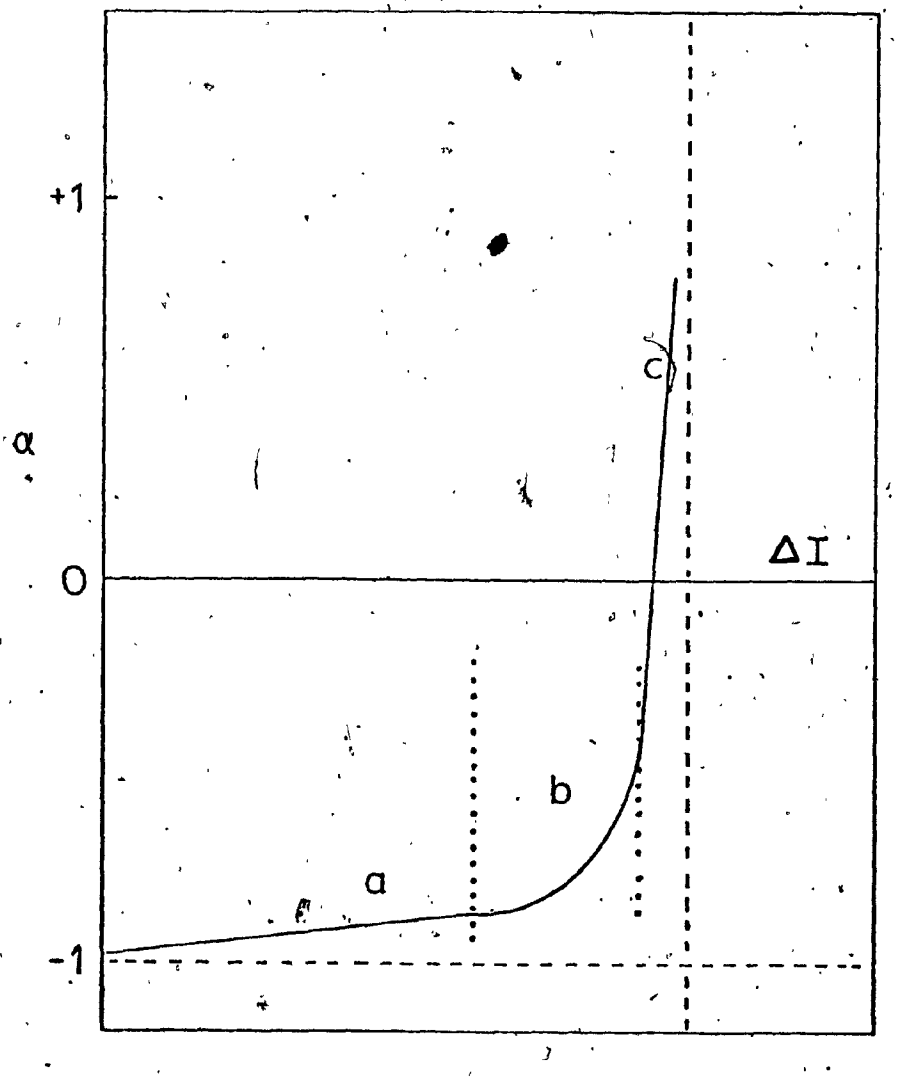

Figure 9 :- EFFECT OF MEASURED INTENSITY UNCERTAINTY LIMITS ON THE VALUE OF α - COEFFICIENTS

TABLE 6

EXPERIMENTAL UNCERTAINTIES FOR α_{ij} COEFFICIENTS *

Elements j	Elements i: Al	P	Cl	K	Ca	Cr	Mn	Fe	Co	Ni	Cu	Zn	Cd	Sn
M	0.2	0.08	0.04	0.04	0.04	0.03	0.02	0.02	0.01	0.02	0.008	0.008	0.004	0.004
Na	nd	0.09	nd	0.05	0.04	0.03	0.01	0.01	0.009	0.004	0.006	0.01	nd	nd
Mg	nd	0.7	0.3	0.07	0.07	0.03	0.04	0.05	0.03	0.04	0.02	0.02	0.04	nd
Al		0.4	0.2	0.08	0.07	0.04	0.05	0.03	0.02	0.03	0.03	0.02	0.06	nd
P	nd		0.1	0.05	0.05	0.02	0.02	0.02	0.01	0.007	0.009	0.005	nd	nd
Cl	0.2	0.1		0.06	0.07	0.06	0.03	0.03	0.03	0.03	0.02	0.05	nd	0.05
K	nd	0.3	0.2		0.14	0.02	0.02	0.05	0.02	0.01	0.01	0.01	nd	nd
Ca	nd	0.4	0.2	0.04		0.08	0.02	0.02	0.01	0.02	0.02	0.01	nd	nd
Cr	nd	0.1	0.1	0.03	0.04		nd	0.03	0.04	0.02	0.04	0.06	0.02	0.05
Mn	0.3	0.1	0.1	0.04	0.04	0.02		0.04	0.07	0.03	0.04	0.05	0.03	0.04
Fe	0.3	0.2	0.07	0.09	0.07	0.04	0.01		0.05	0.05	0.03	0.05	0.06	0.03
Co	nd	0.4	0.1	0.05	0.02	0.01	0.02	0.01		0.02	0.04	0.03	0.06	0.05
Ni	0.4	0.5	0.2	0.04	0.04	0.05	0.03	0.02	0.02		0.02	0.05	0.04	0.04
Cu	0.2	nd	0.1	0.05	0.04	0.03	0.3	0.02	0.02	0.03		0.02	0.05	0.04
Zn	nd	0.3	0.2	0.06	0.04	0.04	0.04	0.02	0.02	0.02	0.03		0.03	0.03
Cd	nd	nd	0.1	nd	0.07	0.04	0.07	0.03	0.04	0.04	0.02	0.02		nd
Pb	nd	nd	nd	nd	0.04	nd	0.04	0.03	0.03	0.03	0.02	0.03	0.1	nd

* Uncertainties expressed on basis of standard deviation of overall acceptable results.

Tables 7 and 8 show operating conditions and previously determined coefficients (87,92,94) respectively. Although some significant difference in results occurs, a linear correlation is evident in most cases which suggests that the data are similar although obtained under different conditions.

Verification of the validity of the coefficient values is generally obtained by noticing the trends in plots of α-coefficient values versus the atomic number of the influencing element.

2.5 Theoretical Models for Evaluating α-Coefficients

In the experimental approach, emphasis is made relative to the importance to the coefficients of certain assumptions in the derivation of the original Lachance-Traill equations (which are known to be invalid to a certain degree). Inadequate treatment of the polychromatic nature of the primary x-ray beam, and enhancement effects, may affect their theoretical derivations significantly. This in turn may affect the coefficients if theoretically calculated using their model. In order to show that the experimental coefficients do represent true coefficients including deviations caused by deficiencies in the derivations, correlations between these and the coefficients theoretically calculated

TABLE 7

OPERATING CONDITIONS [87]

Element	Cl	Cr	Mn	Fe	Co	Ni	Cu	Zn	Cd	Sn	Pb
Target	Cr	W	W	W	W	W	W	W	W	W	W
kV	50	50	50	50	50	50	50	50	50	50	50
Collimator	coarse	fine	fine	fine	fine	fine	fine	fine	fine	fine	fine
Crystal	PET	LiF	LiF	LiF	LiF	LiF	LiF	LiF	LiF	LiF	LiF
Counter	PF	Sc	Sc	Sc	Sc	Sc	Sc	Sc	Sc	Sc	Sc
Time *	20s	10s	10s	10s	10s	10s	10s	10s	10s	20s	20s
Radiation	K	K	K	K	K	K	K	K	K	K	L
Path	He	air	air	air	air	air	air	air	air	air	air

* Fixed time counts -- all determinations were average of 5 counting periods.

TABLE 8

α_{ij}-CORRECTION COEFFICIENTS PREVIOUSLY DETERMINED[87]

j \ i	Cl	Cr	Mn	Fe	Co	Ni	Cu	Zn	Cd	Sn	Pb
M	-0.33^{6}	-0.847^{1}	-0.863^{7}	-0.896^{7}	-0.922^{3}	-0.917^{1}	-0.925^{9}	-0.942^{9}	-0.965^{6}	-0.954^{0}	-0.969^{9}
Cl		0.46^{6}	0.29^{2}	0.04^{7}	-0.172^{6}	-0.16^{2}	-0.25^{0}	-0.32^{7}	-0.857^{6}	-0.846^{9}	-0.695^{6}
Cr	0.39^{6}		0.8^{2}	1.47^{9}	1.05^{3}	1.00^{5}	0.89^{4}	0.54^{0}			
Mn	0.66^{7}	-0.30^{1}		-0.31^{9}	1.24^{3}	1.21^{5}	1.0^{4}	0.63^{1}			
Fe	1.12^{7}	-0.49^{3}	-0.28^{1}		-0.22^{4}	1.32^{5}	1.25^{3}	0.6^{5}	-0.47^{6}		
Co	1.24^{2}	-0.55^{1}	-0.67^{4}	-0.23^{4}		-0.17^{5}	1.5^{1}	0.9^{4}			
Ni	1.26^{1}	-0.38^{9}	-0.39^{1}	-0.63^{3}	-0.37^{4}		-0.07^{4}	1.1^{6}			
Cu	1.40^{0}	-0.51^{0}	-0.50^{9}	-0.62^{1}	-0.66^{5}	-0.3^{5}		-0.26^{0}		-0.25^{2}	0.19^{7}
Zn	1.8^{3}	-0.38^{8}	-0.46^{0}	-0.61^{5}	-0.61^{0}	-0.52^{3}	-0.207^{2}			-0.23^{5}	0.35^{7}
Cd	1.31^{3}			1.12^{8}							
Sn	1.79^{6}			1.48^{6}			0.68^{4}	0.37^{9}			-0.26^{4}
Pb							0.51^{5}	0.26^{8}		1.03^{5}	

by various models must be evaluated. The models chosen must pertain to the same type of sample and also the same statistical data treatment.

Two models are chosen: firstly, the basic equation suggested by Lachance-Traill (48,50-52) ; secondly a fundamental parameters approach (5,6,19); additionally comparison with coefficients found in the literature, provided these were obtained under similar conditions experimentally (ie. same x-ray tube targets, same spectrometer geometries, etc.). These are often not included in full detail.

2.5.1 The Lachance-Traill model

In the first model Equation 26 is used to find the α-coefficients for the effect of an element j on an analyte i:

$$\alpha_{ij} = \left(\frac{(\mu_1 \csc\psi_1 + \mu_2 \csc\psi_2)_j}{(\mu_1 \csc\psi_1 + \mu_2 \csc\psi_2)_i} - 1 \right) \quad (26)$$

where $(\mu_1)_i$ and $(\mu_1)_j$ are the mass absorption coefficients for the elements i and j at the effective wavelength for the excitation of the i radiation; $(\mu_2)_i$ and $(\mu_2)_j$ are the mass absorption coefficients of the elements i and j at the wavelength of the characteristic radiation of the analyte i;

and ψ_1 and ψ_2 are the angle of incidence of the primary x-ray beam and the angle of emergence of the secondary x-radiation respectively. The advantage of the method is that the coefficients can be calculated very easily by means of a table of mass absorption coefficients and do not require more complex methods employing different mathematical techniques. One of the disadvantages stems from its derivation. Firstly, it is assumed that the primary x-radiation is monochromatic, suggesting that a single wavelength could be used to represent the whole primary spectrum that is responsible for exciting the characteristic lines of an analyte. Existence of such a wavelength causes various problems arising especially in its choice, which is important in order to obtain reliable coefficients. The uncertainty which thus arises over this λ_{eff} value and derivation, as previously discussed, adds to the problem. A second disadvantage arises from the inadequate treatment of enhancement effects. Accordingly, by considering only an absorption effect the following equation can be written for the analyte intensity assuming a $45^{\circ}/45^{\circ}$ geometry:

$$I_{i(1)} = g\, c_i \int_{\lambda_{min}}^{\lambda_i\,edge} \frac{\left(\mu_{i(\lambda)} \cdot I^{o}\right)}{\left(\mu_{m(\lambda)} + \mu_{m(\lambda_i)}\right)} \cdot d\lambda \qquad (27)$$

where: $\mu_{m(\lambda)} = \left(\sum_j c_j \mu_j\right)_\lambda$ and $\mu_{m(\lambda_i)} = \left(\sum_j c_j \mu_j\right)_{\lambda_i}$;

and g is a constant for the spectrometer; c_j is the concentration of the element j; λ_i is the analyte wavelength and μ_j is the mass absorption coefficient of the element j at the appropriate wavelength indicated and I^0 is the intensity of the primary x-ray continuum.

With respect to obtaining the λ_{eff}, Equation 27 can be expressed in a variety of ways. Graphically it can be illustrated as depicted by various authors (27,30,96,97), as shown in Figure 10. In Equation 26, Lachance suggests the use of a wavelength for λ_{eff} which is just short of the absorption edge of the analyte for which the mass absorption coefficients of the elements i and j can be used. This corresponds to Figure 10(b) and 10(c), where it can be seen that the effectivenesss is maximum for this wavelength in both the analyte and the sample. In their case, they have neglected totally the tube target continuum and characteristic lines (Figure 10(a)), which do have some significance as shown in Figure 10(d). If the continuum and lines are considered a completely different picture is obtained, where a definite maximum can most often be found. If the continuum is used, the choice of tube-target type is also important, since the primary spectrum will vary with differ-

Figure 10

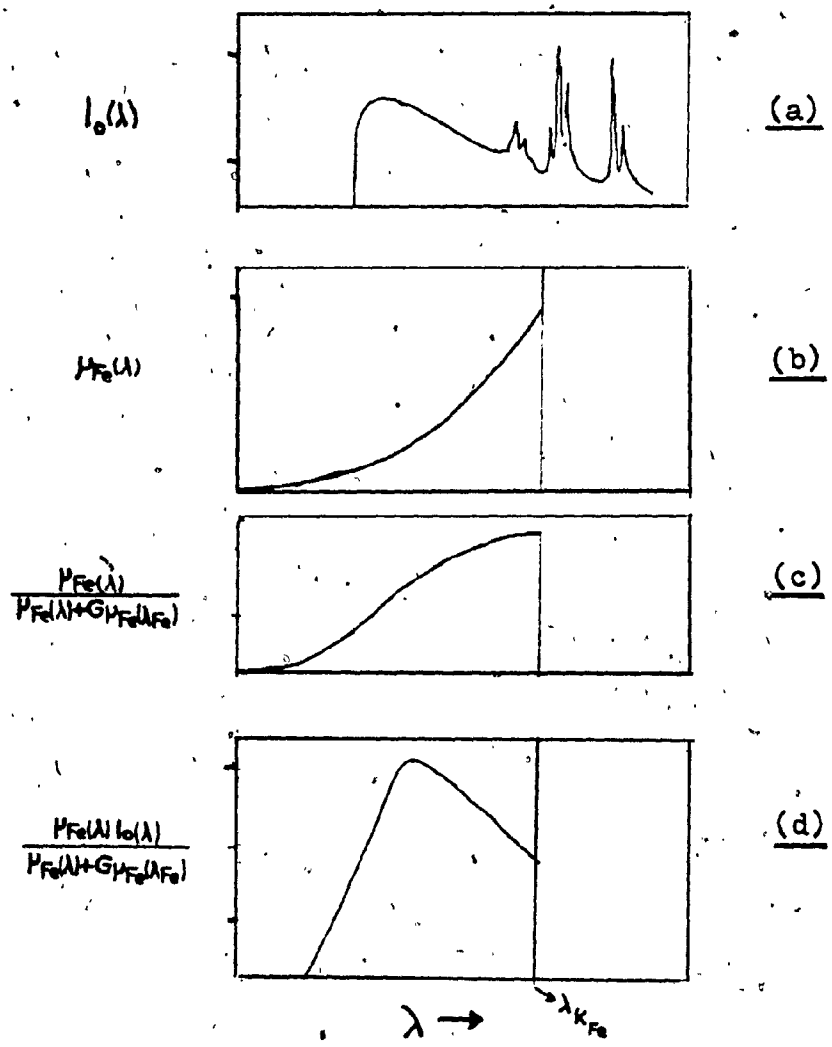

Effectiveness with respect to XRF excitation: (a) Intensity distribution of the incident x-ray spectrum; (b) atomic effectiveness; (c) sample effectiveness; (d) effectiveness of sample and x-ray tube association. (ref. 27,29,55,73)

ent targets due to the different characteristic lines responsible for excitation. Some authors (29,30) have indicated that, in practice, where characteristic tube-target lines are unimportant in the excitation process, (ie. where L or M characteristic lines occur to the short wavelength side of the absorption edge value of the excited element), λ_{eff} should be taken according to the two-thirds rule (31). This value lies between the maximum wavelength of the continuum and a wavelength which is just short of the absorption edge of the analyte. Where K-lines from the tube target element occur to the short wavelength side of the analyte absorption edge, λ_{eff} should be taken as being equal to the Kα-lines of the target element. As previously mentioned in the introduction several other definitions for λ_{eff} can be obtained, thus leading to a variety of coefficients.

2.5.2 The fundamental parameters approach

The second model chosen employs a fundamental parameters approach. This technique is important since coefficients can be obtained through the use of a theoretical method which includes both absorption and enhancement effects, as well as the polychromatic nature of the primary x-ray beam, in the derivation. This allows comparison of coefficients calculated for the same conditions as the experimental

coefficients are evaluated. Various computer programs developed in this study to calculate theoretical intensities are shown in Appendix B. The algorithm employs the equations developed by Fujino and Shiraiwa (6,7) evaluated by the simplified method of Criss and Birks (19). Since only binary systems are used with a matrix of very low atomic number, no tertiary effects should occur. Accordingly, evaluation of only the primary and secondary integrals is performed. These equations have the advantage over Equation 26 of being theoretically sound, and have been used for many years as the most satisfactory model satisfying the full requirements for evaluating theoretical intensities of any multi-component system. The disadvantages, (ie. uncertainty in the parameters used), have been circumvented by a strict analysis and best statistical choice from the most recent literature data available (Appendix C).

Once the intensities have been obtained for a series of binary solutions, the α-coefficients can be calculated in the same manner as the experimental data. Due to the flexibility of the calculation, coefficients can be obtained for different conditions, (ie. different geometries, sample concentrations, etc.), which would otherwise be impossible to evaluate experimentally due to the large number of samples and different instruments required.

Tables 9(a) and 9(b) represent the α_{ij}-coefficients obtained through these simulation studies under similar conditions as the experimental data.

Additionally, the method also provides a means of verifying certain data which cannot be experimentally determined due to either low concentrations or dissolution problems. Various enhancement contributions and other data can be obtained much more easily and faster especially for difficult cases.

2.5.3 Results and Discussion

If λ_{eff} is calculated by the various methods presented, a comparison between these can be shown as in Figure 11 for the elements of higher atomic number utilizing a tungsten tube for excitation. In the diagram, an approximate λ_{eff} value obtained from the experimental coefficients is also shown with the result that only two of the techniques given are most satisfactory for the calculation of coefficients from Equation 26. In most cases the λ_{median} is as good a representation as the two-thirds rule. It has also been found to be especially useful for the case of the light elements using a chromium tube, which gives a good match with the experimental coefficients. However a marked deviation occurs in this particular case if the chromium K-α

TABLE 9(a)

THEORETICAL α_{ij} - COEFFICIENTS*

Elements j	Elements i: Mg	Al	Si	P	Cl	K	Ca	Ti
M	3.18	1.92	0.844	0.22	-0.43^{8}	-0.712	-0.778	-0.804
Mg		6.73	4.03	2.42	0.65	-0.12	-0.31	-0.37
Al	-0.12		5.21	3.23	1.05	0.09^{6}	-0.14	-0.21
Si	0.09	-0.06^{5}		4.80	1.71	0.41	-0.00^{3}	-0.03
P	0.24	0.08^{5}	-0.17		2.33	0.73	0.34	0.19
Cl	0.49	0.37	0.07	-0.07^{4}		1.52	0.95	0.74
K	0.87	0.71	0.35	0.16	-0.13		1.88	1.57
Ca	1.2^{9}	1.7^{4}	0.48	0.22	-0.13^{6}	-0.35		2.10
Ti	2.5^{2}	1.67	0.83	0.33	-0.24	-0.51	-0.56	
Cr	4.8^{8}	3.28	1.81	0.93	-0.05	-0.47	-0.58	-0.57
Mn	5.9^{4}	4.02	2.29	1.24	0.09	-0.41	-0.54	-0.56
Fe	7.6^{7}	5.22	3.06	1.76	0.33	-0.30	-0.46	-0.52
Co	8.7^{2}	6.04	3.62	2.14	0.52	-0.19	-0.38	-0.45
Ni	8.6^{8}	6.12	3.75	2.28	0.63	-0.12	-0.31	-0.40
Cu	9.3^{9}	6.6^{3}	4.10	2.52	0.75	-0.05	-0.26	-0.36
Zn	11.2^{6}	8.0	4.98	3.12	1.04	0.10	-0.14	-0.25
Sn	nd	5.02	3.34^{5}	2.30^{8}	1.03	nd	nd	2.67
Pb	12.83	4.66	3.33^{3}	2.46^{3}	2.07	nd	nd	2.34
Bi	13.29	15.42	7.62	nd	nd	nd	nd	2.50

* coefficients determined with the use of a chromium x-ray tube target.

TABLE 9(b)

THEORETICAL α_{ij} - COEFFICIENTS

Elements j	Elements i: Cr	Mn	Fe	Co	Ni	Cu	Zn	Sn	Pb	Bi
H	-0.841	-0.863	-0.877	-0.897	-0.905	-0.911	-0.923	-0.980	-0.974	-0.973
Mg	-0.47	-0.54	-0.57	-0.64	-0.67	-0.69	-0.73	-0.949[3]	-0.896	-0.903
Al	-0.34	-0.42	-0.48	-0.56	-0.59	-0.61	-0.66	-0.938	-0.87	-0.878
Si	-0.20	-0.31	-0.38	-0.48	-0.52	-0.54	-0.61	-0.923	-0.85	-0.861
P	-0.02[5]	-0.16	-0.24	-0.36	-0.41	-0.45	-0.52	-0.909	-0.82	-0.832
Cl	0.43	0.23	0.11	-0.06[7]	-0.14	-0.19	-0.30	-0.87	-0.74	-0.75
K	1.08	0.79	0.58	0.34	0.24	0.15	-0.00[4]	-0.81[8]	-0.63	-0.66
Ca	1.49	1.14	0.91	0.59	0.47	0.37	0.18	-0.78[1]	-0.56	-0.59
Ti	1.62	1.30	1.11	0.80	0.69	0.61	0.41	-0.73[4]	-0.45	-0.49
Cr		-0.09	1.87	1.42	1.25	1.13	0.85	-0.64[9]	-0.29	-0.34
Mn	-0.11		-0.09[6]	1.69	1.51	1.36	1.05	-0.64[9]	-0.23	-0.28
Fe	-0.59	-0.14		-0.13	1.59	1.48	1.18	-0.56[8]	-0.14	-0.19
Co	-0.56	-0.60	-0.12		-0.08	1.90	1.54	-0.53[7]	-0.014	-0.074
Ni	-0.54	-0.59	-0.59	-0.23		-0.06	1.61	-0.42[6]	0.04[4]	-0.01[4]
Cu	-0.47	-0.58	-0.60	-0.65	-0.27		-0.12	-0.40[3]	0.11	0.04
Zn	-0.44	-0.52	-0.55	-0.63	-0.63	-0.17		-0.34	0.29	0.21
Cd	1.86	1.50[5]	1.28	0.94	0.80	0.69	0.48	nd	nd	nd
Sn	2.11	1.74	1.51	1.14	1.00	0.88	0.65		-0.48	-0.49
Pb	1.96	1.65	1.51	1.17	1.11	1.07	0.88	0.522		-0.40
Bi	1.82	1.79	1.70	nd	1.20	1.16	0.95	0.59[4]	0.01[1]	

* coefficients determined with the use of a tungsten x-ray tube target.

Figure 11

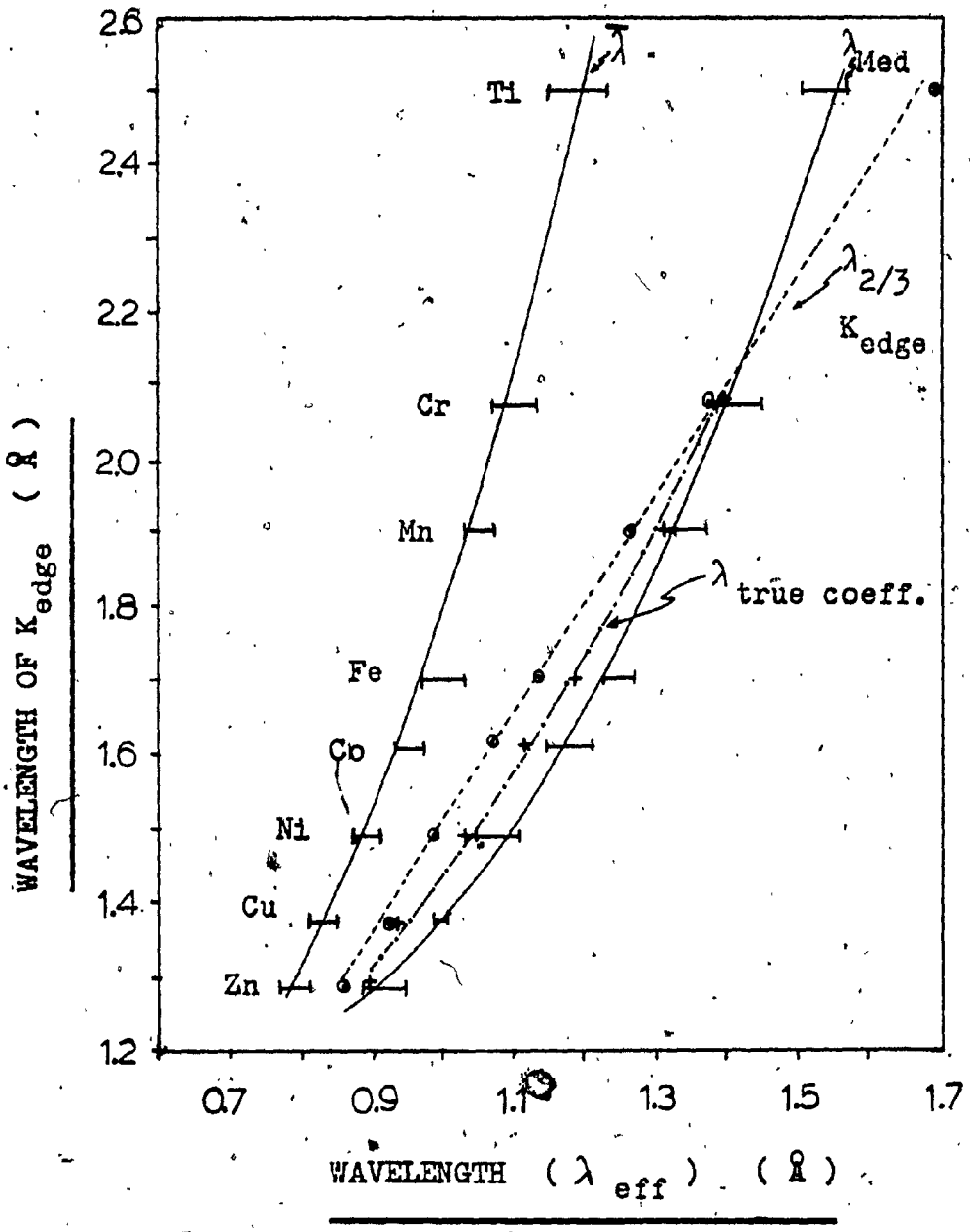

Calculation of λ_{eff} by various methods.

lines of the x-ray tube are used as indicated by the two-thirds rule. This deviation with decreasing atomic number elements, suggests that λ_{eff} can be best shown by λ_{median} which can be calculated from Equation 26 and experimental coefficients.

In view of these results and from the fact that experimental coeffecients do not exist to permit comparison, the use of the two-thirds rule, for simplicity, was used to evaluate Equation 26.

In order to further validate the two-thirds rule, investigation of the contribution of the L characteristic lines of a tungsten tube target in the excitation process for the α-coefficients was conducted. Coefficients were theoretically calculated using the fundamental parameters approach for the effects of various elements on the analytes titanium and iron using two different x-ray tube targets (ie. chromium and tungsten) for the excitation. The results are shown in Figure 12. These clearly indicate that for the analyte element, iron, in which the chromium K-lines from the primary continuum do not play a part in the excitation process of the iron K-lines, that exactly the same results are obtained when using a tungsten tube target which has only L and M characteristic lines in the

Figure 12

Effect of x-ray tube target on α-coefficients

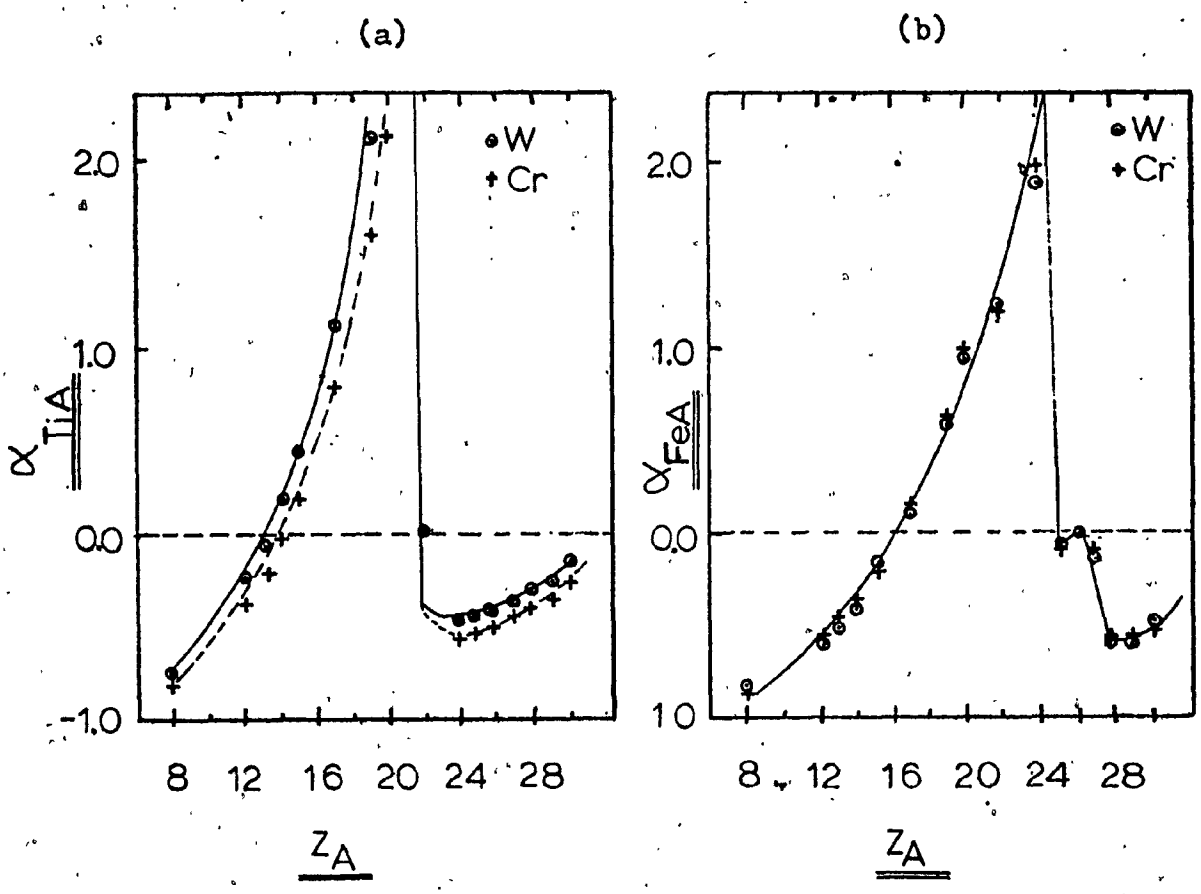

continuum. In contrast, when titanium is used as the analyte a significant difference occurs in the α-coefficients due to the participation of the chromium K-lines in the excitation process. These differences can be explained by the fact that the K-lines from the continuum can also excite the analyte K-lines more effectively than the L or M-lines can. The chromium K-lines constitute approximately 75% of the chromium tube primary continuum while the L and M-lines of the tungsten tube constitute only about 25% of the continuum. However, with decreasing atomic number of the analyte, the contribution from the tube chromium K-lines in the excitation process does seem to fall, since λ_{eff}, if judged on the basis of λ_{median}, shifts to longer wavelengths. This shows an average wavelength between the characteristic tube lines, and the analyte excitation wavelength exists as indicated for the tungsten tube by the two-thirds rule.

Correction coefficients were then calculated using both methods. The results are compared with the experimental coefficients in Figure 13 for the light elements ($Z \leq 22$) using a chromium tube-target and in Figure 14 for the heavier elements ($Z > 22$) using a tungsten tube-target. In all cases, it can be seen that the theoretical coefficients obtained from the fundamental parameters

Figure 13 (a)

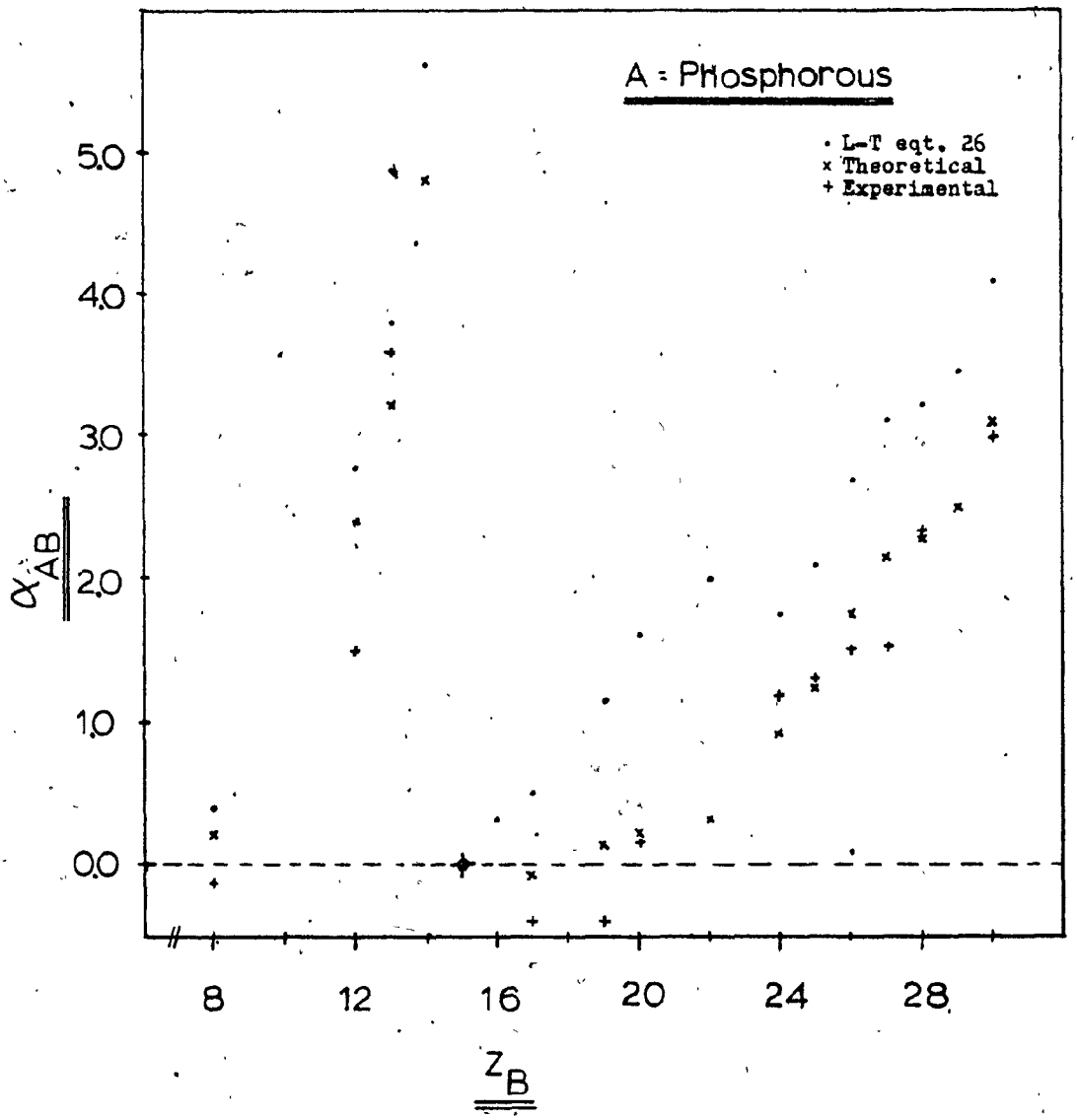

Graphs depicting correlations of α-correction coefficients where the analyte elements A are of atomic number less than 22, versus the atomic number of the interfering element B.

Figure 13 (b)

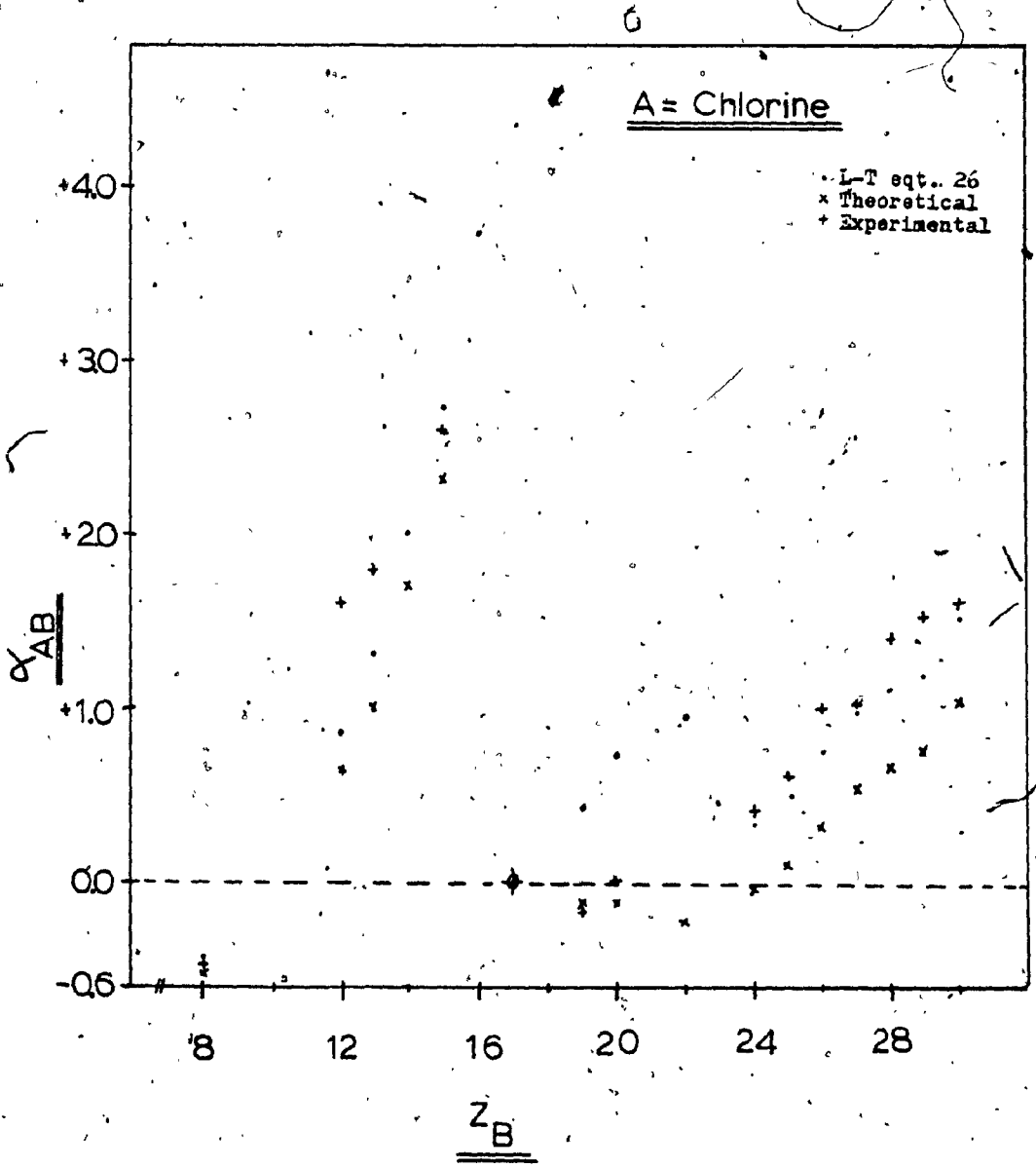
A = Chlorine
L-T eqt. 26
Theoretical
Experimental
+4.0
+3.0
+2.0
+1.0
0.0
-0.6
α_{AB}
8
12
16
20
24
28
Z_B

Figure 13 (c)

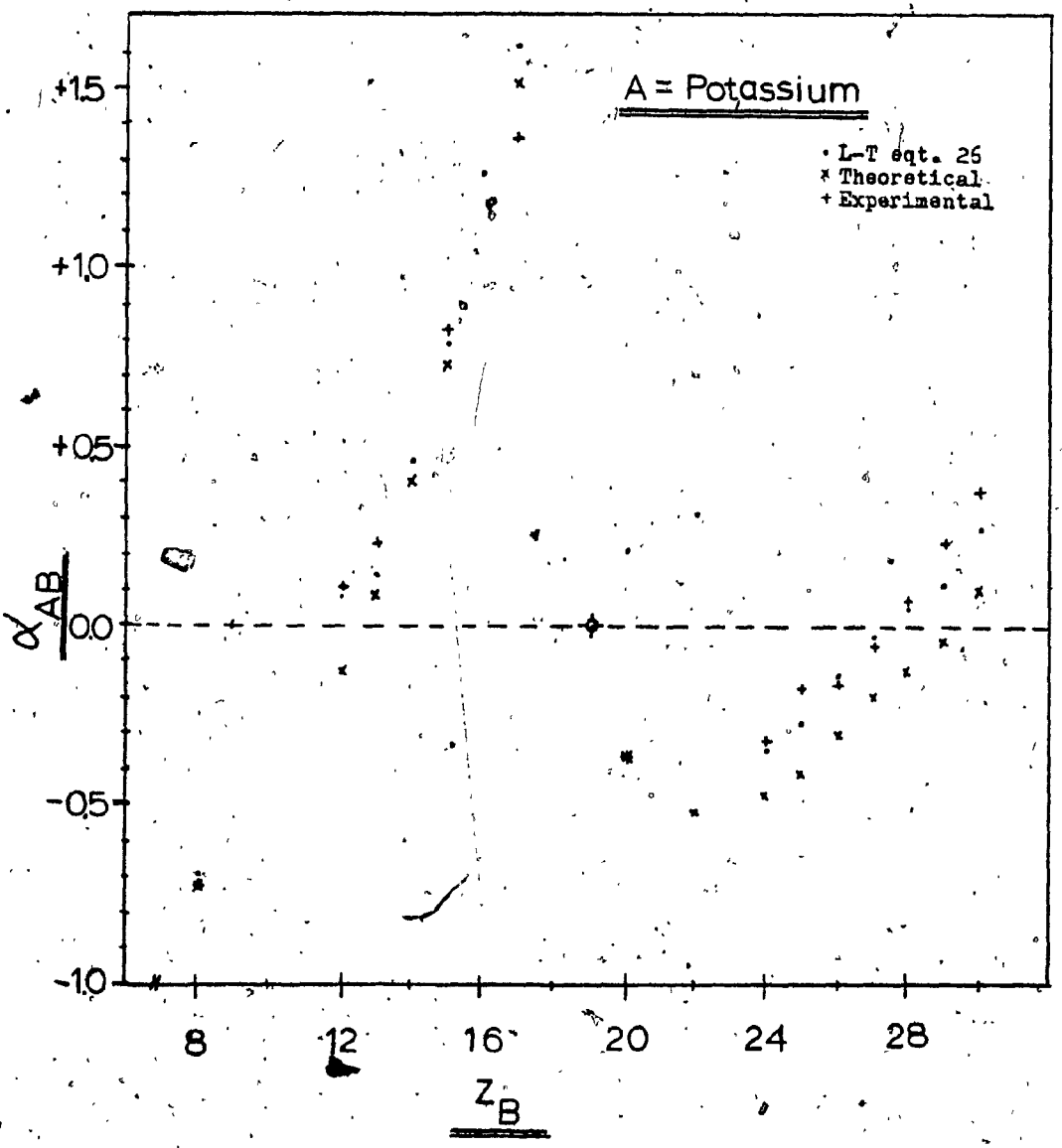
A = Potassium
· L-T eqt. 26
× Theoretical
+ Experimental
+1.5
+1.0
+0.5
0.0
-0.5
-1.0
α_{AB}
8
12
16
20
24
28
Z_B

Figure 13 (d)

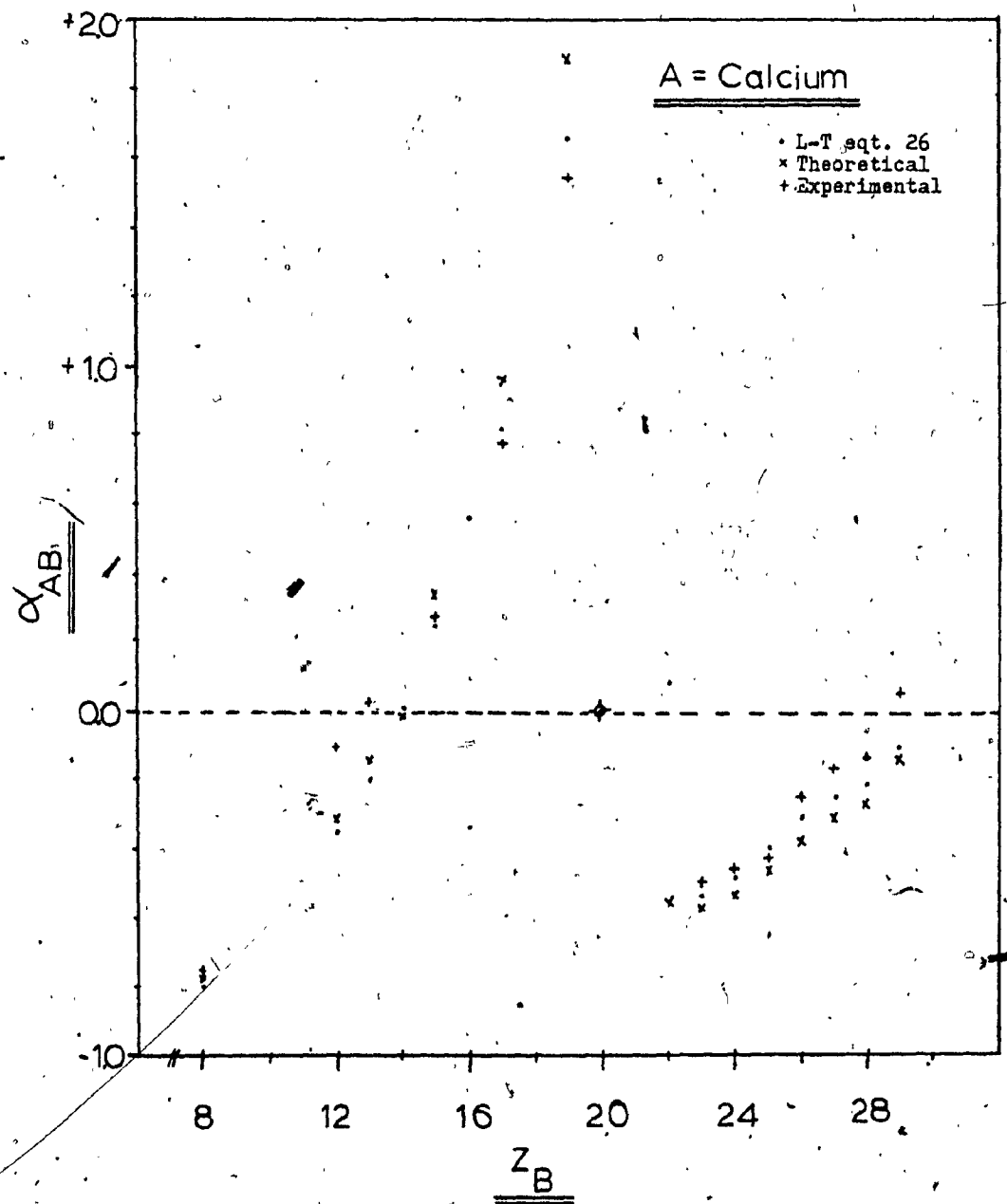
A = Calcium
· L-T eqt. 26
× Theoretical
+ Experimental
+2.0
+1.0
0.0
-1.0
α_{AB}
8
12
16
20
24
28
Z_B

Figure 14 (a)

Graphs depicting correlations of α-correction coefficients where the analyte elements A are of atomic number greater than 22, versus the atomic number of the interfering element B.

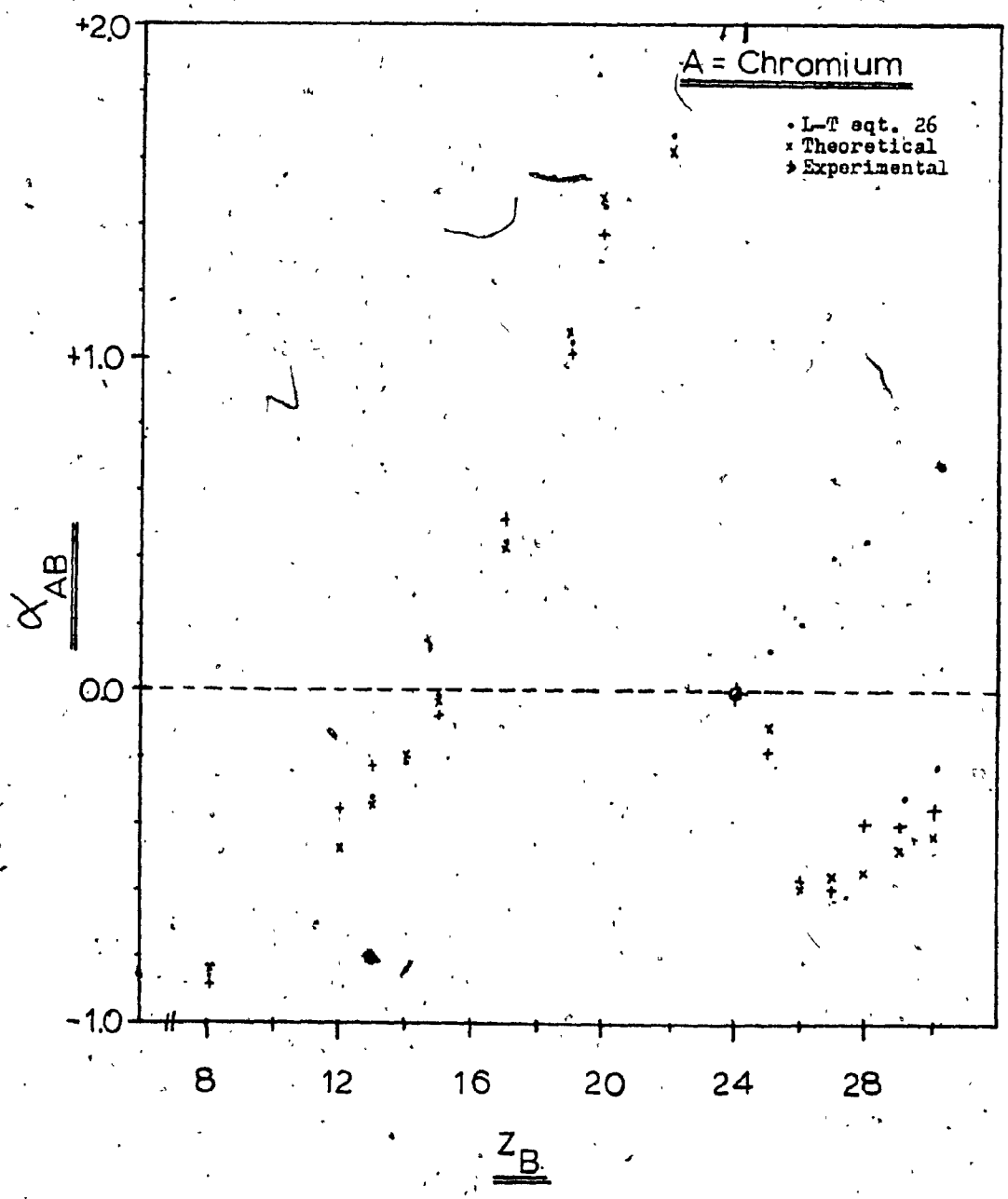

Figure 14 (b)

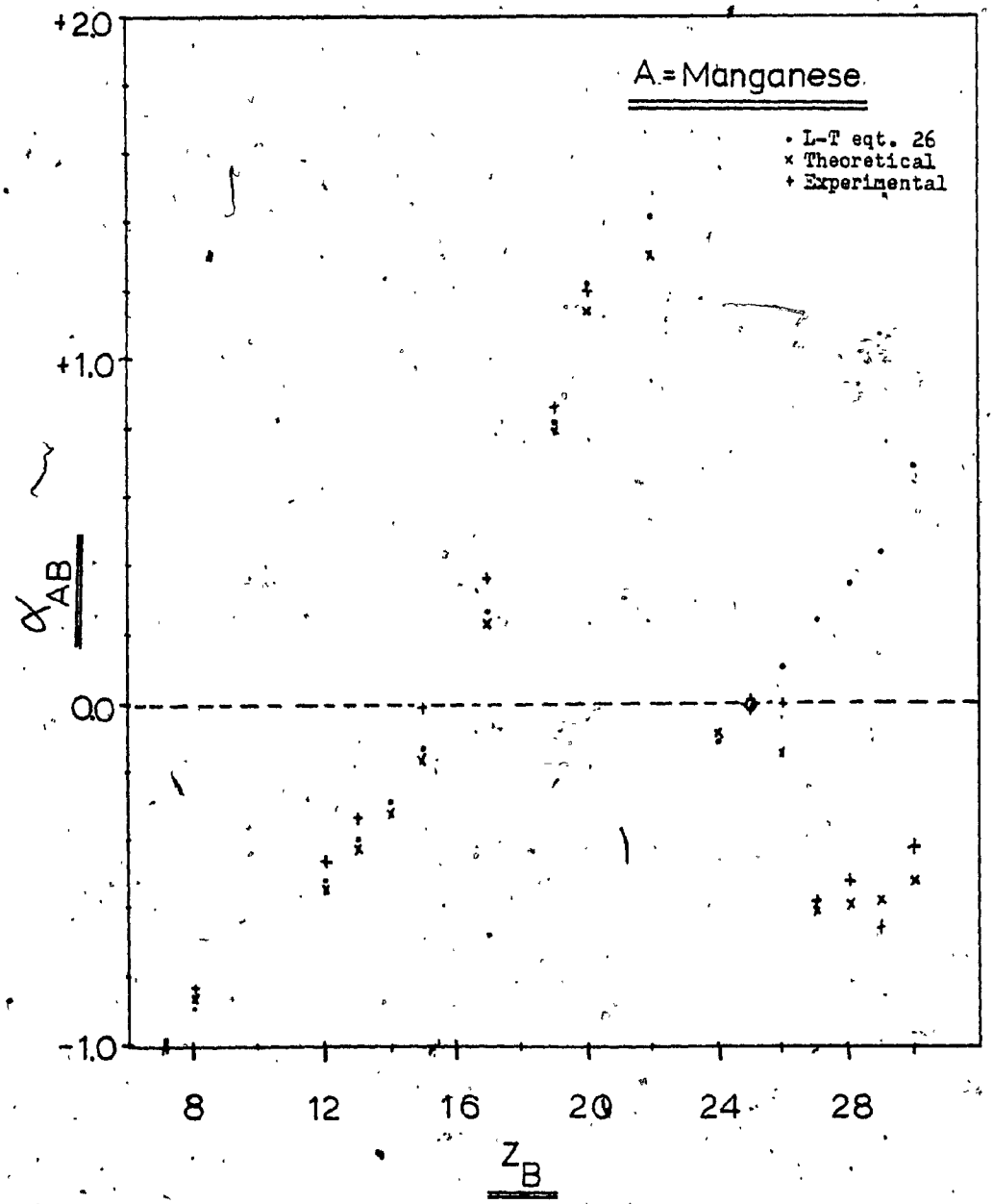
A.=Manganese.
• L-T eqt. 26
× Theoretical
+ Experimental
+2.0
+1.0
0.0
-1.0
α_{AB}
8
12
16
20
24
28
Z_B

Figure 14 (c)

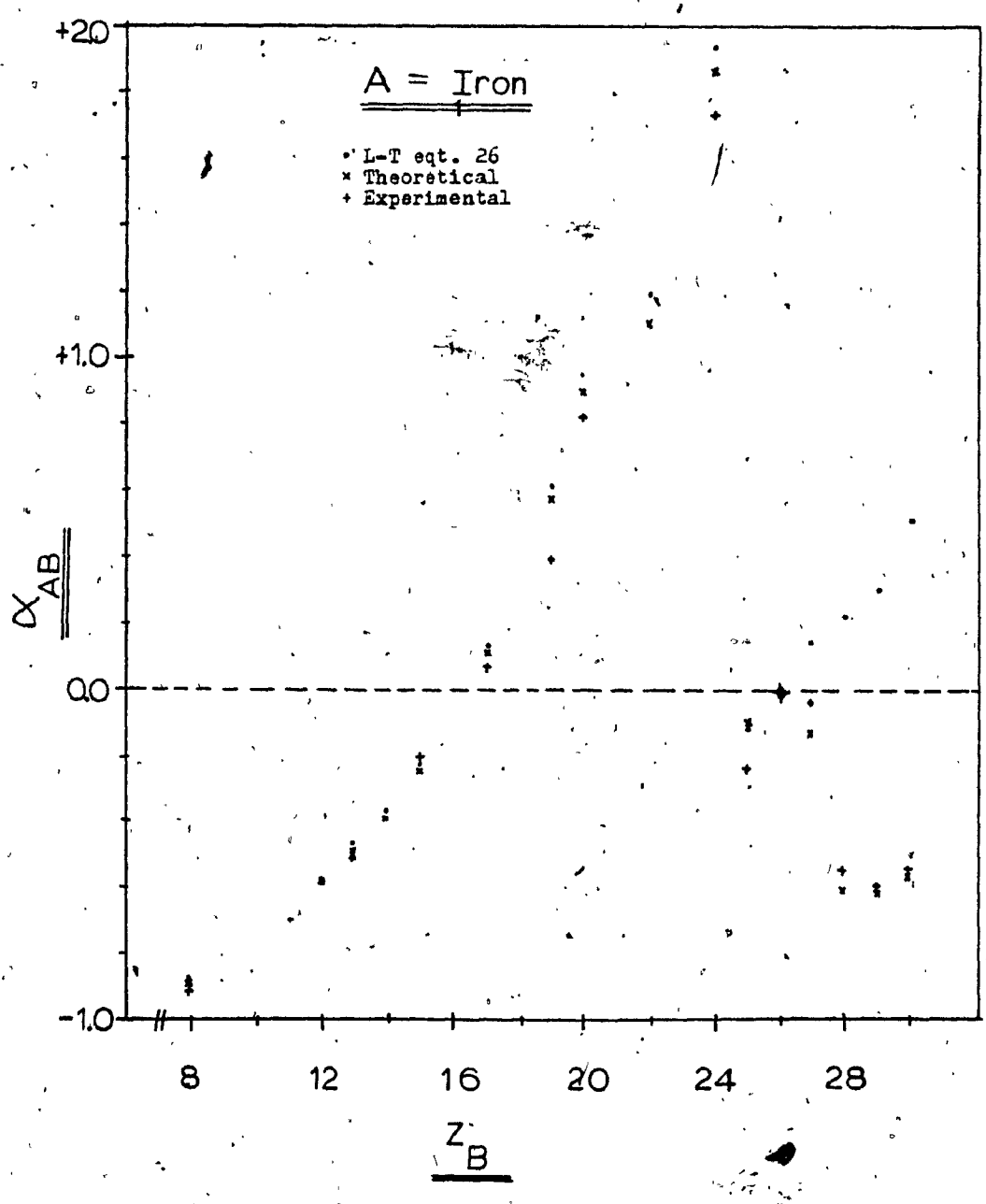
A = Iron
• L-T eqt. 26
× Theoretical
+ Experimental
+2.0
+1.0
0.0
-1.0
α_{AB}
8
12
16
20
24
28
Z_B

Figure 14 (d)

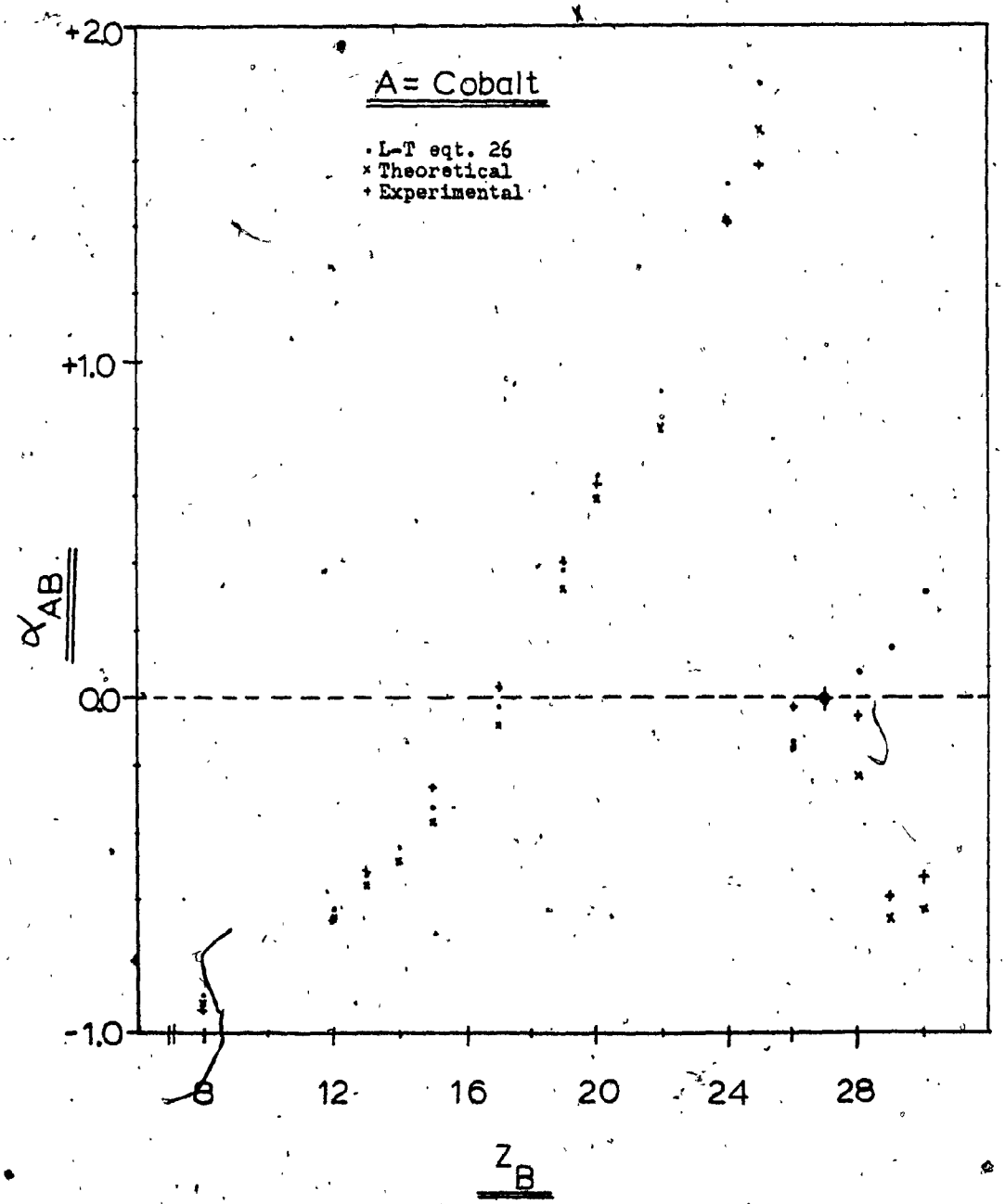
A = Cobalt
· L-T eqt. 26
× Theoretical
+ Experimental
+2.0
+1.0
0.0
-1.0
α_{AB}
8
12
16
20
24
28
Z_B

Figure 14 (e)

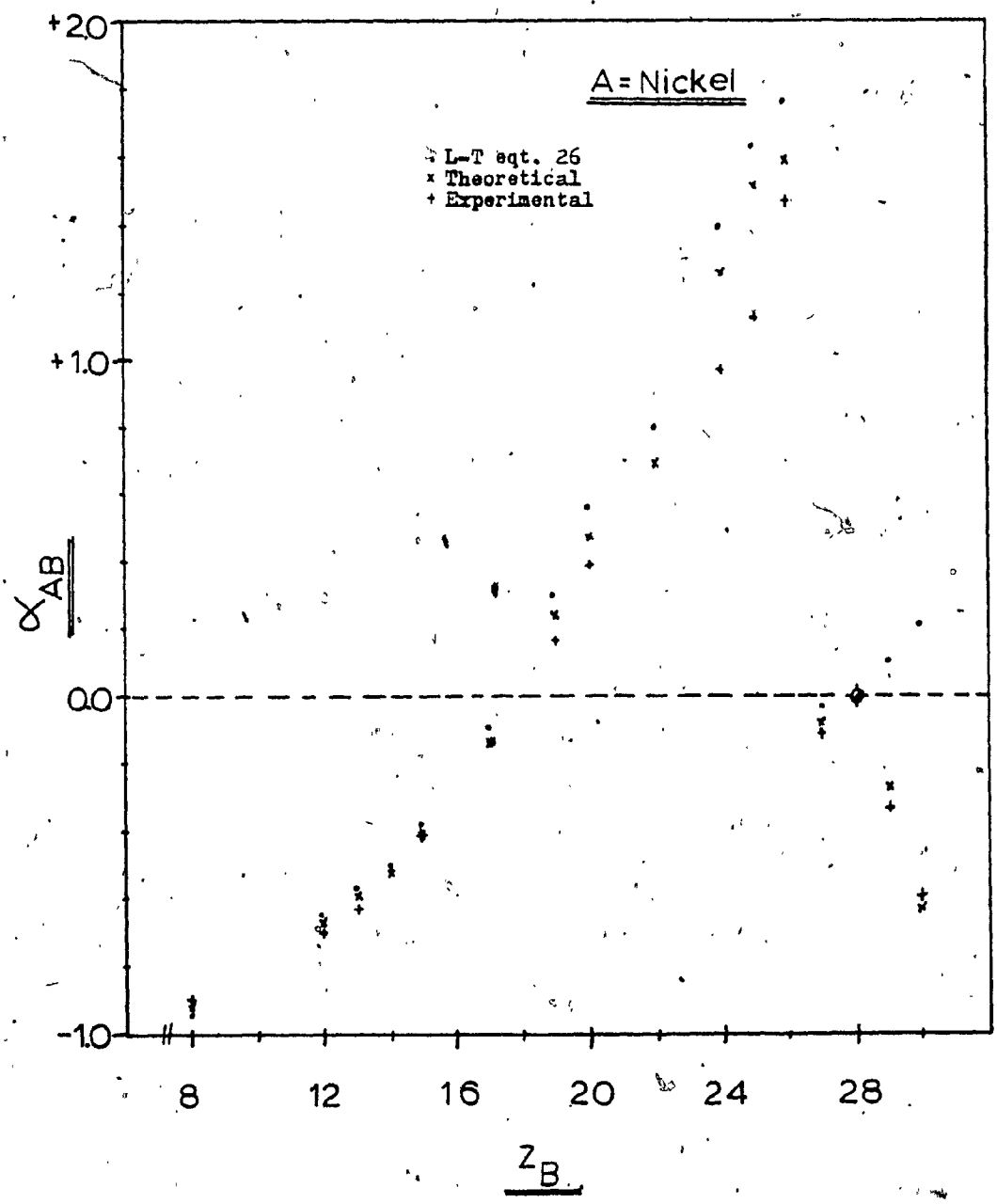
A = Nickel
L-T eqt. 26
Theoretical
Experimental
+2.0
+1.0
0.0
-1.0
α_{AB}
8
12
16
20
24
28
Z_B

Figure 14 (f)

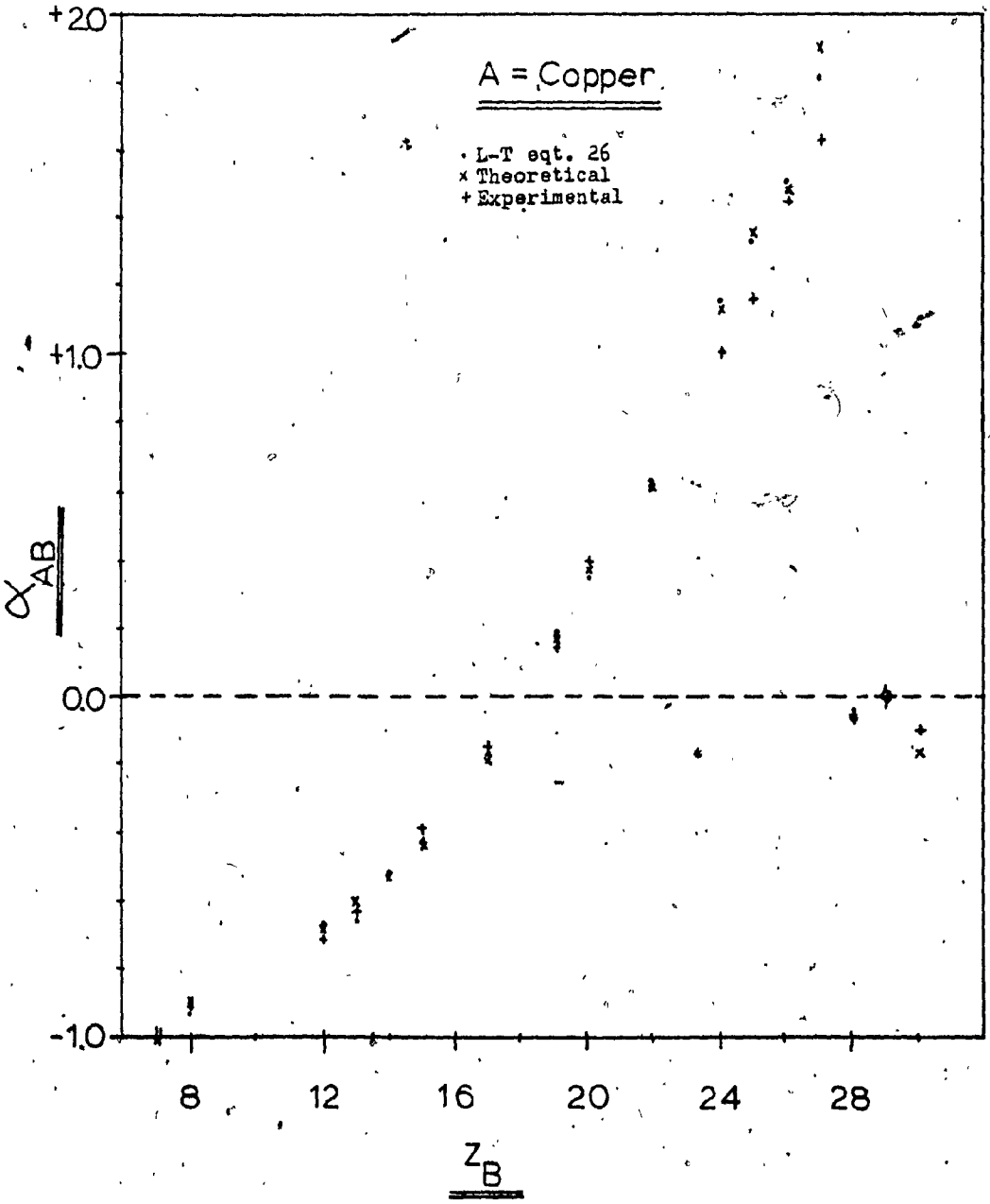
+2.0
+1.0
0.0
-1.0
α_{AB}
A = Copper
· L-T eqt. 26
× Theoretical
+ Experimental
8
12
16
20
24
28
Z_B

Figure 14 (g)

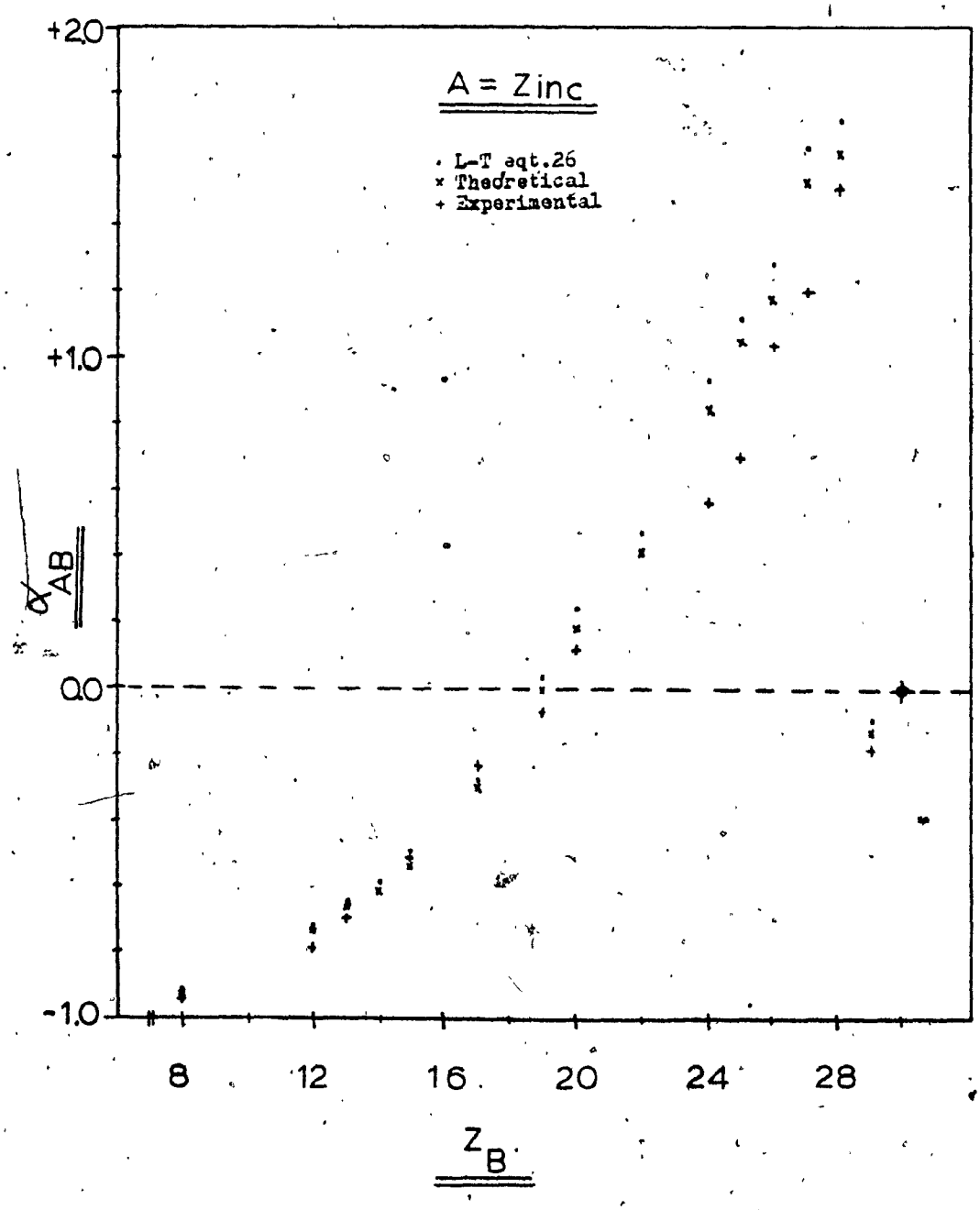
A = Zinc
· L-T eqt.26
× Theoretical
+ Experimental
+2.0
+1.0
0.0
-1.0
α_{AB}
8
12
16
20
24
28
Z_B

method gives better agreement with the experimental coefficients than does Equation 26. This also proves the hypothesis that the experimental coefficients do take into consideration certain features which were not included in their original derivation, mainly the enhancement effects. Equation 26 can be effectively used in cases where absorption is predominant but when enhancement effects occur a marked deviation in coefficients does occur which is very significant for the light elements. This, as well as the fact that λ_{eff} is hard to choose accurately, if it does exist, without extra data, makes it somewhat invalid for use in evaluating experimental data.

In the case of the fundamental parameters method, deviations in the coefficients do occur for the light elements compared to the experimental coefficients when enhancement effects occur. However, this can be attributed partially to the lower intensities obtained in experiments with the lighter elements contributing a higher degree of error.

From these diagrams, certain trends can be observed for the α-coefficients for a particular analyte as the atomic number (Z) of the interfering element is increased.

For both the light and heavy elements, in the case of

"pure" absorption, (ie. before the analyte absorption edge), a steep increase in α occurs up to a particular maximum value. At low Z, these elements constitute a very light absorption of the analyte radiation and have negative coefficients. The α-values then increase to a more neutral absorption effect in the region where $\alpha = 0$, and increase steadily to more positive values for the heavier absorbers until a maximum value is reached. This value occurs at different positions for the light elements (ie. Z_A-1) and for the heavy elements (ie. Z_A-2).

In the case of the light elements, once a maximum positive coefficient is reached, there is then a steep decrease at the analyte Z to a value of 0 for the effects of self-absorption. After this value the main contributions to the system are the enhancement effects. The coefficients then decrease to negative values for the greatest enhancement effect occurring at Z_A+1 and steadily increasing positively as Z increases.

In contrast, for the heavy elements a rapid decrease from the maximum value occurs at the element with Z_A-2 to a slightly negative value showing a nearly neutral absorption effect or equivalent to the analyte self-absorption. This is due to the particular characteristic present in the

elements with $Z > 22$, where the absorption edge of the interfering element Z_A-1 lies between the analyte Kα -line and the analyte K-edge. Accordingly, it can not absorb much of the analyte radiation, being almost equivalent in absorbing power, and thus gives a very slight drop in the coefficient value indicating a nearly neutral absorption. The coefficients then increase to a value of 0 for the effect of self-absorption of the analyte, after which again a distinct feature for the heavy elements occurs. The interfering element Z_A+1 also shows a neutral absorption or one approximately equal to the analyte, since the interfering element has a Kα -line which occurs to the long wavelength side of the analyte absorption edge and the analyte Kα-line. It can, therefore, not excite the analyte K-lines. In this case no enhancement from these Kα -lines can occur. The enhancement contribution which occurs comes from the weaker Kβ lines of the Z_A+1 element, which have a lower enhancing power and, therfore, yield a slightly negative coefficient indicating an almost neutral effect. The greatest degree of enhancement occurs for the element Z_A+2 which gives the most negative coefficient in this region indicating a light to medium absorption. As Z increases from this element, the enhancement contribution decreases and the absorption contribution increases such that the coefficients go to more

positive values ascending to zero. For $\alpha > 0$ the absorption contribution predominates over enhancement to the point that the latter becomes negligible.

These qualitative deductions can further be substantiated by theoretical calculations for several systems which show these particular trends. Table 10 gives some results for the effect of various elements on the analyte element iron at a particular concentration.

In general, it has been found that enhancement effects can contribute as much as 30% in certain cases, which is a very significant amount. As the Z_B increases the enhancement contributions decrease to $< 0.1\%$ at high Z_B and can become negligible at this level.

In summary, the most favourable correlation between experimental and theoretical coefficients shows the reliability of the experimental data obtained. On the other hand, coefficients calculated by the first method are reasonable only in cases of "pure" absorption, deviating significantly when enhancement effects occur. This coupled with the difficulty in the choice of the proper λ_{eff} required for the calculation, makes this method unsatisfactory for quantitative analysis.

Deviations which exist between the experimental and

TABLE 10

SPECIFIC CONTRIBUTIONS FOR THE IRON SYSTEM

(C_{Fe} = 0.5 and C_B = 0.5)

Element B	% Enhancement	% Absorption
Co	2.1	97.9
Ni	17.9	82.1
Cu	17.0	83.0
Zn	16.3	83.7
Br	10.6	89.4
Cd	1.6	98.4
Sn	0.8	99.2

theoretical coefficients when considering the light elements can be accounted for in the lower precision of the experimental data due to the very low intensities obtained in this long wavelength region. One of the advantages of the theoretical technique is that such problems can be overcome by direct calculation of the coefficients from the theoretically calculated intensities. This is especially useful for the determination of coefficients in certain cases, (ie. refractory oxides and low atomic numbered elements), where solutions are very difficult to obtain due to low solubilities.

The trends observed among the correction coefficients can be very useful in determining data for other systems where data has not been evaluated for these elements.

It is, therefore, evident that the theoretical method used should yield optimum results when used to solve model systems quantitatively. The method's flexibility is also shown, in that coefficients for different instrument geometries can easily be calculated without the need of redoing all the experimental work. Tables 11(a) and 11(b) give α-correction coefficients for a $60^{\circ}/30^{\circ}$ instrument, which is in common use nowadays.

TABLE 11(a)

THEORETICAL α_{ij} - COEFFICIENTS *

Elements j	Elements i: Mg	Al	Si	P	Cl	K	Ca	Ti
M	3.67	2.36	1.19	0.488	-0.292	-0.635	-0.719	-0.756
Mg		7.87	4.95	3.15	1.07	0.11	-0.13	-0.22
Al	-0.09^{4}		6.35	4.14	1.57	0.38	0.08^{5}	-0.02^{4}
Si	0.16	-0.03		6.06	2.42	0.78	0.25	0.21
P	0.31	0.13	-0.15		3.20	1.19	0.69	0.48
Cl	0.61	0.43	0.10^{3}	-0.07		2.19	1.47	1.17
K	1.03	0.82	0.40	0.18	-0.13		2.64	2.20
Ca	1.57	1.99	0.62	0.31	-0.10^{4}	-0.33		2.87
Ti	3.09	2.13	1.18	0.59	-0.11	-0.44	-0.52	
Cr	5.69	4.01	2.39	1.38	0.21	-0.33	-0.48	-0.51
Mn	6.90	4.88	2.97	1.77	0.39	-0.25	-0.42	-0.49
Fe	8.[illegible]	6.28	3.89	2.41	0.69	-0.10	-0.31	-0.41
Co	10.05	7.21	4.55	2.87	0.93	0.04	-0.20	-0.33
Ni	9.92	7.28	4.69	3.03	1.07	0.13	-0.12	-0.25
Cu	10.66	7.84	5.09	3.32	1.21	0.21	-0.05	-0.19
Zn	12.74	9.37	6.12	4.05	1.58	0.41	0.10	-0.06
Sn	nd	5.47	3.72	2.61	1.20	nd	nd	3.55
Pb	nd	4.98	3.62	2.71	2.49	nd	nd	3.10
Bi	nd	17.49	8.81	nd	nd	nd	nd	3.30

* coefficients determined with the use of a chromium tube target and 60°/30° geometry.

TABLE 11(b)

THEORETICAL α_{ij} – COEFFICIENTS *

Elements j	Elements i: Cr	Mn	Fe	Co	Ni	Cu	Zn	Sn	Pb	Bi
H	-0.803	-0.830	-0.849	-0.874	-0.844	-0.892	-0.906	-0.935	-0.968	-0.970
Hg	-0.35	-0.43	-0.47	-0.56	-0.59	-0.62	-0.66	-0.94	-0.88	-0.89
Al	-0.19	-0.29	-0.36	-0.46	-0.49	-0.52	-0.58	-0.92	-0.85	-0.86
Si	-0.01	-0.14	-0.23	-0.36	-0.41	-0.45	-0.52	-0.90[5]	-0.83	-0.84
P	0.21	0.04[6]	-0.07	-0.22	-0.28	-0.33	-0.41	-0.86	-0.80	-0.81
Cl	0.77	0.53	0.37	0.14	0.06	-0.01[3]	-0.14	-0.84	-0.70[5]	-0.72
K	1.58	1.22	0.95	0.65	0.51	0.41	0.22	-0.77	-0.59	-0.62
Ca	2.10	1.66	1.36	0.96	0.80	0.67	00.44	-0.73	-0.51	-0.54
Ti	2.23	1.85	1.58	1.20	1.06	0.95	0.72	-0.67	-0.39	-0.42
Cr		-0.09[4]	2.52	1.96	1.76	1.59	1.27	-0.56	-0.21	-0.26
Mn	-0.10		-0.10	2.30	2.07	1.88	1.52	-0.56	-0.13	-0.18
Fe	-0.55	-0.11		-0.13	2.16	2.00	1.66	-0.46	-0.04[5]	-0.096
Co	-0.50	-0.55	-0.093		-0.083	2.52	2.11	-0.42	0.10[1]	0.04
Ni	-0.44	-0.51	-0.54	-0.19		-0.06	2.18	-0.28	0.16	0.10
Cu	-0.41	-0.49	-0.53	-0.60	-0.23		-0.11	-0.25	0.23	0.165
Zn	-0.30	-0.41	-0.46	-0.56	-0.58	-0.13		-0.17	0.44	0.36
Cd	2.53	2.11	1.91	1.38	1.21	1.07	0.83	nd	nd	nd
Sn	2.84	2.39	2.19	1.62	1.44	1.30	1.03		-0.37	-0.41
Pb	2.61	2.24	2.02	1.61	1.51	1.43	1.21	0.90		-0.04
Bi	2.41	2.41	2.27	nd	1.62	1.55	1.30	1.00	0.02	

* coefficients determined with the use of a tungsten tube target and $60^{\circ}/30^{\circ}$ geometry.

3. APPLICATION OF MODIFIED LACHANCE-TRAILL APPROACH TO CHEMICAL ANALYSIS

3.1 Introduction

When considering chemical analyses of multi-component systems in XRF, a significantly more complex situation occurs as compared to the determinations previously evaluated using binary solutions. The physical nature of the specimen must be considered. Solids must have some type of surface finish to limit the grain size and distribution effects. Particle size, surface conditions and heterogeneity effects must all be considered if using solids or powders. In the case of aqueous specimens these effects are nonexistent, and homogeneity is ensured once the sample is dissolved.

In this section a variety of complex systems are analyzed and compared to evaluate the modified Lachance-Traill approach on a practical basis.

3.2 Purposes of the XRF Investigation

Previous works(87-89) have shown the applicability of the aqueous solution method to the analysis of several alloy systems. In this investigation several different problems are dealt with.

Firstly, the determination of the validity of the new experimental α-correction coefficients, as well as the theoretical coefficients, when applied to solid and aqueous specimens, and their ability to yield satisfactory results when applied to complex systems.

Secondly, the establishment of some correlation between experimental and theoretical data systems, with a view to determining the sources of error which arise during analytical applications. This is accomplished by simulating XRF intensities for multi-component systems through the use of a suitable computer program developed for this purpose.

Finally, an attempt is made to develop a method for applying the modified Lachance-Traill system to solid-solution specimens. This is especially important in the analysis of geological materials.

With these purposes in view, the analyses of several systems were carried out on solution as well as on solid specimens. Intensities appear in Appendix D for all systems.

3.3 Examination of Copper Base Alloys

3.3.1 Experimental approach

Two series of copper alloys were individually analyzed

in both solid and aqueous systems. The solids had a surface finish prepared by anodic electrolysis. The aqueous solutions were prepared by using 1.000 gram samples of drillings from each alloy. These were subsequently dissolved and digested in a mixture of HNO_3:HCl. The final dilution was made to 50.00 grams with water. The concentration ranges and standard concentrations are presented in Tables 12 and 13 respectively.

It is important to note that the two series were analyzed on different days and therefore analytical results have been calculated separately. The final results have then been grouped for comparison purposes.

The series were each evaluated by the Lachance-Traill and direct ratio (DR) approaches using a single standard in each case. The analytical results appear in Tables 14 and 15 for solid and aqueous specimens respectively.

In the Lachance-Traill technique the theoretical α-correction coefficients (ie. Table 11) are used in the calculations instead of the experimental coefficients. This is shown to be adequate since no significant difference occur in data results as seen in Table 16.

Table 17 represents the combined absolute percent relative errors obtained in the solid and aqueous solution specimens using both approaches. It can readily be seen

TABLE 12

CONCENTRATION RANGES FOR COPPER ALLOYS*

Element	Solid (%)	Aqueous Solution (%)
Copper	85.4-93.0	1.71-1.86
Tin	4.2-6.6	0.08-0.13
Lead	0.55-6.25	0.011-0.125
Iron	0.01-0.13	0.0002-0.0026
Nickel	0.01-0.40	0.0002-0.0080
Zinc	1.50-4.10	0.03-0.08

*Alloys 2 and 8.

TABLE 13

COMPOSITION OF COPPER BASE ALLOYS*

Alloy	Cu	Sn	Pb	Fe	Ni	Zn.
2-1	89.05	4.22	4.01	0.10	0.22	2.40
2-2	86.94	4.84	3.95	0.11	0.24	3.92
2-3	84.96	6.05	3.96	0.12	0.26	4.65
2-5	84.28	6.00	4.87	0.13	0.27	4.34
2-9	85.97	4.80	6.16	0.12	0.38	2.58
2-10	85.39	4.94	6.25	0.12	0.40	2.86
8-1	93.03	4.83	0.60	0.01	0.01	1.49
8-8	90.19	5.63	1.81	0.02	0.07	2.27
8-13	87.59	6.61	2.78	0.03	0.11	2.88

* Copper base alloys 2 and 8

TABLE 14

RESULTS FOR COPPER ALLOYS 2 AND 8 - SOLID SPECIMEN

	Cu		Sn		Pb		Fe		Ni		Zn	
Alloy	A	B	A	B	A	B	A	B	A	B	A	B
2-1	88.96	*	4.11	*	3.97	*	0.07	*	0.27	*	2.59	*
2-2	86.67	86.09	5.09	5.19	3.87	3.92	0.12	0.13	0.26	0.21	3.99	3.67
2-3	84.99	83.85	6.02	6.10	3.88	3.94	0.12	0.12	0.25	0.20	4.74	4.32
2-5	85.04	83.91	5.91	5.97	4.17	4.25	0.13	0.13	0.25	0.20	4.49	4.08
2-9	85.81	84.68	4.83	4.81	5.86	5.95	0.11	0.11	0.40	0.32	2.98	2.68
2-10	85.38	84.78	4.85	4.80	6.33	6.43	0.11	0.10	0.41	0.32	2.91	2.61
8-1	92.98	*	4.78	*	0.60	*	0.02	*	0.00	*	1.62	*
8-3	89.00	88.30	6.65	6.63	0.59	0.60	0.02	0.02	0.00	0.01	3.73	3.36
8-8	90.45	90.87	5.47	5.40	1.86	1.87	0.02	0.01	0.07	0.24	2.15	1.93
8-13	88.33	88.60	6.31	6.15	2.34	2.36	0.01	0.01	0.13	0.46	2.88	2.55

Column A Results using the Lachance-Traill correction method
Column B Results using the Direct Ratio method (DR)
* Alloy No. used as standard for the Direct Ratio method

TABLE 15

RESULTS FOR COPPER ALLOYS 2 AND 8 - AQUEOUS SOLUTION

	Cu		Sn		Pb		Fe		Ni		Zn	
Alloy	A	B	A	B	A	B	A	B	A	B	A	B
2-1	88.75	*	4.17	*	4.15	*	0.11	*	0.25	*	2.59	*
2-2	86.53	80.86	4.98	4.89	4.11	3.79	0.13	0.11	0.25	0.20	4.00	3.45
2-3	85.04	86.04	5.84	5.88	3.92	3.84	0.13	0.12	0.25	0.22	4.83	4.46
2-5	84.46	88.25	5.94	6.28	4.70	4.86	0.13	0.13	0.24	0.23	4.53	4.33
2-9	85.29	92.26	4.92	5.10	6.37	6.71	0.12	0.12	0.37	0.36	2.95	2.92
2-10	85.09	97.85	4.81	5.21	6.70	7.44	0.11	0.12	0.38	0.39	2.92	3.08
8-1	93.48	*	4.17	*	0.57	*	0.02	*	0.03	*	1.75	*
8-3	89.49	94.67	5.85	7.09	0.60	0.65	0.02	0.01	0.02	0.01	4.03	3.61
8-8	91.02	96.77	4.79	5.76	1.75	1.89	0.02	0.01	0.08	0.03	2.35	2.11
8-13	88.45	92.01	5.65	6.70	2.74	2.95	0.02	0.01	0.13	0.05	3.04	2.64

Column A Results using the Lachance-Traill correction method
Column B Results using the Direct Ratio method (DR)
* Alloy No. used as standard for the Direct Ratio method

TABLE 16

DIFFERENCE BETWEEN $\alpha_{expt.}$ AND $\alpha_{theo.}$ IN THE ANALYSIS OF COPPER ALLOYS

	SOLID					AQUEOUS SOLUTION			
Element	A	B	C	D	E	B	C	D	E
Cu	88.76	88.96	88.97	0.01	0.01	88.75	88.77	0.02	0.02
Sn	4.22	4.11	4.13	0.02	0.48	4.17	4.15	0.02	0.48
Pb	3.89	3.97	3.97	0.00	0.00	4.15	4.13	0.02	0.48
Fe	0.10	0.09	0.09	0.00	1.06	0.11	0.11	0.00	0.00
Ni	0.22	0.27	0.27	0.00	0.00	0.25	0.26	0.01	3.85
Zn	2.81	2.59	2.57	0.02	0.78	2.59	2.60	0.01	0.38

Column A Standard composition of Copper Alloy 2-1'
Column B Composition using theoretical coefficients
Column C Composition using experimental coefficients
Column D Absolute error between Columns B and C
Column E Absolute % Relative Error

TABLE 17

COMPARISON OF RESULTS* - ABSOLUTE % RELATIVE ERROR

Element	Solid		Aqueous Solution	
	A	B	A	B
Copper	0.34	0.87	0.58	6.78
Tin	2.22	3.07	7.02	3.60
Lead	5.15	5.97	4.15	10.66
Iron	9.9	9.80	11.20	2.84
Nickel	9.09	19.66	8.40	12.88
Zinc	5.55	9.59	6.32	8.10

Column A Results by the Lachance-Traill method
Column B Results by the Direct Ratio Method (DR)

* Data for Copper Alloys 2 and 8

TABLE 18

ABSOLUTE % RELATIVE ERRORS FOR COPPER ALLOYS 2 AND 8

	SOLID		AQUEOUS SOLUTION	
Element	A	B	A	B
Copper	0.34	1.45	0.58	1.80
Tin	2.22	2.01	7.02	14.62
Lead	5.14	3.39	4.15	4.63
Iron	9.90	--	11.2	--
Nickel	9.09	--	8.4	--
Zinc	5.55	5.84	6.32	5.57

Column A Results from present work
Column B Results from ref. 87

that no major differences occur in the case of copper alloys of this type where the major species are copper, zinc, tin and lead. Significant differences are evident in the DR method where the solid samples yield a lower relative error in certain cases. In the solid specimens the relative constancy of the general matrix permits the use of the DR method without the introduction of undue inaccuracy. The high relative errors, in some cases, arise out of a few very poor results within the series. Prior rejection of these values would improve the overall accuracy appreciably. This is especially significant for minor elements such as iron and nickel, where the main problem of low concentration arises, and contributes to very low intensities posing extra difficulties for aqueous solution specimens.

Comparison of the results with previous data (87) (Table 18) shows little difference in the Lachance-Traill approach in solid or aqueous solution media.

The relative errors appear to be quite high but the α-correction method does seem to show a slight improvement, especially in the ease of application and simultaneous determination of all elements present.

3.3.2 Theoretical approach

In view of the high relative errors obtained, and also the unavailability of more types of copper alloy standards, a computer program involving a theoretical model simulating XRF intensities obtained from the instrument was developed using Equation 4 (Appendix E). The Lachance-Traill and DR approaches were then applied as previously stated and data results compared.

The first series (Series J) involves the analysis of copper alloy brasses and bronzes similar in composition to alloys 2 and 8 used in the experimental section. Concentration ranges and standard concentrations are shown in Tables 19 and 20 respectively. Analytical results for both solid and aqueous specimens appear in Tables 21 and 22 respectively. Table 23 shows the relative errors for both the Lachance-Traill and DR approaches.

It is evident that the α-correction method does give better accuracy especially in the case of aqueous solutions. However, it must be emphasized that in using the theoretical model a truly homogeneous sample is used with no surface or other physical interferences occurring. Another factor is that the calculated intensities are not subject to the experimental variability which causes significant differences when considering analytes of low concentration. Accordingly, results for minor components show little deviation.

TABLE 19

CONCENTRATION RANGES FOR COPPER ALLOY BRONZES*

Element	Solid (%)	Aqueous Solution (%)
Copper	83.0-93.0	1.60-1.80
Tin	2.5-6.5	0.08-1.20
Lead	0.5-8.0	0.06-0.16
Iron	0.01-0.15	0.00-0.004
Nickel	0.01-0.16	0.00-0.006
Zinc	1.80-4.60	0.06-0.15

*Copper alloys Series J

TABLE 20

COMPOSITION OF COPPER BASE ALLOYS*

Alloy	Cu	Sn	Pb	Fe	Ni	Zn
J-1	88.73	4.22	3.94	0.09	0.22	2.80
J-2	85.32	5.91	3.85	0.11	0.26	4.55
J-3	84.50	5.91	4.87	0.12	0.27	4.33
J-4	83.56	5.92	5.92	0.14	0.20	4.26
J-5	85.52	4.86	5.87	0.13	0.37	3.25
J-6	83.73	5.86	6.22	0.12	0.31	3.76
J-7	81.82	2.71	8.01	0.09	0.16	7.22
J-8	92.76	4.88	0.55	0.01	0.005	1.80
J-9	90.69	5.26	1.72	0.02	0.07	2.25
J-10	87.74	6.50	2.80	0.03	0.11	2.81

* Copper Base Alloys - Series J

TABLE 21

RESULTS FOR COPPER ALLOYS SERIES J - SOLID SPECIMEN

	Cu		Sn		Pb		Fe		Ni		Zn	
Alloy	A	B	A	B	A	B	A	B	A	B	A	B
J-1	88.74	*	4.24	*	3.91	*	0.09	*	0.22	*	2.80	*
J-2	85.26	85.16	5.96	5.96	3.87	3.99	0.11	0.11	0.26	0.25	4.54	4.53
J-3	84.59	84.39	5.82	5.81	4.89	5.11	0.12	0.11	0.27	0.27	4.31	4.31
J-4	83.79	83.46	5.70	5.68	5.94	6.28	0.14	0.13	0.20	0.20	4.23	4.24
J-5	85.75	85.54	4.68	4.65	5.84	6.08	0.13	0.12	0.37	0.36	3.24	3.24
J-6	84.00	83.65	5.61	5.58	6.23	6.61	0.12	0.11	0.30	0.30	3.73	3.74
J-7	82.25	82.10	2.49	2.43	7.81	8.01	0.09	0.09	0.16	0.17	7.21	7.20
J-8	92.26	92.28	5.36	5.36	0.55	0.54	0.01	0.01	0.005	0.005	1.81	1.80
J-9	90.34	90.35	5.60	5.60	1.73	1.72	0.017	0.018	0.068	0.068	2.25	2.25
J-10	87.48	87.38	6.73	6.74	2.84	2.92	0.032	0.031	0.114	0.112	2.81	2.81

Column A Results using the Lachance-Traill correction method
Column B Results using the Direct Ratio method (DR)
* Alloy No. used as standard for the Direct Ratio method

TABLE 22

RESULTS FOR COPPER ALLOYS SERIES J - AQUEOUS SOLUTION

	Cu		Sn		Pb		Fe		Ni		Zn	
Alloy	A	B	A	B	A	B	A	B	A	B	A	B
J-1	88.78	*	4.22	*	3.92	*	0.09	*	0.22	*	2.80	*
J-2	85.32	85.28	5.92	5.91	3.85	3.90	0.11	0.11	0.26	0.26	4.55	4.54
J-3	**	**	**	**	**	**	**	**	**	**	**	**
J-4	83.67	84.13	5.80	5.42	5.93	5.83	0.14	0.14	0.20	0.20	4.26	4.28
J-5	85.63	85.91	4.76	4.54	5.85	5.80	0.13	0.13	0.37	0.37	3.25	3.26
J-6	83.85	84.36	5.72	5.30	6.23	6.11	0.12	0.12	0.31	0.31	3.76	3.79
J-7	**	**	**	**	**	**	**	**	**	**	**	**
J-8	92.62	92.26	5.04	5.38	0.54	0.56	0.01	0.01	0.005	0.005	1.79	1.79
J-9	90.59	90.34	5.37	5.59	1.71	1.76	0.017	0.017	0.067	0.067	2.24	2.23
J-10	87.67	87.30	6.57	6.85	2.80	2.90	0.032	0.031	0.114	0.113	2.81	2.81

Column A Results using the Lachance-Traill correction method
Column B Results using the Direct Ratio method (DR)
* Alloy No. used as standard for the Direct Ratio method
** Data unavailable for sample

TABLE 23

COMPARISON OF RESULTS* - ABSOLUTE % RELATIVE ERROR

Element	Solid		Aqueous Solution	
	A	B	A	B
Copper	0.28	0.25	0.10	0.45
Tin	4.24	5.10	1.62	6.64
Lead	0.76	3.34	0.41	2.01
Iron	0.37	5.31	0.22	1.85
Nickel	0.79	2.16	0.00	0.63
Zinc	0.40	0.31	0.17	0.45

Column A Results by the Lachance-Traill method
Column B Results by the Direct Ratio method (DR)

* Data for Copper Alloys Series J

The DR method does under the same conditions show a lower accuracy and thus gives an indication of the presence of absorption-enhancement effects which seem to be compensated by the Lachance-Traill approach. The usefulness of the theoretical model in these studies is further substantiated by the possibility of calculating the degrees of the absorption and enhancement effects, (ie. Table 24).

Severe enhancement effects are evident for both iron and nickel in solid and aqueous specimens, the latter being significantly lower. The enhancement effects arise basically from the high copper and zinc concentrations and, to a lower degree, from the lead and tin contents. Lead and tin are free from enhancement effects since their absorption edges are well separated from the other analytes.

A second series (Series K) consisting of complex brasses was also investigated. The relevant analytical data and results appear in Tables 25 through 29. Again, the Lachance - Traill approach shows a significant higher accuracy than the DR approach especially in aqueous media. In this case, the major enhancement effects occur for manganese, iron and nickel, and are basically due to copper and zinc. The effects are significantly decreased in aqueous solution.

The DR method does show significant differences over

TABLE 24

THEORETICAL CONTRIBUTIONS FROM ABSORPTION AND ENHANCEMENT EFFECTS IN COPPER ALLOYS - SERIES J

SOLID SPECIMEN

Analyte Element	Absorption (%)	Enhancement (%)	Major Contributors (%)			
			Cu	Zn	Pb	Sn
Fe	67	33	31	1.5	0.3	0.1
Ni	85	15	11	3.0	0.8	0.2
Cu	98	2		0.3	1.4	0.3
Zn	98	2			1.6	0.4
Sn	100					
Pb	100					

AQUEOUS SOLUTION

Analyte Element	Absorption (%)	Enhancement (%)	Major Contributors (%)			
			Cu	Zn	Pb	Sn
Cl	>97	<3	2.1	0.1		0.5
Fe	85	15	14	0.7	0.3	
Ni	94	6	4	1.2	0.7	0.1
Cu	>99	<1		0.1	0.1	0.6
Zn	99	1			0.8	0.2
Sn	100					
Pb	100					

TABLE 25

CONCENTRATION RANGES FOR COPPER ALLOYS*

Element	Solid (%)	Aqueous Solution (%)
Copper	59.0-66.0	0.001-0.050
Tin	0.1-1.5	0.60-0.70
Lead	0.2-2.5	0.002-0.030
Iron	0.06-1.50	0.002-0.020
Nickel	0.02-1.30	0.001-0.025
Zinc	29.0-36.0	1.0-1.3
Manganese	0.1-3.0	0.01-0.06
Aluminum	0.1-2.5	0.004-0.050

*Complex brasses Series K

TABLE 26

COMPOSITION OF COPPER BASE ALLOYS*

Alloy	Mn	Fe	Ni	Zn	Sn	Pb	Al	Cu
K-1	1.50	1.23	0.53	34.92	1.28	0.21	0.63	59.70
K-2	1.90	0.79	0.27	36.02	0.10	0.51	0.41	60.00
K-3	1.98	0.72	0.17	34.82	0.68	0.82	0.21	60.60
K-4	2.90	0.28	0.39	35.56	0.29	1.07	0.11	59.40
K-5	0.94	1.54	0.06	34.15	1.48	0.36	0.82	60.65
K-6	1.45	0.68	1.32	33.84	0.29	0.20	2.52	59.70
K-7	2.58	1.30	0.72	33.20	0.10	0.80	1.50	59.80
K-8	0.20	0.06	0.02	29.39	1.07	1.50	1.86	65.90
K-9	0.10	0.09	0.03	29.99	0.79	1.73	1.27	66.00
K-10	0.50	0.14	0.04	29.36	0.50	2.49	0.87	66.10

* Data for Copper Alloy Complex Brasses - Series K

TABLE 27

RESULTS FOR COPPER ALLOYS SERIES K - SOLID SPECIMEN

	Mn		Fe		Ni		Zn	
Alloy	A	B	A	B	A	B	A	B
K-1	1.50	*	1.23	*	0.53	*	34.92	*
K-2	1.88	1.95	0.78	0.81	0.27	0.28	36.23	36.12
K-3	1.98	1.99	0.72	0.72	0.17	0.17	34.94	35.03
K-4	2.89	2.92	0.28	0.28	0.39	0.39	35.65	35.63
K-5	0.95	0.93	1.55	1.52	0.06	0.06	34.20	34.41
K-6	1.44	1.48	0.67	0.69	1.32	1.34	33.97	33.60
K-7	2.56	2.63	1.29	1.32	0.72	0.72	33.22	33.26
K-8	0.20	0.19	0.06	0.06	0.02	0.02	29.66	29.88
K-9	0.10	0.10	0.09	0.09	0.03	0.03	30.31	30.48
K-10	0.51	0.48	0.14	0.14	0.04	0.04	29.64	29.87

	Sn		Pb		Al		Cu	
Alloy	A	B	A	B	A	B	A	B
K-1	1.28	*	0.21	*	0.63	*	59.70	*
K-2	0.10	0.10	0.50	0.49	0.31	0.31	59.91	59.95
K-3	0.67	0.66	0.81	0.81	0.18	0.18	60.51	60.44
K-4	0.28	0.28	1.06	1.06	0.09	0.09	59.35	59.35
K-5	1.47	1.46	0.36	0.36	0.85	0.85	60.56	60.41
K-6	0.29	0.29	0.20	0.20	2.03	2.01	60.07	60.39
K-7	0.10	0.10	0.79	0.81	1.15	1.17	60.17	59.99
K-8	1.03	0.98	1.50	1.46	1.78	1.74	65.75	65.67
K-9	0.76	0.72	1.72	1.67	1.14	1.11	65.84	65.80
K-10	0.47	0.45	2.47	2.44	0.73	0.73	66.00	65.81

Column A Results using the Lachance-Traill correction method

Column B Results using the Direct Ratio method (DR)

* Alloy No. used as standard for the Direct Ratio method

TABLE 28

RESULTS FOR COPPER ALLOYS SERIES K - AQUEOUS SOLUTION

	Mn		Fe		Ni		Zn	
Alloy	A	B	A	B	A	B	A	B
K-1	1.50	*	1.23	*	0.53	*	34.89	*
K-2	1.90	1.89	0.79	0.78	0.27	0.27	35.99	36.05
K-3	1.97	1.96	0.72	0.71	0.17	0.17	34.80	34.87
K-4	2.90	2.89	0.28	0.28	0.39	0.39	35.55	35.58
K-5	0.94	0.93	1.53	1.53	0.06	0.06	34.12	34.16
K-6	1.44	1.43	0.68	0.66	1.32	1.30	33.80	33.74
K-7	2.57	2.52	1.29	1.27	0.72	0.71	33.20	33.16
K-8	0.20	0.20	0.06	0.06	0.02	0.02	29.39	29.47
K-9	0.10	0.10	0.09	0.09	0.03	0.03	30.00	30.06
K-10	0.50	0.50	0.14	0.14	0.04	0.04	29.40	29.41

	Sn		Pb		Al		Cu	
Alloy	A	B	A	B	A	B	A	B
K-1	1.28	*	0.21	*	0.63	*	59.66	*
K-2	0.10	0.11	0.51	0.51	0.39	0.42	59.97	59.97
K-3	0.65	0.71	0.82	0.84	0.21	0.24	60.60	60.51
K-4	0.28	0.29	1.07	1.07	0.11	0.11	59.39	59.39
K-5	1.44	1.53	0.36	0.37	0.81	0.89	60.65	60.54
K-6	0.27	0.31	0.20	0.21	2.43	2.89	59.70	59.47
K-7	0.09	0.11	0.80	0.84	1.44	1.83	59.85	59.57
K-8	1.06	1.06	1.50	1.50	1.84	1.87	65.93	65.86
K-9	0.77	0.78	1.73	1.73	1.24	1.28	66.03	65.93
K-10	0.48	0.50	2.48	2.53	0.85	0.93	66.17	65.95

Column A Results using the Lachance-Traill correction method

Column B Results using the Direct Ratio method (DR)

* Alloy No. used as standard for the Direct Ratio method

TABLE 29

COMPARISON OF RESULTS* - ABSOLUTE % RELATIVE ERROR

Element	Solid		Aqueous Solution	
	A	B	A	B
Copper	0.24	0.38	0.04	0.17
Tin	2.11	3.89	3.49	5.10
Lead	0.67	1.72	0.04	1.87
Iron	0.75	0.76	0.14	0.95
Nickel	0.00	0.58	0.17	0.32
Zinc	0.47	0.86	0.06	0.16
Manganese	0.59	1.99	0.26	0.78
Aluminum	13.6	14.8	1.94	7.80

Column A Results by the Lachance-Traill method
Column B Results by the Direct Ratio method (DR)

* Data for Copper Alloys Series K

over the previous system. In the case of aluminum high errors do occur in solid specimens even for the Lachance-Traill approach but these are adequately compensated for in dilute solution. As shown in Table 30, the degree of enhancement is subject to high variability in solid specimens over a range of 7 to 32 percent, appearing to affect the compensation powers of the Lachance-Traill approach. However, in aqueous media, where the range is decreased to 4 to 7 percent, significantly lower effects are observed and better compensation results. The major effects arise from the tin L-lines in both cases. It can also be noted that the acid (HCl) concentration does show some effect due to enhancement of the analyte by the chloride content to approximately 4 percent. Absorption and enhancement contributions for the other elements present are given in Table 31.

Comparison of Tables 23 and 29 for the Lachance-Traill approach does not show any differences in relative errors even though samples of different composition and contents are used. The results also show that under conditions of true homogeneity as well as significant intensities (ie. high peak to background) for the minor elements, the Lachance-Traill approach is capable of less than 2 percent relative error in all cases for copper alloys (Table 32).

TABLE 30

THEORETICAL CONTRIBUTIONS FROM ABSORPTION AND ENHANCEMENT EFFECTS IN COPPER ALLOYS - SERIES K (DATA FOR ALUMINUM)

SOLID SPECIMEN

Alloy	Absorption (%)	Enhancement (%)	Major Contributors (%)			
			Cu	Zn	Mn	Sn
K-1	70.5	29.5	2.1	1.3	0.1	25.9
K-2	92.4	7.6	2.8	1.8	0.2	2.7
K-3	80.4	19.6	2.4	1.5	0.2	15.5
K-4	88.2	11.8	2.6	1.7	0.3	7.2
K-5	67.9	32.1	2.0	1.3	0.1	28.6
K-6	87.9	12.1	2.7	1.6	0.2	7.5
K-7	92.6	7.4	2.7	1.6	0.3	2.7
K-8	74.0	26.0	2.5	1.2	0.02	22.2
K-9	78.7	21.3	2.7	1.4	0.01	17.3
K-10	84.3	15.7	2.8	1.4	0.05	11.5

AQUEOUS SOLUTION

Alloy	Absorption (%)	Enhancement (%)	Major Contributors (%)			
			Cu	Zn	Sn	Cl*
K-1	93.4	6.6	0.3	0.2	3.5	2.5
K-2	96.1	3.9	0.3	0.2	0.3	3.1
K-3	94.2	5.8	0.3	0.2	1.7	3.6
K-4	95.8	4.2	0.3	0.2	0.8	2.9
K-5	92.6	7.4	0.3	0.2	3.8	3.1
K-6	95.0	5.0	0.3	0.2	0.7	3.8
K-7	95.0	5.0	0.3	0.2	0.2	4.3
K-8	94.0	6.0	0.3	0.2	2.9	2.6
K-9	95.0	5.0	0.3	0.2	2.1	2.7
K-10	95.0	5.0	0.3	0.2	1.3	3.2

* Hydrochloric acid concentrations of 0.2 to 4.0 percent

TABLE 31

THEORETICAL CONTRIBUTIONS FROM ABSORPTION AND ENHANCEMENT EFFECTS IN COPPER ALLOYS - SERIES K

SOLID SPECIMEN

Analyte Element	Absorption (%)	Enhancement (%)	Major Contributors (%)	
			Cu	Zn
Mn	67	33	21	11
Fe	64	36	24	12
Ni	71	29	7	22
Cu	98	<2		2
Zn	>99	<1		
Sn	100			
Pb	100			

AQUEOUS SOLUTION

Analyte Element	Absorption (%)	Enhancement (%)	Major Contributors (%)	
			Cu	Zn
Mn	95	5	3	2
Fe	94	6	4	2
Ni	96	4	1	3
Cu	99.6	0.4		0.4
Zn	>99.96	<0.04		
Sn	100			
Pb	100			

TABLE 32

ABSOLUTE % RELATIVE ERRORS ACCUMULATED FOR COPPER ALLOYS

	SOLID		AQUEOUS SOLUTION	
Element	A	B	A	B
Copper	0.28	0.24	0.10	0.04
Tin	4.24	2.11	1.62	3.49
Lead	0.76	0.67	0.41	0.04
Iron	0.37	0.75	0.22	0.14
Nickel	0.79	0.00	0.00	0.17
Zinc	0.40	0.47	0.17	0.06
Aluminum	--	13.6	--	1.94
Manganese	--	0.59	--	0.26

Column A Results for simple copper alloys
Column B Results for complex copper alloys

3.4 Examination of Geological Specimens

3.4.1 Introduction

When considering alloy specimens, homogeneity is easily obtained, since most of the analytes are in the elemental form in a relatively constant matrix,(ie. copper in copper alloys). Also, very few elements are present in significant concentrations and consist usually of atomic numbers greater than 24.

The systems involving materials of geological origin pose an entirely different problem. The presence of mixed oxide systems of unknown distributions and differing particle sizes give rise to problems of nonhomogeneity. As a result a raw pressed specimen (even of very low particle size) should yield significantly different results than a truly homogeneous sample. The question of how to obtain a homogeneous sample can be considered to contribute another problem. Since it has been shown that an aqueous solution technique can be applied in alloy systems, it would be reasonable to adopt this method to a powdered specimen. However, most rocks and minerals do not dissolve readily or to a high degree in acid solutions. Accordingly, the method is quite inadequate if a significant amount of material is required in order to obtain high intensities.

One technique generally used in emission spectroscopy and XRF is fusion with a flux of low atomic number elements, (ie. Li, B, O and N). This alternative will yield what is commonly referred to as a solid-solution, (ie. a glass); where most mineral structures have been decomposed. Use of lithium tetraborate provides a clear glass when fused at 1200 ^{o}C with most samples. The glass can be poured while hot into a mold and flattened for direct XRF analysis. The technique if properly applied will be free of surface effects. However, it is tedious and sometimes quite hard to obtain a specimen which is free of imperfections throughout, (ie. air bubbles, warped surface due to crucible, etc.). Also, some glasses are hygroscopic and surface changes can be noted. These can be circumvented by crushing the homogeneous glass to a fine powder in a ball mill and pressing the powder into a disc for XRF analysis. Use of boric acid as a backing material for the disc provides a very stable support. The use of platinum crucibles is suggested. However, due to the high cost, and if many samples are to be prepared, graphite crucibles are suitable especially in yielding a glass button of proper shape for crushing in a ball mill. Contamination with a little carbon powder is evident but poses no difficulties since carbon is of very low atomic number. A much more severe problem occurs due to

the presence of some analytes with atomic number lower than 24 which give very low intensities, especially magnesium and aluminum.

When considering geological materials, an additional determination is required for loss on ignition during fusion. This is due to water content, as well as loss of other volatiles and structural decompositions which occur on high temperature heating. This can be obtained by weighing a dried specimen, fusing with a flux and determining the weight of the glass after fusion.

3.4.2 Analysis of Allard Lake standards

These standards were obtained from the Quebec Iron and Titanium Corporation in Quebec. The concentration ranges and standard concentrations are given in Tables 33 and 34 respectively. It is readily evident that problems in analysis will result due to the large concentration spans involved. Typical data results appear in Tables 35 to 37. In the case of fused specimens, the magnesium content was not determined due to the very low intensities. Table 37 does show the Lachance-Traill approach to give higher accuracy in fused specimens but still at a greater than 4 percent value. However, due to the complexity of the sys-

TABLE 33

CONCENTRATION RANGES FOR ALLARD LAKE STANDARDS*

Element	Solid (%)	Fused (%)
Magnesium	1.4-2.3	0.14-0.23
Aluminum	0.7-12.0	0.07-1.20
Silicon	0.7-22.5	0.07-2.25
Calcium	0.3-5.6	0.03-0.56
Titanium	2.0-22.0	0.20-2.20
Chromium	0.0-0.07	0.00-0.007
Manganese	0.0-1.3	0.00-0.13
Iron	4.9-41.8	0.49-4.20

*Series ALS and TALS

TABLE 34

COMPOSITION OF ALLARD LAKE STANDARDS*

Ore No.	Ti	Fe	Al	Si	Ca	Mg	Mn	Cr
ALS-2	14.09	27.9	5.27	8.50	2.16	2.32	0.09	0.06
ALS-4	19.48	37.6	2.22	3.15	0.81	2.01	0.12	0.07
ALS-5	16.25	32.0	3.92	5.88	1.48	2.33	0.11	0.06
ALS-6	8.51	17.8	9.65	14.77	3.51	1.95	0.06	0.03
ALS-7	11.63	23.9	6.64	11.19	2.74	2.09	0.08	0.04
ALS-8	2.34	6.8	11.86	21.43	5.25	1.67	0.03	0.01
ALS-10	6.65	13.9	10.14	17.42	4.35	1.39	0.05	0.02
ALS-11	21.64	41.8	0.67	0.65	0.25	1.97	0.13	0.08
ALS-12	2.04	4.9	12.44	22.51	5.58	1.42	0.03	0.00

* Data for Series ALS and TALS

TABLE 35

RESULTS FOR THE ALLARD LAKE STANDARDS - SOLID SPECIMEN**

	Ti		Fe		Al		Si	
Ore No.	A	B	A	B	A	B	A	B
ALS-2	14.02	*	28.85	*	7.05	*	8.78	*
ALS-4	23.41	21.14	50.97	34.40	6.59	3.99	4.13	3.34
ALS-5	15.62	16.82	32.36	30.39	3.04	2.13	6.39	6.33
ALS-6	8.22	8.79	15.55	20.3	8.82	7.77	11.60	12.41
ALS-7	11.11	11.56	20.86	23.57	8.16	6.71	10.36	10.63
ALS-8	1.87	2.04	4.96	9.30	10.63	11.05	14.94	17.44
ALS-10	6.23	6.55	11.50	16.50	9.76	9.20	13.31	14.70
ALS-11	23.78	23.77	55.40	37.50	1.32	0.74	0.97	0.80
ALS-12	1.86	2.01	4.45	8.35	10.80	11.37	15.42	18.07

	Ca		Mg		Mn	
Ore No.	A	B	A	B	A	B
ALS-2	2.36	*	2.26	*	0.093	*
ALS-4	1.02	0.85	3.19	2.66	0.161	0.115
ALS-5	1.64	1.62	2.63	2.51	0.110	0.102
ALS-6	3.07	2.93	1.54	1.85	0.053	0.069
ALS-7	2.72	2.55	1.82	2.05	0.070	0.079
ALS-8	4.33	4.16	0.93	1.30	0.023	0.041
ALS-10	3.74	3.53	1.15	1.47	0.043	0.061
ALS-11	0.20	0.19	3.81	2.94	0.170	0.119
ALS-12	4.41	4.20	0.86	1.22	0.027	0.048

Column A Results using the Lachance-Traill correction method
Column B Results using the Direct Ratio method (DR)
* Ore No. used as standard for the Direct Ratio method
** Data for Allard Lake Standards - Series ALS

TABLE 36

RESULTS FOR ALLARD LAKE STANDARDS - FUSED SPECIMEN**

	Ti		Fe		Al		Si		Ca		Mn	
Rock No.	A	B	A	B	A	B	A	B	A	B	A	B
ALS-2	13.54	*	27.20	*	5.21	*	8.62	*	2.23	*	0.09	*
ALS-4	18.17	19.50	35.65	33.87	2.24	2.21	3.11	3.04	0.81	0.81	0.11	0.11
ALS-5	18.91	15.36	37.48	28.88	4.04	3.66	6.32	5.38	9.65	8.20	0.12	0.09
ALS-6	8.97	8.76	18.22	19.77	8.10	8.06	14.22	13.58	3.42	3.10	0.06	0.07
ALS-7	12.05	10.30	23.95	21.50	6.58	5.51	11.26	9.14	2.83	2.24	0.08	0.07
ALS-8	2.32	1.83	6.67	6.97	11.84	9.93	21.87	17.33	5.41	3.95	0.03	0.03
ALS-10	7.08	6.01	14.61	14.65	9.39	8.26	17.20	14.45	4.30	3.39	0.05	0.05
ALS-11	19.32	22.42	38.93	38.11	1.07	1.11	0.77	0.80	0.17	0.18	0.12	0.12
ALS-12	2.14	1.94	5.69	6.86	12.08	12.01	22.47	20.94	5.52	4.66	0.03	0.04

Column A Results using the Lachance-Traill correction method
Column B Results using the Direct Ratio method (DR)
* Rock No. used as standard for DR method ** Data for Series ALS

TABLE 37

COMPARISON OF RESULTS* - ABSOLUTE % RELATIVE ERROR

Element	Solid		Fused	
	A	B	A	B
Magnesium	33.7	17.3	---	---
Aluminum	26.5	22.6	4.04	10.8
Silicon	22.9	14.0	4.09	13.08
Calcium	14.6	15.8	2.12	17.33
Titanium	8.6	5.19	6.56	7.48
Manganese	13.8	20.1	5.47	10.08
Iron	16.9	20.7	6.38	8.21

Column A Results by the Lachance-Traill method
Column B Results by the Direct Ratio method (DR)

* Data for Allard Lake Standards - Series ALS

tem and the simultaneous determination of seven elements, this appears reasonable and acceptable. Wet chemical analysis of such specimens is quite time consuming and tedious with various precipitations and separations.

To investigate this system further, in hope of finding some idea of the causes of error, a theoretical system (Series TALS) was analyzed and pertinent data are given in Tables 38 through 40. The theoretical data, it must be stressed, used a truly homogeneous specimen where no structural differences occur in the specimen (ie. oxides, etc.). The data shows that the solid results for the Lachance-Traill approach are significantly improved over the experimental data. This shows that even though the powdered specimens are of small particle size, the different distributions affect the intensities significantly. However, the DR technique does not show any improvement when considering fused specimens. The Lachance-Traill approach does effectively compensate for the absorption-enhancement effects present. Such elements as chromium, titanium, calcium, silicon, aluminum and magnesium in solids are affected significantly with a range of 2 to 20 percent enhancement mainly due to iron and titanium as shown in Table 41. In fused specimens less than 10 percent enhancement is evident. Graphical data of intensities versus concentration shows

TABLE 38

RESULTS FOR THE ALLARD LAKE STANDARDS - SOLID SPECIMEN**

	Ti		Fe		Al		Si	
Ore No.	A	B	A	B	A	B	A	B
TALS-2	13.86	*	27.51	*	5.20	*	8.38	*
TALS-4	18.16	20.01	35.63	32.16	2.15	1.95	3.02	2.97
TALS-5	15.65	16.63	31.10	30.09	3.84	3.69	5.74	5.73
TALS-6	8.72	8.15	18.00	21.45	9.69	11.51	14.93	15.65
TALS-7	11.66	11.47	23.85	25.81	6.61	7.10	11.14	11.53
TALS-8	2.47	2.15	7.01	10.76	12.17	17.61	22.18	25.32
TALS-10	6.89	6.21	14.14	18.00	10.23	13.07	17.71	19.36
TALS-11	19.58	22.61	38.70	33.81	0.64	0.56	0.61	0.60
TALS-12	2.15	1.84	5.06	7.93	12.78	19.34	23.35	27.06

	Ca		Mg		Mn		Cr	
Ore No.	A	B	A	B	A	B	A	B
TALS-2	2.14	*	2.30	*	0.090	*	0.063	*
TALS-4	0.78	0.85	1.96	1.75	0.120	0.107	0.064	0.061
TALS-5	1.45	1.52	2.29	2.19	0.100	0.102	0.059	0.059
TALS-6	3.57	3.27	1.95	2.34	0.060	0.072	0.027	0.030
TALS-7	2.75	2.67	2.08	2.24	0.080	0.082	0.041	0.043
TALS-8	5.45	4.66	1.69	2.52	0.030	0.045	0.007	0.009
TALS-10	4.45	3.98	1.39	1.79	0.050	0.057	0.026	0.023
TALS-11	0.23	0.27	1.90	1.62	0.120	0.108	0.075	0.072
TALS-12	5.79	4.88	1.44	2.24	0.030	0.047	0.00	0.00

Column A Results using the Lachance-Traill correction method
Column B Results using the Direct Ratio method (DR)
* Ore No. used as standard for the Direct Ratio method
** Data for Allard Lake Standards - Series TALS

TABLE 39

RESULTS FOR THE ALLARD LAKE STANDARDS - FUSED SAMPLES**

	Ti		Fe		Al		Si	
Ore No.	A	B	A	B	A	B	A	B
TALS-2	14.13	*	27.82	*	5.25	*	8.50	*
TALS-4	19.47	19.68	37.34	35.06	2.21	2.18	3.15	3.13
TALS-5	16.27	16.37	31.86	31.15	3.91	3.89	5.88	5.86
TALS-6	8.54	8.38	17.83	19.20	9.62	9.83	14.77	14.85
TALS-7	11.66	11.57	23.88	24.68	6.62	6.69	11.19	11.23
TALS-8	2.35	2.27	6.85	8.07	11.82	12.31	21.41	21.78
TALS-10	6.67	6.50	13.95	15.40	10.11	10.41	17.41	17.61
TALS-11	21.60	21.99	41.44	37.96	0.67	0.66	0.65	0.64
TALS-12	2.04	1.97	4.94	5.85	12.40	12.96	22.49	22.91

	Ca		Mg		Mn		Cr	
Ore No.	A	B	A	B	A	B	A	B
TALS-2	2.16	*	2.32	*	0.093	*	0.061	*
TALS-4	0.81	0.82	2.01	1.98	0.122	0.116	0.068	0.066
TALS-5	1.48	1.49	2.33	2.32	0.107	0.106	0.061	0.060
TALS-6	3.50	3.44	1.95	1.99	0.061	0.065	0.027	0.028
TALS-7	2.74	2.72	2.09	2.11	0.077	0.079	0.041	0.042
TALS-8	5.22	5.07	1.67	1.74	0.030	0.034	0.007	0.008
TALS-10	4.33	4.24	1.39	1.42	0.046	0.050	0.020	0.021
TALS-11	0.25	0.26	1.97	1.93	0.130	0.121	0.082	0.078
TALS-12	5.54	5.37	1.42	1.48	0.031	0.036	0.00	0.00

Column A Results using the Lachance-Traill correction method
Column B Results using the Direct Ratio method (DR)
* Ore No, used as standard for the Direct Ratio method
** Data for Allard Lake Standards - Series TALS

TABLE 40

COMPARISON OF RESULTS* - ABSOLUTE % RELATIVE ERROR

Element	Solid		Fused	
	A	B	A	B
Magnesium	1.26	25.2	0.00	2.19
Aluminum	2.01	24.2	0.33	2.16
Silicon	2.72	9.31	0.02	0.99
Calcium	2.93	7.17	0.20	2.29
Titanium	4.32	4.96	0.21	1.77
Chromium	1.74	12.2	0.02	4.98
Manganese	3.92	23.3	0.46	7.81
Iron	2.91	27.2	0.49	9.83

Column A Results by the Lachance-Traill method
Column B Results by the Direct Ratio method (DR)

* Data for Allard Lake Standards - Series TALS

TABLE 41

THEORETICAL CONTRIBUTIONS FROM ABSORPTION AND ENHANCEMENT EFFECTS IN ALLARD LAKE STANDARDS - SERIES TALS

SOLID SPECIMEN

Analyte Element	Absorption (%)	Enhancement (%)	Major Contributors (%)				
			Al	Si	Ca	Ti	Fe
Mg	91.3-93.6	6.4-8.7	<1.	<2	<2	<5	<3.5
Al	91.0-94.0	6.0-9.0		<2	<2	<5	<3.6
Si	90.5-96.4	3.6-9.5			<2	<6	<3.7
Ca	84.0-97.5	2.5-16.0				<10	<6.5
Ti	86.7-97.4	2.6-13.3					<12.3
Cr	78.3-94.6	5.4-21.7					<21.7
Mn	>97.0	<3.0					< 3.0
Fe	100.0						

FUSED SPECIMEN

Analyte Element	Absorption (%)	Enhancement (%)	Major Contributors (%)				
			Al	Si	Ca	Ti	Fe
Mg	97.3-98.9	1.1-2.7	<0.1	<3.0	<0.4	<1.3	<1.5
Al	97.3-98.9	1.1-2.7		<0.3	<0.4	<1.3	<1.6
Si	96.8-99.2	0.8-3.2			<0.5	<1.4	<1.6
Ca	95.0-99.0	1.0-5.0				<2.5	<2.9
Ti	94.7-99.2	0.8-5.3					<5.3
Cr	89.4-98.3	1.7-10.6					<10.6
Mn	>99.0	<1.0					<1.0
Fe	100.0						

why the DR approach is unsuitable due to the high degree of curvature (Figure 15). However, the Lachance-Traill approach provides a simple and accurate method of compensation over a wide range of concentrations.

3.4.3 Analysis of bauxite and aluminum containing ores

3.4.3.1 Introduction

Having considered a system most closely resembling iron-base or titanium-base ores both experimentally and theoretically we have a somewhat clearer idea of the effects present and the compensating powers of the Lachance-Traill approach.

A totally different type of specimen encountered are the bauxites. Bauxite is commonly referred to as an aggregate of aluminous minerals consisting chiefly of aluminum hydrate or hydroxide but may contain amorphous aluminous material (Table 42).

The potential sources of aluminum other than bauxite include aluminum phosphate rocks, aluminous shale, alunite, dawsonite, high alumina clay, igneous rocks, metamorphic rocks, saprolite and sillimanite group minerals. (98).

Figure 15.

GRAPH OF I_{Fe} VERSUS C_{Fe} (Series TALS - solid)

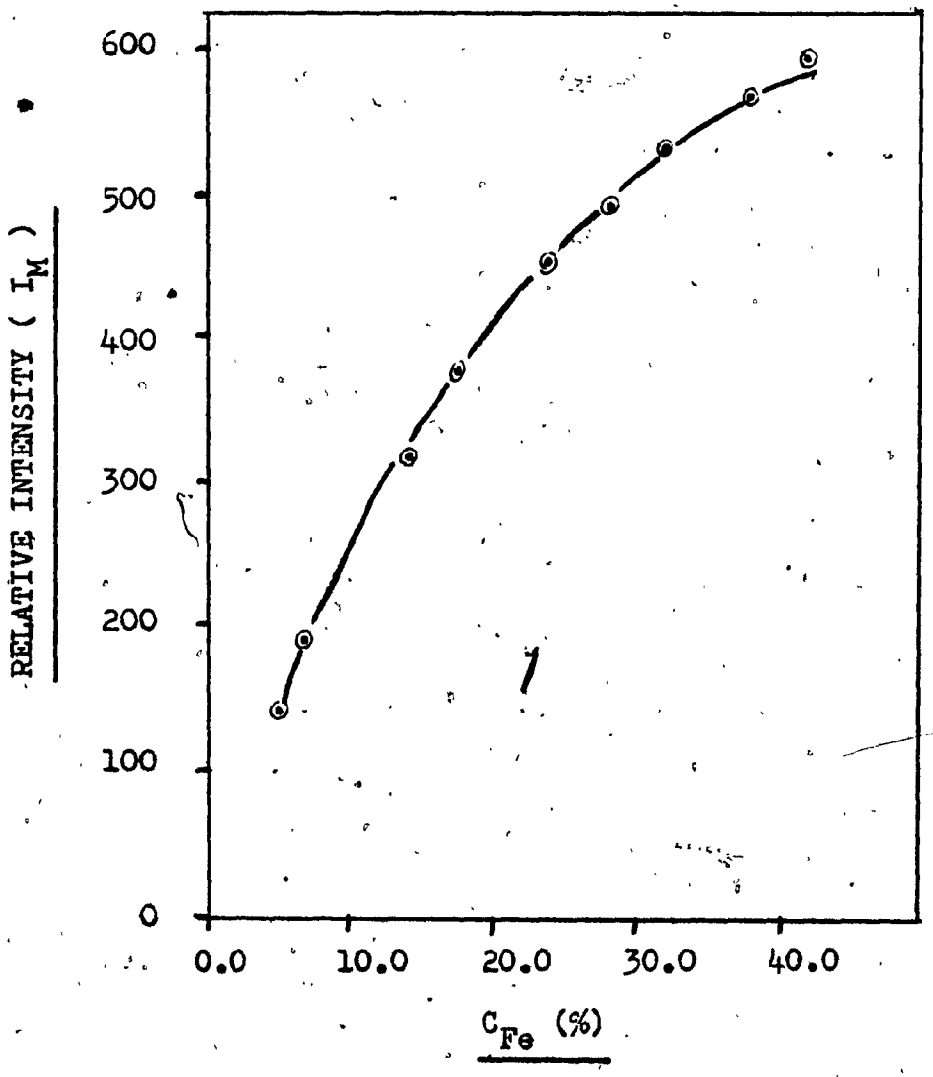

TABLE 42 (98)

Mineral Contents:

trihydrate	chiefly gibbsite	$Al_2O_3 \cdot 3H_2O$
monohydrate	chiefly boehmite	$Al_2O_3 \cdot H_2O$
kaolinite		$Al_2O_3 \cdot 2SiO_2 2H_2O$
mixed bauxite	both gibbsite and boehmite	
hematite		Fe_2O_3
goethite		$Fe_2O_3 \cdot H_2O$
quartz		SiO_2
anatase		TiO_2

Bauxites exist in a number of different forms and their physical properties vary appreciably. Bauxites may be massive or earthy, pisolitic, oolitic, brecciated, nodular, botryoidal, cellular, platy or vermicular.(98) Many pisolites consist of concentric layers, and banding is common in other structures. Some high grade bauxites are light gray or nearly white, but shades of brown, yellow, red, pink and purple are common and those rich in organic matter are nearly black. The hardness and specific gravity of the bauxite minerals are summarized in Table 43. (98)

Mineral impurities present are iron, titanium, clay and silica minerals.

The iron minerals hematite (Fe_2O_3) and goethite ($Fe_2O_3 \cdot H_2O$) are the most abundant impurities. They occur as nodules, concretions and as finely disseminated forms intergrown with aluminous minerals. They are the chief causes of the red and brown colours that are characteristic of many bauxites. Magnetite ($FeFe_2O_4$) and ilmenite ($FeTiO_3$) are common in some bauxites particularly those that have altered from basic igneous rocks. Maghemite (γ-Fe_2O_3), has been identified in several bauxite deposits and pyrite (FeS_2) and siderite ($FeCO_3$) occur in a few deposits. (98)

The titanium minerals in bauxite include the primary

TABLE 43 (98)

COMPOSITION OF BAUXITES

Type	Structure	Alumina content (%)	Water content (%)	Specific Gravity	Hardness Mohrs Scale
Gibbsite	Monoclinic	65.35	34.65	2.3-2.4	2.2-3.5
Boehmite	Orthorhombic	84.97	15.03	3.01-3.06	4.0-5.0
Diaspore*	Orthorhombic	84.98	15.02	3.3-3.5	6.5-7.0

* differs from Boehmite by a more closely-packed and tightly-bonded atomic structure.

minerals ilmenite ($FeTiO_3$ or $FeO \cdot TiO_2$), rutile (TiO_2) and titaniferrous magnetite; and the secondary minerals, anatase (TiO_2) and leucoxene (TiO_2), formed during weathering. Titaniferrous hematite and sphene ($CaTiSiO_5$ or $CaO \cdot TiO_2 \cdot SiO_2$) are also present. (98)

The kaolin minerals - kaolinite ($(OH)_8Si_4Al_4O_{10}$), halloysite ($(OH)_8Si_4Al_4O_{10}$) and endellite ($(OH)_8Si_4Al_4O_{10} \cdot 4H_2O$), the hydrated form of halloysite - are the most common clay minerals associated with bauxite deposits. (98) They occur virtually pure in pockets, veins and concretions, and are intergrown with aluminum and iron bearing minerals. Kaolinite is the most common mineral in the group.

Nearly all the silica in many high-grade bauxite deposits is in the form of kaolin minerals, but some deposits contain minor quantities of quartz and in a few deposits this is the major impurity. (98)

Other accessory and minor mineral impurities which occur are zircon, tourmaline, kyanite and garnet as well as chamosite to a lesser degree. (98)

This brief description shows the complexities which do occur in any one specimen for analysis.

3.4.3.2 Analysis of a series of high grade bauxite ores of the same relative composition

The first series (Series BXT) include high grade ores containing 16 to 31 percent aluminum (58). These are basically boehmite (ie. samples B61 and B62) consisting of about 10 to 20 percent water, the other samples being gibbsite with about 20 to 30 percent water. Tables 44 through 48 give the data results. The fused specimens are based on data corrected for loss on ignition when calculated. The Lachance-Traill approach gives effective compensation for absorption-enhancement effects and shows significant improvements over the DR technique. Little difference can be distinguished between solid or fused samples. However, since true homogeneity is assumed in the theoretical model, experimentally the situation may be quite different for raw solid specimens due to sample composition. When considering fused specimens, where the sample matrix has been destroyed, the approach may be valid. Table 49 shows that the main enhancement effects are due to iron and titanium with a maximum value of 10 percent, except for certain elements (ie. chromium).

3.4.3.3 Analysis of a mixture of typical bauxite ore deposits

The next series (Series DX) consists of a mixture of

TABLE 44

CONCENTRATION RANGES FOR BAUXITE SAMPLES*

Element	Solid (%)	Fused (%)
Magnesium	0.00-0.40	0.00-0.10
Aluminum	18.0-31.0	4.00-9.00
Silicon	0.20-12.0	0.04-1.60
Calcium	0.00-0.80	0.00-0.30
Titanium	0.60-1.80	0.10-0.50
Chromium	0.01-0.08	0.00-0.01
Manganese	0.00-0.40	0.00-0.10
Iron	0.90-19.0	0.20-5.00
Phosphorus	0.00-2.90	0.00-0.80
Potassium	0.00-1.70	0.00-0.40

*Series BXT, samples B61 - B70

TABLE 45

COMPOSITION OF BAUXITE SAMPLES*

Ore No.	Mg	Al	Si	P	K	Ca	Ti	Cr	Mn	Fe	LOI
B-61	0.32	29.30	2.14	0.03	0.08	0.47	1.56	0.06	0.01	16.44	12.50
B-62	0.42	30.90	1.73	0.04	0.45	0.75	1.68	0.03	0.11	13.84	12.75
B-63	0.24	25.29	0.16	0.16	0.27	0.04	1.70	0.08	0.10	14.18	27.32
B-64	0.25	25.29	2.16	2.93	1.39	1.02	1.29	0.03	0.42	11.00	23.00
B-65	0.18	31.04	2.37	0.03	0.17	0.04	1.52	0.02	0.01	4.50	26.65
B-66	0.15	34.13	0.24	0.06	0.09	0.01	1.76	0.05	0.01	0.90	30.20
B-67	0.11	22.04	12.29	0.04	0.01	0.01	0.62	0.01	0.01	5.68	22.60
B-68	0.20	23.12	0.70	0.08	0.17	0.01	1.33	0.05	0.015	18.86	24.80
B-69	0.09	30.83	2.42	0.03	0.01	0.022	1.47	0.015	0.007	5.12	26.50
B-70	0.09	18.76	6.26	0.02	0.13	0.008	1.01	0.024	0.008	19.32	21.45

* Data for Bauxites - Series BXT

TABLE 46

RESULTS FOR BAUXITE SAMPLES - SOLID SPECIMEN**

	Hg		Al		Si		Ca		Ti	
Ore No.	A	B	A	B	A	B	A	B	A	B
B-61	0.315	*	29.36	*	2.13	*	0.47	*	1.56	*
B-62	0.420	0.230	31.01	32.16	1.73	1.72	0.75	0.73	1.68	1.62
B-63	0.243	0.240	25.58	25.22	0.16	0.17	0.04	0.04	1.71	1.91
B-64	0.253	0.270	25.31	26.84	2.16	2.39	1.01	0.96	1.28	1.19
B-65	0.180	0.220	31.71	37.53	2.40	2.53	0.038	0.04	1.54	1.64
B-66	0.150	0.190	35.09	44.16	0.24	0.25	0.007	0.008	1.78	1.94
B-67	0.110	0.130	22.44	26.35	12.40	15.15	0.008	0.008	0.65	0.65
B-68	0.200	0.190	23.30	21.56	0.70	0.74	0.008	0.009	1.33	1.50
B-69	0.090	0.110	31.48	36.93	2.45	2.58	0.022	0.020	1.49	1.60
B-70	0.095	0.090	18.85	17.52	6.24	7.12	0.008	0.008	1.01	1.11

	Cr		Mn		Fe		P		K	
Ore No.	A	B	A	B	A	B	A	B	A	B
B-61	0.061	*	0.009	*	16.45	*	0.026	*	0.079	*
B-62	0.026	0.025	0.105	0.105	13.84	14.00	0.035	0.035	0.455	0.450
B-63	0.080	0.090	0.100	0.110	14.28	15.86	0.160	0.180	0.270	0.300
B-64	0.030	0.030	0.420	0.430	10.90	11.44	2.89	3.16	1.38	1.38
B-65	0.015	0.016	0.007	0.009	4.57	5.95	0.029	0.030	0.173	0.180
B-66	0.049	0.050	0.007	0.009	0.92	1.30	0.057	0.060	0.093	0.100
B-67	0.008	0.009	0.008	0.010	5.75	7.45	0.040	0.038	0.006	0.006
B-68	0.045	0.050	0.015	0.016	19.04	19.96	0.075	0.082	0.170	0.190
B-69	0.015	0.016	0.007	0.009	5.19	6.75	0.030	0.030	0.006	0.006
B-70	0.024	0.030	0.008	0.008	19.47	20.14	0.016	0.017	0.130	0.140

Column A Results using the Lachance-Traill correction method

Column B Results using the Direct Ratio method (DR)

* Ore No. used as standard for DR method ** Data for Series BXT

TABLE 47

RESULTS FOR BAUXITE SAMPLES - FUSED SPECIMEN**

	Mg		Al		Si		Ca		Ti	
Ore No.	A	B	A	B	A	B	A	B	A	B
B-61	0.31	*	29.34	*	2.14	*	0.470	*	1.56	*
B-62	0.42	0.49	30.95	35.72	1.73	1.98	0.750	0.850	1.68	1.90
B-63	0.24	0.33	25.34	34.71	0.16	0.22	0.036	0.050	1.70	2.35
B-64	0.25	0.34	25.52	33.50	0.22	0.29	1.02	1.27	1.29	1.59
B-65	0.18	0.25	31.10	44.18	2.37	3.20	0.037	0.050	1.51	2.04
B-66	0.15	0.23	34.20	51.91	0.24	0.33	0.007	0.010	1.75	2.47
B-67	0.11	0.14	22.08	29.60	12.28	16.76	0.008	0.010	0.62	0.79
B-68	0.20	0.27	23.16	30.15	0.70	0.93	0.008	0.010	1.33	1.80
B-69	0.09	0.13	30.89	43.70	2.42	3.26	0.022	0.030	1.47	1.98
B-70	0.10	0.12	18.78	23.46	6.26	8.22	0.008	0.010	1.01	1.31

	Cr		Mn		Fe		P		K	
Ore No.	A	B	A	B	A	B	A	B	A	B
B-61	0.061	*	0.009	*	16.45	*	0.026	*	0.08	*
B-62	0.026	0.030	0.105	0.120	13.86	15.96	0.035	0.040	0.45	0.52
B-63	0.080	0.110	0.100	0.140	14.18	19.30	0.160	0.220	0.27	0.37
B-64	0.030	0.040	0.425	0.540	11.04	14.14	2.94	3.90	1.39	1.78
B-65	0.015	0.020	0.007	0.010	4.53	6.68	0.029	0.040	1.69	0.23
B-66	0.048	0.070	0.007	0.011	9.09	1.45	0.056	0.080	0.091	0.13
B-67	0.008	0.010	0.008	0.011	5.72	8.11	0.039	0.050	0.006	0.008
B-68	0.045	0.060	0.015	0.020	18.84	24.32	0.076	0.100	0.173	0.230
B-69	0.015	0.020	0.007	0.011	5.16	7.58	0.029	0.040	0.006	0.008
B-70	0.023	0.030	0.008	0.010	19.30	24.06	0.016	0.020	0.133	0.170

Column A Results using the Lachance-Traill correction method
Column B Results using the Direct Ratio method (DR)
* Ore No. used as standard for DR method ** Data for Series BXT

TABLE 48

COMPARISON OF RESULTS* - ABSOLUTE % RELATIVE ERROR

Element	Solid		Fused	
	A	B	A	B
Magnesium	0.85	17.4	0.79	2.75
Aluminum	1.20	12.6	0.25	2.84
Silicon	0.49	8.62	0.21	1.89
Calcium	0.37	6.57	2.00	0.55
Titanium	0.71	8.65	0.21	1.74
Chromium	0.32	9.29	1.32	0.0
Manganese	0.09	14.3	0.85	3.54
Iron	0.98	18.5	0.39	5.38
Phosphorus	0.92	5.84	0.16	0.29
Potassium	0.96	4.75	0.37	0.12

Column A Results by the Lachance-Traill method
Column B Results by the Direct Ratio method (DR)

* Data for Bauxite Samples - Series BXT

TABLE 49

THEORETICAL CONTRIBUTIONS FROM ABSORPTION AND ENHANCEMENT EFFECTS IN BAUXITE SAMPLES - SERIES BXT

SOLID SPECIMEN

Analyte Element	Absorption (%)	Enhancement (%)	Major Contributors (%)			
			Al	Si	Ti	Fe
Mg	93.0-95.7	4.3-7.0	<3	<0.5	<0.6	<3.7
Al	94.0-99.0	1.0-6.0		<0.5	<0.7	<4.0
Si	94.7-99.0	1.0-5.3			<0.7	<4.0
P	96.0-99.0	1.0-4.0			<0.7	<4.0
K	94.0-98.7	1.3-6.0			<1.0	<5.3
Ca	93.0-98.0	2.0-7.0			<1.2	<6.5
Ti	89.0-99.2	0.8-11.0				<11.0
Cr	77.7-98.4	1.6-22.3				<22.3
Mn	97.0-99.8	0.2-3.0				<3.0
Fe	100.0					

FUSED SPECIMEN

Analyte Element	Absorption (%)	Enhancement (%)	Major Contributors (%)			
			Al	Si	Ti	Fe
Mg	97.0-98.8	1.2-3.0	<0.8		<0.3	<1.9
Al	97.0-99.6	0.4-3.0			<0.3	<2.0
Si	97.0-99.5	0.5-3.0			<0.3	<2.0
P	97.8-99.6	0.4-2.2			<0.3	<2.0
K	96.9-99.4	0.6-3.1			<0.4	<2.8
Ca	96.0-98.6	1.4-4.0			<0.6	<3.5
Ti	94.0-98.3	1.7-6.0				<6.0
Cr	87.0-99.2	0.8-13.0				<13.0
Mn	98.4-99.9	0.1-1.6				<1.6
Fe	100.0					

typical bauxites. (98) The associated parent rocks are presented in Table 50.

Data results for this series are presented in Tables 51 through 56. The DR method in these cases employs two standards to obtain better results for comparison purposes. The Lachance-Traill approach shows acceptable results as compared to the DR method under the theoretical assumption of homogeneity. Experimentally, raw specimens would likely be impractical for analysis due to the large concentration ranges present as well as variations in mineral and water contents. Fusion may also be a problem due to the high silica content, but addition of certain oxidizers or modification of the flux may help in matrix dissolution (ie. carbonate fusion).

3.4.3.4 Analysis of a typical aluminum phosphate rock deposit

Major deposits of aluminum phosphate rock (Series APD) occur in friable, leached, phosphatic sand above calcium phosphate zones in Florida. The aluminum bearing minerals are crandallite ($CaAl_3(PO_4)_2(OH)_3 \cdot H_2O$), millsite ($(NaK)CaAl_6(PO_4)_4(OH)_9 \cdot 3H_2O$), wavelite ($Al_3(PO_4)_2(OH)_3 \cdot 5H_2O$) and kaolinite ($(OH)_8Si_4Al_4O_{10}$). In addition to the aluminous forms, some of the phosphate occurs as carbonatefluorapatite ($Ca_{10}(PO_4CO_3)_6F_{2-3}$).

TABLE 50 (98)

Parent Rocks Series DX:

1. Nepheline syenite
2. Dolerite
3. Hornblende schist
4. Primary laterite
5. Solid hornblende basalt, chloritized and saussuritized
6. Residual kaolinitic clay
7. Yellowish-white pisolitic bauxite
8. Green shale
9. Diabase
10. Compact superficial gibbsitic laterite

TABLE 51

CONCENTRATION RANGES FOR BAUXITE SAMPLES*

Element	Solid (%)	Fused (%)
Magnesium	0.00-8.00	0.00-1.60
Aluminum	6.00-33.30	1.30-9.70
Silicon	0.20-26.4	0.00-6.2
Calcium	0.00-8.4	0.00-1.70
Titanium	0.30-2.80	0.00-0.70
Chromium	---	---
Manganese	0.00-0.40	0.00-0.70
Iron	0.40-17.6	0.10-4.30
Phosphorus	0.00-0.06	0.00-0.04
Potassium	0.00-5.30	0.00-1.20

*Series IX

TABLE 52

COMPOSITION OF BAUXITE SAMPLES*

Ore No.	Mg	Al	Si	Ca	Ti	Cr	Mn	Fe	P	K	LOI
DX-1	0.29	11.17	26.42	0.64	0.30	----	0.19	1.63	0.026	5.26	10.85
DX-2	4.19	9.15	24.31	6.29	0.32	----	0.38	8.45	0.004	0.15	3.03
DX-3	5.75	6.45	23.26	8.43	2.76	----	0.37	7.70	0.026	0.09	1.58
DX-4	0.03	15.43	10.93	0.007	2.44	----	0.008	15.59	0.004	0.058	18.24
DX-5	4.22	7.41	22.79	5.65	0.66	----	0.15	10.81	0.06	0.37	6.22
DX-6	0.15	17.42	16.92	0.007	2.04	----	0.008	9.48	0.056	0.008	13.51
DX-7	0.11	33.32	0.19	0.004	2.33	----	0.008	0.44	0.15	0.008	31.57
DX-8	1.66	9.63	28.50	0.45	0.59	----	0.33	3.28	0.002	2.50	8.35
DX-9	8.00	6.54	23.97	7.62	0.42	----	0.008	7.09	0.048	0.34	1.77
DX-10	0.006	31.86	0.61	0.12	0.62	----	0.008	2.73	0.004	0.004	33.37

* Data for Bauxites - Series DX

TABLE 53

RESULTS FOR BAUXITE SAMPLES - SOLID SPECIMEN**

	Mg		Al		Si		Ca		Ti	
Ore No.	A	B	A	B	A	B	A	B	A	B
DX-1	0.29	0.33	11.19	13.32	26.50	27.86	0.64	0.57	0.30	0.37
DX-2	4.11	4.07	9.23	9.18	24.15	24.05	6.21	6.40	0.32	0.37
DX-3	5.47	5.50	6.48	6.53	22.79	23.65	8.24	8.53	2.71	1.81
DX-4	0.03	0.04	15.38	13.43	10.93	12.44	0.007	0.008	2.42	2.56
DX-5	4.14	3.85	7.46	7.30	22.54	22.88	5.58	5.89	0.66	0.61
DX-6	0.15	*	17.49	*	17.07	*	0.007	*	2.04	*
DX-7	0.11	0.13	34.27	37.16	0.20	5.53	0.004	0.004	2.36	2.60
DX-8	1.66	1.79	9.72	11.06	28.69	29.56	0.45	0.44	0.59	0.62
DX-9	7.81	*	6.64	*	23.75	*	7.52	*	0.42	*
DX-10	0.006	0.017	32.77	34.14	0.63	5.77	0.13	0.16	0.63	0.83

	Mn		Fe		P		K	
Ore No.	A	B	A	B	A	B	A	B
DX-1	0.190	0.230	1.63	4.57	0.026	0.026	5.27	5.22
DX-2	0.037	0.039	8.34	7.90	0.004	0.004	0.15	0.15
DX-3	0.360	0.330	7.53	7.01	0.026	0.026	0.09	0.09
DX-4	0.008	0.010	17.37	13.53	0.004	0.005	0.06	0.07
DX-5	0.150	0.160	10.64	9.04	0.060	0.060	0.37	0.38
DX-6	0.008	*	9.42	*	0.057	*	0.008	*
DX-7	0.008	0.013	0.45	3.92	0.150	0.190	0.008	0.010
DX-8	0.330	0.420	3.92	5.62	0.002	0.002	2.52	2.47
DX-9	0.008	*	7.00	*	0.049	*	0.34	*
DX-10	0.008	0.014	2.77	7.09	0.004	0.005	0.004	0.005

Column A Results using the Lachance-Traill correction method
Column B Results using the Direct Ratio method (DR)
* Ore Nos. used as standards for DR method ** Data for Series DX

TABLE 54

RESULTS FOR BAUXITE SAMPLES - FUSED SPECIMEN**

	Mg		Al		Si		Ca		Ti	
Ore No.	A	B	A	B	A	B	A	B	A	B
DX-1	0.29	0.30	11.18	11.58	26.39	26.04	0.62	0.59	0.30	0.32
DX-2	4.18	4.17	9.19	9.17	24.24	24.14	6.29	6.32	0.32	0.34
DX-3	5.74	5.71	6.48	6.48	23.20	23.48	8.42	8.48	2.76	2.35
DX-4	0.03	0.03	15.44	14.93	10.91	11.75	0.007	0.007	2.45	2.47
DX-5	4.21	4.16	7.44	7.38	22.74	22.72	5.65	5.69	0.66	0.64
DX-6	0.15	*	17.44	*	16.90	*	0.007	*	2.04	*
DX-7	0.11	0.12	33.40	34.36	0.19	2.80	0.004	0.004	2.33	2.30
DX-8	1.66	1.68	9.64	8.89	28.41	27.90	0.45	0.44	0.58	0.60
DX-9	7.98	*	6.58	*	23.92	*	7.61	*	0.42	*
DX-10	0.006	0.007	31.92	32.56	0.61	3.03	0.12	0.12	0.62	0.65

	Mn		Fe		P		K	
Ore No.	A	B	A	B	A	B	A	B
DX-1	0.19	0.20	1.63	2.55	0.026	0.025	5.26	5.12
DX-2	0.04	0.04	8.40	8.28	0.004	0.004	0.15	0.15
DX-3	0.37	0.35	7.65	7.26	0.026	0.026	0.091	0.090
DX-4	0.008	0.008	17.37	15.49	0.004	0.004	0.058	0.060
DX-5	0.15	0.15	10.73	10.04	0.061	0.060	0.37	0.37
DX-6	0.008	*	9.42	*	0.057	*	0.008	*
DX-7	0.008	0.009	0.44	1.25	0.120	0.150	0.008	0.008
DX-8	0.29	0.32	2.86	3.76	0.002	0.002	2.46	2.41
DX-9	0.008	*	7.06	*	0.050	*	0.34	*
DX-10	0.008	0.009	2.73	3.45	0.004	0.004	0.004	0.004

Column A Results using the Lachance-Traill correction method
Column B Results using the Direct Ratio method (DR)
* Ore Nos. used as standards for the DR method ** Data for Series DX

TABLE 55

COMPARISON OF RESULTS* - ABSOLUTE % RELATIVE ERROR

Element	Solid		Fused	
	A	B	A	B
Magnesium	0.97	10.4	0.72	4.13
Aluminum	1.11	8.59	0.27	2.00
Silicon	1.49	4.35	0.17	2.16
Calcium	3.08	9.88	0.62	2.86
Titanium	0.57	17.0	0.21	4.99
Manganese	0.53	20.1	0.07	6.27
Iron	1.23	13.7	0.43	11.4
Phosphorus	0.39	9.32	0.76	1.20
Potassium	0.21	17.4	0.44	1.20

Column A Results by the Lachance-Traill method
Column B Results by the Direct Ratio method (DR)

* Data for Bauxite Samples - Series DX

TABLE 56

THEORETICAL CONTRIBUTIONS FROM ABSORPTION AND ENHANCEMENT EFFECTS IN BAUXITE SAMPLES - SERIES DX

SOLID SPECIMEN

Analyte Element	Absorption (%)	Enhancement (%)	Major Contributors* (%)					
			Al	Si	Ca	Ti	Fe	K
Mg	93.5-96.0	4.0-6.5	3.3	3.0	2.7	0.8	3.1	2.0
Al	93.0-99.0	1.0-7.0		3.2	2.8	0.8	2.0	2.0
Si	95.0-99.0	1.0-5.0			3.2	0.9	3.3	0.1
P	96.0-98.0	2.0-4.0			2.8	0.9	3.3	
K	94.0-98.6	1.4-6.0			4.2	1.3	2.7	
Ca	93.0-98.5	1.5-7.0				1.6	5.6	
Ti	94.0-99.6	0.4-6.0					6.0	
Mn	97.3-99.5	0.5-6.7					2.7	
Fe	100.0							

FUSED SPECIMEN

Analyte Element	Absorption (%)	Enhancement (%)	Major Contributors* (%)					
			Al	Si	Ca	Ti	Fe	K
Mg	97.5-98.7	1.3-2.5	0.8	0.6	1.0	0.4	1.6	0.6
Al	97.5-99.5	0.5-2.5		0.6	1.1	0.4	1.7	0.7
Si	97.9-99.5	0.5-2.1			1.2	0.4	1.7	0.7
P	97.8-99.7	0.3-2.2			1.3	0.7	1.8	
K	97.0-99.6	0.4-3.0			1.7	1.0	2.4	
Ca	97.9-99.1	0.9-2.1				0.6	3.0	
Ti	97.1-99.8	0.2-2.9					2.9	
Mn	98.6-99.9	0.1-1.4					1.4	
Fe	100.0							

* The indicated percentages are ranges representing zero to the indicated maximum percent.

The aluminum phosphate minerals form 20 to 30 percent of the rock and more than 60 percent is quartz sand. The quartz is coarser than 150 mesh and virtually all the phosphatic material is finer than 150 mesh or can be disaggregated to this size.

Though much of the rock contains from 8 to 15 percent alumina, the alumina, phosphate and uranium contents can be increased three-fold by removing the +150 mesh quartz sand.

Tables 57 through 61 show typical data results, with the Lachance-Traill approach showing higher accuracy over the DR technique even when two standards are used. Experimentally the magnesium concentration is much too low for analysis. Enhancement is minimal at less than 10 percent in the raw solid and less than 4 percent in fused specimens (Table 62).

Separation of the coarser quartz may be advantageous for experimental determinations since the silica content is very high and will certainly pose dissolution problems.

3.4.4 Analysis of a series of rocks and minerals

In many analyses involving geological materials, standard reference materials are used for calibration purposes. These are usually standard rocks and minerals which can be

TABLE 57

CONCENTRATION RANGES FOR ALUMINUM PHOSPHATE ROCKS*

Element	Solid (%)	Fused (%)
Magnesium	0.006	0.0013
Aluminum	3.00-8.00	0.60-1.80
Silicon	19.0-32.0	4.40-7.10
Calcium	0.10-6.00	0.03-1.40
Titanium	0.20-0.40	0.04-0.09
Chromium	0.00-0.30	0.00-0.08
Manganese	0.10-1.70	0.01-0.09
Iron	0.90-1.80	0.20-0.42
Phosphorus	4.90-8.60	1.10-2.10
Potassium	0.00-0.013	0.00-0.004

*Series APD

TABLE 58

COMPOSITION OF ALUMINUM PHOSPHATE ROCKS*

Rock No.	Mg	Al	Si	Ca	Ti	Cr	Mn	Fe	P	K	LOI
APD-1	0.006	4.37	24.06	6.42	0.22	0.007	0.54	1.93	8.61	0.0083	7.70
APD-2	0.006	3.16	29.26	5.90	0.22	0.07	0.41	2.00	5.94	0.0042	5.79
APD-3	0.006	6.61	19.13	5.72	0.24	0.08	1.66	1.83	9.07	0.0083	12.63
APD-4	0.006	7.50	26.76	2.22	0.38	0.34	0.12	1.52	5.58	0.0083	9.72
APD-5	0.006	4.32	32.47	0.64	0.19	0.01	0.12	0.92	5.07	0.0042	8.05
APD-6	0.006	4.97	31.82	0.14	0.25	0.014	0.11	0.93	4.94	0.0125	9.07
APD-7	0.006	7.89	23.99	0.86	0.39	0.007	0.10	1.53	7.14	0.0166	13.21

Data for Aluminum Phosphate Deposits - Series APD

TABLE 59

RESULTS FOR THE ALUMINUM PHOSPHATE ROCKS - SOLID SPECIMEN**

	Mg		Al		Si		Ca		Ti	
Rock No.	A	B	A	B	A	B	A	B	A	B
APD-1	0.006	0.006	4.40	3.67	24.28	24.55	6.50	6.14	0.22	0.17
APD-2	0.006	0.006	3.16	1.97	29.25	29.77	5.89	5.61	0.21	0.17
APD-3	0.006	*	6.66	*	19.46	*	5.85	*	0.24	*
APD-4	0.006	0.006	7.48	8.38	27.14	25.24	2.24	2.22	0.38	0.35
APD-5	0.006	0.006	4.34	4.00	33.18	32.95	0.64	0.63	0.19	0.18
APD-6	0.006	*	4.99	*	32.57	*	0.14	*	0.25	*
APD-7	0.006	0.006	7.96	9.05	24.77	23.11	0.88	0.88	0.39	0.39

	Cr		Mn		Fe		P		K	
Rock No.	A	B	A	B	A	B	A	B	A	B
APD-1	0.007	0.005	0.54	0.41	1.94	1.88	8.65	8.27	0.008	0.008
APD-2	0.070	0.050	0.41	0.32	1.99	2.00	5.93	5.84	0.004	0.004
APD-3	0.080	*	1.68	*	1.85	*	9.14	*	0.008	*
APD-4	0.340	0.031	0.12	0.11	1.53	1.66	5.60	5.57	0.008	0.009
APD-5	0.010	0.010	0.12	0.12	0.93	0.87	5.12	5.02	0.004	0.004
APD-6	0.014	*	0.12	*	0.94	*	4.99	*	0.013	*
APD-7	0.007	0.007	0.10	0.10	1.56	1.92	7.26	6.94	0.017	0.017

Column A Results using the Lachance-Traill correction method
Column B Results using the Direct Ratio method (DR)
* Rock Nos. used as standards for the DR method ** Data for Series APD

TABLE 60

RESULTS FOR THE ALUMINUM PHOSPHATE ROCKS - FUSED SPECIMEN**

	Mg		Al		Si		Ca		Ti	
Rock No.	A	B	A	B	A	B	A	B	A	B
APD-1	0.006	0.006	4.39	4.35	24.27	24.32	6.46	6.39	0.22	0.20
APD-2	0.006	0.006	3.16	3.12	29.33	29.52	5.89	5.89	0.22	0.20
APD-3	0.006	*	6.66	*	19.35	*	5.77	*	0.24	*
APD-4	0.006	0.006	7.49	7.51	26.85	26.39	2.23	2.24	0.38	0.37
APD-5	0.006	0.006	4.31	4.31	32.55	32.60	0.64	0.64	0.19	0.19
APD-6	0.006	0.*	4.95	*	31.92	*	0.14	*	0.25	*
APD-7	0.006	0.006	7.90	7.94	24.17	23.72	0.86	0.87	0.39	0.39

	Cr		Mn		Fe		P		K	
Rock No.	A	B	A	B	A	B	A	B	A	B
APD-1	0.007	0.006	0.54	0.48	1.93	1.94	8.63	8.57	0.008	0.008
APD-2	0.007	0.063	0.41	0.37	2.00	2.04	5.94	5.99	0.004	0.004
APD-3	0.080	*	1.66	*	1.83	*	9.11	*	0.008	*
APD-4	0.34	0.33	0.12	0.11	1.53	1.59	5.60	5.59	0.008	0.008
APD-5	0.01	0.01	0.12	0.12	0.92	0.90	5.07	5.07	0.004	0.004
APD-6	0.014	*	0.11	*	0.93	*	4.94	*	0.013	*
APD-7	0.007	0.007	0.10	0.10	1.53	1.68	7.16	7.01	0.017	0.017

Column A Results using the Lachance-Traill correction method
Column B Results using the Direct Ratio method (DR)
* Rock Nos. used as standards for the DR method ** Data for Series APD

TABLE 61

COMPARISON OF RESULTS - ABSOLUTE % RELATIVE ERROR

Element	Solid		Fused	
	A	B	A	B
Magnesium	1.19	0.00	3.33	0.00
Aluminum	0.48	12.5	0.30	0.54
Silicon	1.70	2.92	0.56	0.98
Calcium	0.99	2.63	0.30	0.54
Titanium	0.80	13.4	0.00	4.86
Chromium	0.00	15.2	0.10	6.63
Manganese	0.94	12.5	0.03	6.76
Iron	1.03	8.55	0.17	3.82
Phosphorus	0.78	1.92	0.20	0.66
Potassium	3.07	2.01	2.62	1.00

Column A Results by the Lachance-Traill method
Column B Results by the Direct Ratio method (DR)

Data for Aluminum Phosphate Rocks - Series APD

TABLE 62

THEORETICAL CONTRIBUTIONS FROM ABSORPTION AND ENHANCEMENT EFFECTS IN ALUMINUM PHOSPHATE DEPOSITS - SERIES APD

SOLID SPECIMEN

Analyte Element	Absorption (%)	Enhancement (%)	Major Contributors (%) *						
			Al	Si	Ca	Ti	Mn	Fe	P
Mg	90.0-92.0	8.0-10.0	0.7	4.1	2.0	0.1	0.3	0.3	4.8
Al	89.8-92.3	7.7-10.2		4.4	2.2	0.1	0.3	0.4	4.6
Si	91.7-96.2	3.8-8.3			2.4	0.1	0.3	0.4	5.4
Ca	98.7-99.2	0.8-1.3				0.2	0.6	0.7	
Ti	98.8-99.3	0.7-1.2					0.9	1.0	
Cr	97.6-98.6	1.4-2.4					0.2	2.4	
Mn	> 99.8	< 0.3						0.3	
Fe	100.0								

FUSED SPECIMEN

Analyte Element	Absorption (%)	Enhancement (%)	Major Contributors (%) *						
			Al	Si	Ca	Ti	Mn	Fe	P
Mg	96.1-97.7	2.3-3.9	1.5	0.9	0.8	0.1	0.1	0.2	2.2
Al	96.0-97.7	2.3-4.0		0.9	0.9	0.1	0.2	0.2	2.3
Si	96.4-98.5	1.5-3.6			1.0	0.1	0.2	0.2	2.4
Ca	99.6-99.8	0.2-0.4				0.1	0.3	0.3	
Ti	99.3-99.7	0.3-0.7					0.5	0.5	
Cr	98.8-99.4	0.6-1.2					0.1	1.2	
Mn	> 99.9	< 0.1						0.1	
Fe	100.0								

* The indicated percentages are ranges representing zero to the indicated maximum percent

obtained from various sources, ie. USGS, NBS, etc.. Data results on these reference materials appearing in the literature (99) are somewhat confusing, particularly as to the true analytical content. The concentration ranges for the individual elements can be seen to be quite large and in some cases with errors of ± 10 percent or greater. Recently, Abbey (100) has produced a list of "usable" values for most standard reference materials which clears up the situation somewhat.

In the following part of the study two series (Series XY-1 and Series XY-2) were setup from this accumulation of reference standards. Table 63 shows the individual specimens and parent rock or mineral.

Theoretical intensities were evaluated for both series individually. It can be noted that the silica content (1 - 36%) is much too high in certain cases and problems are evident in fusions if high sample weights are used. The major constituents include aluminum, silicon, calcium and iron.

In Series XY-1, Tables 64 through 68 show data results obtained in a similar manner to the previous treatments. It is evident that the Lachance-Traill approach significantly compensated for any absorption-enhancement effects which

TABLE 63 (100)

Parent Rocks or Minerals:

Series XY-1		Series XY-2	
MRG-1	Gabbro	I-1	Aplitic granite
SY-2	Syenite	I-3	Dolerite
SY-3	Syenite	M-2	Pelitic schist
AGV-1	Andesite	M-3	Calc silicate
BCR-1	Basalt	302/1	Iron ore
DTS-1	Dunite	DT-N	Kyanite
G-2	Granite	UB-N	Serpentine
GSP-1	Granodiorite	NIM-S	Syenite
PCC-1	Peridotite	NBS-97a	Flint clay
W-1	Diabase	NBS-99a	Sodium spar

TABLE 64

CONCENTRATION RANGES FOR ROCKS AND MINERALS*

Element	Solid (%)	Fused (%)
Magnesium	0.40-30.0	0.10-6.00
Aluminum	0.10-10.0	0.10-2.20
Silicon	18.0-32.0	3.80-6.50
Calcium	0.10-10.50	0.02-1.60
Titanium	0.00-2.30	0.00-0.50
Chromium	0.00-0.50	0.00-0.09
Manganese	0.05-0.30	0.00-0.06
Iron	1.80-12.50	0.40-2.60
Phosphorus	0.03-0.20	0.00-0.04
Potassium	0.00-5.00	0.00-1.03

*Series XY-1

TABLE 65

COMPOSITION OF ROCK AND MINERAL SAMPLES*

Rock No.	Mg	Al	Si	Ca	Ti	Cr	Mn	Fe	P	K	LOI
MRG-1	8.15	5.13	18.34	10.52	2.25	0.041	0.13	12.45	0.03	0.15	2.91
SY-2	1.62	7.28	28.09	5.72	0.09	0.001	0.25	4.40	0.19	3.74	5.75
SY-3	1.59	7.07	27.90	5.90	0.09	0.001	0.26	4.50	0.24	3.52	6.32
AGV-1	0.93	10.32	27.92	3.57	0.63	0.003	0.077	4.82	0.22	2.43	4.45
BCR-1	2.10	8.20	25.64	4.99	1.33	0.003	0.15	9.46	0.14	1.39	3.32
DTS-1	30.05	0.17	19.02	0.11	0.006	0.44	0.085	6.02	0.004	0.008	0.44
G-2	0.46	9.20	32.34	1.42	0.30	0.001	0.031	1.84	0.06	3.75	5.05
GSP-1	0.58	9.11	31.46	1.44	0.40	0.034	0.12	3.04	0.31	4.95	3.93
PCC-1	26.31	0.44	19.70	0.38	0.006	0.030	0.093	5.78	0.002	0.008	4.70
W-1	4.00	8.91	24.64	7.85	0.64	0.014	0.130	8.77	0.061	0.53	2.63

* Data for Rocks and Minerals - Series XY-1

TABLE 66

RESULTS FOR ROCK AND MINERAL SAMPLES - SOLID SPECIMEN**

	Mg		Al		Si		Ca		Ti	
Rock No.	A	B	A	B	A	B	A	B	A	B
MRG-1	8.07	*	5.11	*	18.35	*	10.55	*	2.26	*
SY-2	1.63	1.93	7.42	9.81	28.39	33.64	5.80	4.96	0.09	0.09
SY-3	1.61	1.89	7.02	9.49	28.20	33.51	5.98	5.17	0.09	0.09
AGV-1	6.95	1.12	10.23	14.28	28.49	31.73	3.63	3.27	0.64	0.73
BCR-1	2.12	2.27	8.12	9.99	25.95	27.98	5.04	4.77	1.34	1.53
DTS-1	30.96	38.61	0.18	0.14	20.01	17.14	0.11	0.12	0.01	0.01
G-2	0.47	0.60	9.11	13.94	33.12	40.00	1.44	1.23	0.31	0.36
GSP-1	0.59	0.73	8.92	13.29	31.87	38.01	1.46	1.19	0.40	0.46
PCC-1	27.16	33.06	0.46	0.37	20.71	18.54	0.40	0.42	0.006	0.009
W-1	3.98	4.35	8.79	10.49	24.73	25.77	7.85	7.46	0.64	0.67

	Cr		Mn		Fe		P		K	
Rock No.	A	B	A	B	A	B	A	B	A	B
MRG-1	0.041	*	0.13	*	12.53	*	0.03	*	0.15	*
SY-2	0.001	0.001	0.26	0.30	4.48	5.39	0.19	0.17	3.81	3.46
SY-3	0.001	0.001	0.27	0.31	4.58	5.52	0.24	0.22	3.58	3.27
AGV-1	0.003	0.004	0.08	0.10	4.92	6.35	0.23	0.20	2.49	2.24
BCR-1	0.003	0.004	0.15	0.18	9.58	11.24	0.14	0.13	1.42	1.31
DTS-1	0.45	0.71	0.09	0.14	6.29	9.76	0.005	0.004	0.008	0.008
G-2	0.001	0.001	0.03	0.04	1.89	2.65	0.06	0.05	3.86	3.36
GSP-1	0.003	0.004	0.12	0.16	3.09	4.09	0.31	0.27	5.04	4.37
PCC-1	0.31	0.49	0.01	0.15	6.04	9.57	0.002	0.002	0.009	0.008
W-1	0.014	0.015	0.13	0.15	8.81	9.97	0.06	0.06	0.53	0.50

Column A Results using the Lachance-Traill correction method
Column B Results using the Direct Ratio method (DR)
* Rock No. used as standard for Direct Ratio method ** Data for Series XY-1

TABLE 67

RESULTS FOR ROCK AND MINERAL SAMPLES - FUSED SPECIMEN**

	Mg		Al		Si		Ca		Ti	
Rock No.	A	B	A	B	A	B	A	B	A	B
NRG-1	8.13	*	5.12	*	18.29	*	10.50	*	2.25	*
SY-2	1.62	1.88	7.25	9.52	28.01	32.65	5.69	4.82	0.09	0.09
SY-3	1.59	1.82	7.04	9.16	27.83	32.34	5.86	4.99	0.09	0.09
AGV-1	0.93	1.10	10.27	14.06	27.86	31.23	3.55	3.21	0.63	0.72
BCR-1	2.10	2.26	8.16	9.95	25.58	27.86	4.97	4.75	1.33	1.52
DTS-1	30.03	39.60	0.17	0.14	19.00	17.57	0.11	0.12	0.006	0.01
G-2	0.46	0.59	9.15	13.63	32.26	39.12	1.41	1.21	0.30	0.35
GSP-1	0.58	0.72	9.06	13.16	31.39	37.61	1.43	1.18	0.40	0.45
PCC-1	26.29	32.45	0.44	0.36	19.68	18.29	0.38	0.41	0.006	0.009
W-1	3.99	4.40	8.89	10.52	24.58	25.85	7.82	7.48	0.64	0.68

	Cr		Mn		Fe		P		K	
Rock No.	A	B	A	B	A	B	A	B	A	B
NRG-1	0.040	*	0.13	*	12.44	*	0.03	*	0.15	*
SY-2	0.001	0.001	0.25	0.29	4.42	5.24	0.19	0.17	3.73	3.56
SY-3	0.001	0.001	0.26	0.30	4.52	5.33	0.24	0.21	3.52	3.16
AGV-1	0.003	0.004	0.08	0.10	4.84	6.25	0.22	0.19	2.43	2.21
BCR-1	0.003	0.004	0.15	0.18	9.48	11.19	0.14	0.13	1.39	1.31
DTS-1	0.44	0.55	0.09	0.14	6.09	10.01	0.005	0.004	0.008	0.008
G-2	0.001	0.009	0.03	0.04	1.85	2.59	0.06	0.05	3.75	3.28
GSP-1	0.003	0.004	0.12	0.15	3.06	4.04	0.31	0.26	4.95	4.33
PCC-1	0.30	0.37	0.09	0.15	5.85	9.39	0.002	0.002	0.008	0.008
W-1	0.014	0.015	0.13	0.15	8.79	10.00	0.06	0.06	0.53	0.50

Column A Results using the Lachance-Traill correction method
Column B Results using the Direct Ratio method (DR)
* Rock No. used as standard for the Direct Ratio method ** Data for Series XY-1

TABLE 68

COMPARISON OF RESULTS* - ABSOLUTE % RELATIVE ERROR

Element	Solid		Fused	
	A	B	A	B
Magnesium	1.66	20.9	0.09	19.3
Aluminum	1.86	30.9	0.33	29.4
Silicon	1.99	14.2	0.22	12.6
Calcium	1.38	10.4	0.41	11.2
Titanium	0.83	19.0	0.00	20.1
Chromium	4.09	26.9	3.77	15.2
Manganese	2.03	32.5	1.60	37.0
Iron	2.14	35.1	0.54	33.5
Phosphorus	3.13	9.39	2.44	10.7
Potassium	2.14	6.62	0.39	7.72

Column A. Results by the Lachance-Traill method
Column B Results by the Direct Ratio method (DR)

* Data for Rocks and Minerals - Series XY-1

occur. Enhancement effects are present at less than 10 percent in all cases (Table 69).

Tables 70 through 74 represent data results for the Series XY-2. The Lachance-Traill approach shows improved accuracy and, even if two standards are used, the DR is inadequate for data treatment. Enhancement effects are present at less than 10 percent level for most elements except titanium and chromium with iron as the major contributor (Table 75).

3.5 Discussion

The modified Lachance-Traill approach has been shown to be suitable for chemical analysis by XRF. The theoretical simulations emphasize the ability of the model to compensate for absorption-enhancement effects. It has also been shown that enhancement effects occur to less than 10 percent and that in this range adequate compensation does occur. The theoretical model, when applied on a homogeneous sample, shows that relative errors of less than 2 percent are easily obtainable for most systems (Tables 32 and 76). Experimentally different errors are evident. Such sources of error arise from low intensities for the minor constituents especially in aqueous or fused specimens. Another source may be traced

TABLE 69

THEORETICAL CONTRIBUTIONS FROM ABSORPTION AND ENHANCEMENT EFFECTS IN ROCK AND MINERAL SAMPLES - SERIES XY-1

SOLID SPECIMEN

Analyte Element	Absorption (%)	Enhancement (%)	Major Contributors (%) *					
			Al	Si	Ca	Ti	Fe	K
Mg	93.0-97.0	3.0-7.0	0.9	3.6	3.4	0.4	1.4	1.0
Al	>93.0	<7.0		4.0	3.5	0.5	1.7	1.1
Si	93.0-97.0	3.0-7.0			4.0	0.5	2.0	1.7
P	93.0-99.0	1.0-7.0			4.0	0.5	1.7	
K	91.0-99.0	1.0-9.0			5.0	0.7	2.5	
Ca	95.0-99.0	1.0-5.0				0.9	3.3	
Ti	95.0-99.0	1.0-5.0					5.0	
Cr	89.0-98.0	2.0-11.0					11.0	
Mn	98.5-99.0	1.0-1.5					1.5	
Fe	100.0							

FUSED SPECIMEN

Analyte Element	Absorption (%)	Enhancement (%)	Major Contributors (%) *					
			Al	Si	Ca	Ti	Fe	K
Mg	97.0-99.0	1.0-3.0	0.1	0.8	1.3	0.1	0.9	0.5
Al	97.0-99.0	1.0-3.0		0.9	1.4	0.1	0.9	0.6
Si	97.0-99.0	1.0-3.0			1.5	0.1	0.9	0.6
P	97.0-99.0	1.0-3.0			1.6	0.1	0.9	
K	96.0-99.0	1.0-4.0			2.2	0.1	1.3	
Ca	98.0-99.0	1.0-2.0				0.4	1.7	
Ti	97.0-99.0	1.0-3.0					2.8	
Cr	94.0-99.0	1.0-6.0					6.0	
Mn	>99.0	<1.0					1.0	
Fe	100.0							

* The indicated percentages are ranges representing zero to the indicated maximum percent

TABLE 70

CONCENTRATION RANGES FOR ROCKS AND MINERALS*

Element	Solid (%)	Fused (%)
Magnesium	0.02-21.4	0.00-4.80
Aluminum	1.50-35.5	0.40-7.20
Silicon	8.30-35.2	1.90-7.40
Calcium	0.08-8.60	0.00-1.80
Titanium	0.03-1.60	0.00-0.30
Chromium	0.02-0.70	0.00-0.14
Manganese	0.00-0.20	0.00-0.05
Iron	0.05-33.3	0.00-7.90
Phosphorus	0.00-0.20	0.00-0.21
Potassium	0.00-12.8	0.00-2.60

*Series XY-2

TABLE 71

COMPOSITION OF ROCK AND MINERAL SAMPLES*

Rock No.	Mg	Al	Si	Ca	Ti	Cr	Mn	Fe	P	K	LOI
I-1	0.66	8.35	35.24	0.57	0.03	0.068	0.023	0.39	0.009	3.55	4.88
I-3	2.52	7.84	23.26	5.86	1.56	0.68	0.17	11.36	0.175	1.19	5.01
M-2	1.48	14.37	22.85	1.25	0.43	0.68	0.20	6.52	0.22	6.56	4.95
M-3	0.73	10.56	25.99	8.58	0.50	0.68	0.22	3.23	0.16	0.59	7.14
302/1	0.87	6.29	8.32	2.89	0.29	0.068	0.22	33.29	0.88	0.46	15.25
DTN	0.024	35.50	17.07	0.029	0.84	0.027	0.008	00.46	0.039	0.10	1.88
UB-N	21.35	1.78	18.66	0.84	0.07	0.23	0.093	5.91	0.013	0.017	11.75
NIM-S	0.28	10.41	29.75	0.47	0.024	0.003	0.008	0.98	0.052	12.77	0.94
NBS-97a	0.91	23.25	20.41	0.079	1.14	0.021	0.016	0.31	0.16	0.42	14.02
NBS-99a	0.012	12.29	30.48	1.53	0.006	0.021	0.016	0.046	0.009	4.32	6.80

* Data for Rocks and Minerals - Series XY-2

TABLE 72

RESULTS FOR ROCK AND MINERAL SAMPLES - SOLID SPECIMEN**

	Mg		Al		Si		Ca		Ti	
Rock No.	A	B	A	B	A	B	A	B	A	B
I-1	0.68	0.66	8.49	8.12	36.36	36.23	0.58	0.57	0.03	0.03
I-3	2.50	1.88	7.86	5.30	23.30	23.71	5.87	6.71	1.56	1.20
M-2	1.47	1.26	14.26	11.85	23.14	22.84	1.28	1.19	0.43	0.33
M-3	0.73	0.64	10.69	9.04	26.30	26.64	8.62	9.69	0.50	0.35
302/1	0.89	0.45	6.38	2.90	8.44	13.59	2.95	4.03	0.29	0.30
DTN	0.02	0.03	36.07	39.59	17.83	17.07	0.03	0.02	0.85	0.79
UBN	21.90	18.62	1.87	0.41	19.43	19.97	0.87	1.11	0.07	0.08
NIM-S	0.28	0.27	10.18	9.94	29.76	30.43	0.48	0.35	0.02	0.02
NBS-97a	0.94	*	23.70	*	21.30	*	0.08	*	1.16	*
NBS-99a	0.01	*	12.36	*	31.20	*	1.55	*	0.006	*

	Cr		Mn		Fe		P		K	
Rock No.	A	B	A	B	A	B	A	B	A	B
I-1	0.07	0.06	0.02	0.02	0.40	0.34	0.009	0.009	3.65	3.47
I-3	0.68	0.52	0.17	0.12	11.37	7.06	0.18	0.18	1.19	1.25
M-2	0.68	0.54	0.20	0.15	6.58	4.45	0.22	0.22	6.61	6.67
M-3	0.68	0.49	0.22	0.16	3.27	2.15	0.16	0.16	0.60	0.60
302/1	0.07	0.07	0.23	0.16	34.5	20.7	0.88	1.07	0.46	0.55
DTN	0.03	0.03	0.008	0.007	0.47	0.44	0.04	0.04	0.10	0.07
UBN	0.24	0.26	0.10	0.10	6.11	5.62	0.01	0.01	0.02	0.01
NIM-S	0.003	0.002	0.008	0.005	0.99	0.66	0.05	0.05	12.81	12.19
NBS-97a	0.021	*	0.017	*	0.32	*	0.16	*	0.43	*
NBS-99a	0.021	*	0.016	*	0.047	*	0.009	*	4.40	*

Column A Results using the Lachance-Traill correction method
Column B Results using the Direct Ratio method (DR)
* Rock No. used as standard for DR method ** Data for Series XY-2

TABLE 73

RESULTS FOR ROCK AND MINERAL SAMPLES - FUSED SPECIMEN**

	Mg		Al		Si		Ca		Ti	
Rock No.	A	B	A	B	A	B	A	B	A	B
I-1	0.66	0.65	8.36	8.30	35.16	35.19	0.57	0.57	0.03	0.03
I-3	2.51	2.40	7.87	7.40	23.19	24.08	5.90	6.27	1.56	1.43
M-2	1.48	1.44	14.38	13.94	22.80	23.48	1.26	1.23	0.43	0.39
M-3	7.28	0.72	10.62	10.35	25.94	26.55	8.60	9.04	0.50	0.43
302/1	0.87	0.76	6.30	5.50	8.30	10.86	2.94	3.28	0.29	0.30
DTN	0.02	0.02	35.55	35.73	17.04	17.71	0.03	0.03	0.84	0.85
UBN	21.33	20.87	1.79	1.54	18.63	19.44	0.85	0.94	0.07	0.08
NIM-S	0.27	0.28	10.42	10.35	29.66	30.43	0.47	0.42	0.02	0.02
NBS-97a	0.90	*	23.28	*	20.38	*	0.08	*	1.13	*
NBS-99a	0.01	*	12.30	*	30.45	*	1.53	*	0.006	*

	Cr		Mn		Fe		P		K	
Rock No.	A	B	A	B	A	B	A	B	A	B
I-1	0.07	0.07	0.023	0.020	0.39	0.38	0.01	0.01	3.55	3.54
I-3	0.69	0.62	0.169	0.150	11.25	9.26	0.17	0.18	1.19	1.23
M-2	0.68	0.63	0.199	0.180	6.48	5.60	0.22	0.22	6.56	6.64
M-3	0.68	0.60	0.219	0.190	3.21	2.71	0.16	0.16	0.59	0.60
302/1	0.07	0.07	0.217	0.190	32.70	25.56	0.87	0.96	0.46	0.50
DTN	0.03	0.03	0.008	0.008	0.46	0.47	0.04	0.04	0.10	0.10
UBN	0.23	0.24	0.093	0.094	5.91	5.84	0.01	0.01	0.02	0.01
NIM-S	0.003	0.003	0.008	0.007	0.97	0.85	0.05	0.05	12.73	12.70
NBS-97a	0.02	*	0.016	*	0.31	*	0.16	*	0.42	*
NBS-99a	0.02	*	0.016	*	0.05	*	0.009	*	4.32	*

Column A Results using the Lachance-Traill correction method
Column B Results using the Direct Ratio method (DR)
* Rock Nos. used as standards for the DR method ** Data for Series XY-2

TABLE 74

COMPARISON OF RESULTS* - ABSOLUTE % RELATIVE ERROR

Element	Solid		Fused	
	A	B	A	B
Magnesium	0.95	15.7	1.83	3.68
Aluminum	1.68	26.7	0.24	4.82
Silicon	2.26	9.99	0.21	6.30
Calcium	1.86	22.2	0.61	6.72
Titanium	0.58	17.4	0.15	7.05
Chromium	0.88	18.1	0.96	6.65
Manganese	2.25	21.0	0.68	9.52
Iron	1.97	24.5	0.54	11.3
Phosphorus	0.75	5.14	1.67	1.74
Potassium	1.57	9.54	0.07	4.55

Column A Results by the Lachance-Traill method
Column B Results by the Direct Ratio method (DR)

* Data for Rocks and Minerals - Series XY-2

TABLE 75

THEORETICAL CONTRIBUTIONS FROM ABSORPTION AND ENHANCEMENT EFFECTS IN ROCK AND MINERAL SAMPLES - SERIES XY-2

SOLID SPECIMEN

Analyte Element	Absorption (%)	Enhancement (%)	Major Contributors* (%)						
			Al	Si	Ca	Ti	Cr	Fe	K
Mg	93.0-95.0	5.0-7.0	2.4	4.0	2.8	0.3		1.7	1.3
Al	92.0-97.0	3.0-8.0		4.5	3.0	0.4		5.0	2.0
Si	93.0-99.0	1.0-7.0			3.2	0.4	0.1	5.1	4.3
P	93.0-99.8	0.2-7.0			3.1	0.4	0.1	5.3	
K	91.0-99.6	0.4-9.0			4.2	0.5	0.2	7.2	
Ca	91.0-99.9	0.1-9.0				2.6	0.2	8.9	
Ti	85.0-99.9	0.1-15.0					0.3	14	
Cr	71.0-99.9	0.1-29.0						28.5	
Mn	95.0-99.9	0.1-5.0						5.0	
Fe	100.0								

FUSED SPECIMEN

Analyte Element	Absorption (%)	Enhancement (%)	Major Contributors* (%)						
			Al	Si	Ca	Ti	Cr	Fe	K
Mg	96.0-98.8	1.2-4.0	0.6	1.0	1.1	0.2		2.7	1.3
Al	96.0-99.1	0.9-4.0		1.0	1.2	0.2		2.8	1.4
Si	96.0-99.8	0.2-4.0			1.3	0.2		2.8	1.6
P	97.0-99.8	0.2-3.0			1.3	0.2		2.9	
K	95.0-99.9	0.1-5.0			1.8	0.2		4.0	
Ca	98.0-99.9	0.1-2.0				0.3	0.1	5.0	
Ti	91.0-99.9	0.1-9.0					0.2	8.4	
Cr	83.0-99.9	0.1-17.0						17.4	
Mn	97.7-99.9	0.1-2.3						2.3	
Fe	100.0								

* The indicated percentages are ranges representing zero to the indicated maximum percent

TABLE 76

ABSOLUTE % RELATIVE ERRORS FOR DIFFERENT SAMPLES

SOLID SPECIMEN

Element	Allard Lake		Bauxites			Rocks and Minerals	
	ALS	TALS	BXT	DX	APD	XY-1	XY-2
Mg	33.7	1.26	0.85	0.97	1.19	1.66	0.95
Al	26.5	2.01	1.20	1.11	0.48	1.86	1.68
Si	22.9	2.72	0.49	1.49	1.70	1.99	2.26
Ca	14.6	2.93	0.37	3.08	0.99	1.38	1.83
P	--	--	0.92	0.39	0.78	3.13	0.75
K	--	--	0.96	0.21	3.07	2.14	1.57
Ti	8.6	4.32	0.71	0.57	0.80	0.83	0.58
Cr	--	1.74	0.32	--	0.00	4.09	0.88
Mn	13.8	3.92	0.09	0.53	0.94	2.03	2.25
Fe	16.9	2.91	0.98	1.23	1.03	2.14	1.97

FUSED SPECIMEN

Element	Allard Lake		Bauxites			Rocks and Minerals	
	ALS	TALS	BXT	DX	APD	XY-1	XY-2
Mg	--	0:00	0.79	0.72	3.33	0.09	1.83
Al	4.04	0.33	0.25	0.27	0.30	0.33	0.24
Si	4.09	0.02	0.21	0.17	0.56	0.22	0.21
Ca	2.12	0.20	2.00	0.62	0.30	0.41	0.61
P	--	--	0.16	0.76	0.20	2.44	1.67
K	--	--	0.37	0.44	2.62	0.39	0.07
Ti	6.56	0.21	0.21	0.21	0.00	0.00	0.15
Cr	--	0.02	1.32	--	0.10	3.77	0.96
Mn	5.47	0.46	0.85	0.07	0.03	1.60	0.68
Fe	6.38	0.49	0.39	0.43	0.17	0.54	0.54

to the efficiency of the acids in dissolving certain alloys (ie. in the case of tin), if present in high concentrations in copper alloys, dissolution is very difficult. In geological material, different fluxes may be required to ensure complete break-down of the mineral matrices present, as well as the often high silica content.

The validity of the Lachance-Traill approach can best be illustrated graphically using data for the Series TALS obtained using solid samples where the concentration span and absorption-enhancement effects are more significant. The calculated intensities (I_{corr}) (Equation 21) and known compositions of the samples are used to plot the various intensity versus concentration graphs. The efficiency of the Lachance-Traill approach in compensating for the absorption-enhancement effects is clearly shown with excellent linear relationships resulting (Figures 16, 17 and 18). This is especially significant in the case of magnesium (Figure 16) where a large scatter in the data points occurs. The data also shows why the Direct Ratio method cannot be successfully applied due to the severe matrix effects present which results in the non-linear plots for measured intensities versus concentration.

The Lachance-Traill approach has been shown to yield

Figure 16

GRAPH OF I_{Mg} VERSUS C_{Mg} (Series TALS - solid)

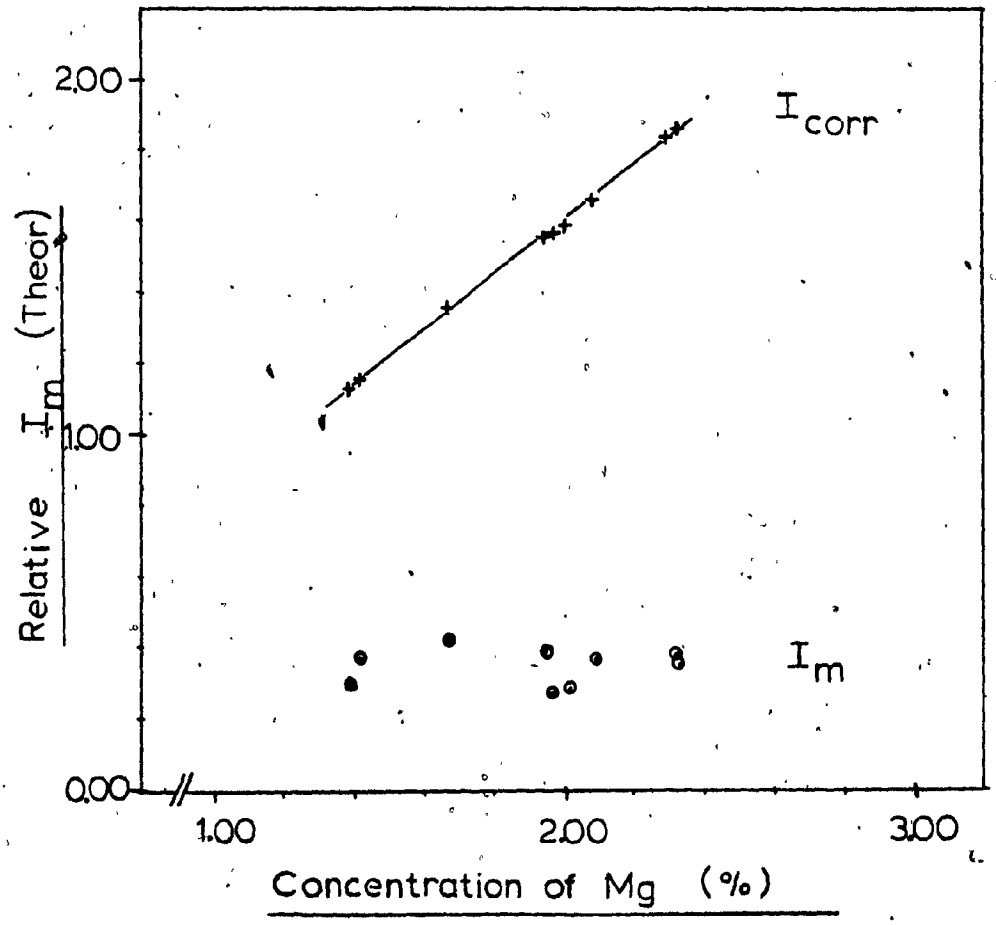

Figure 17

GRAPH OF I_{Al} VERSUS C_{Al} (Series TALS - solid)

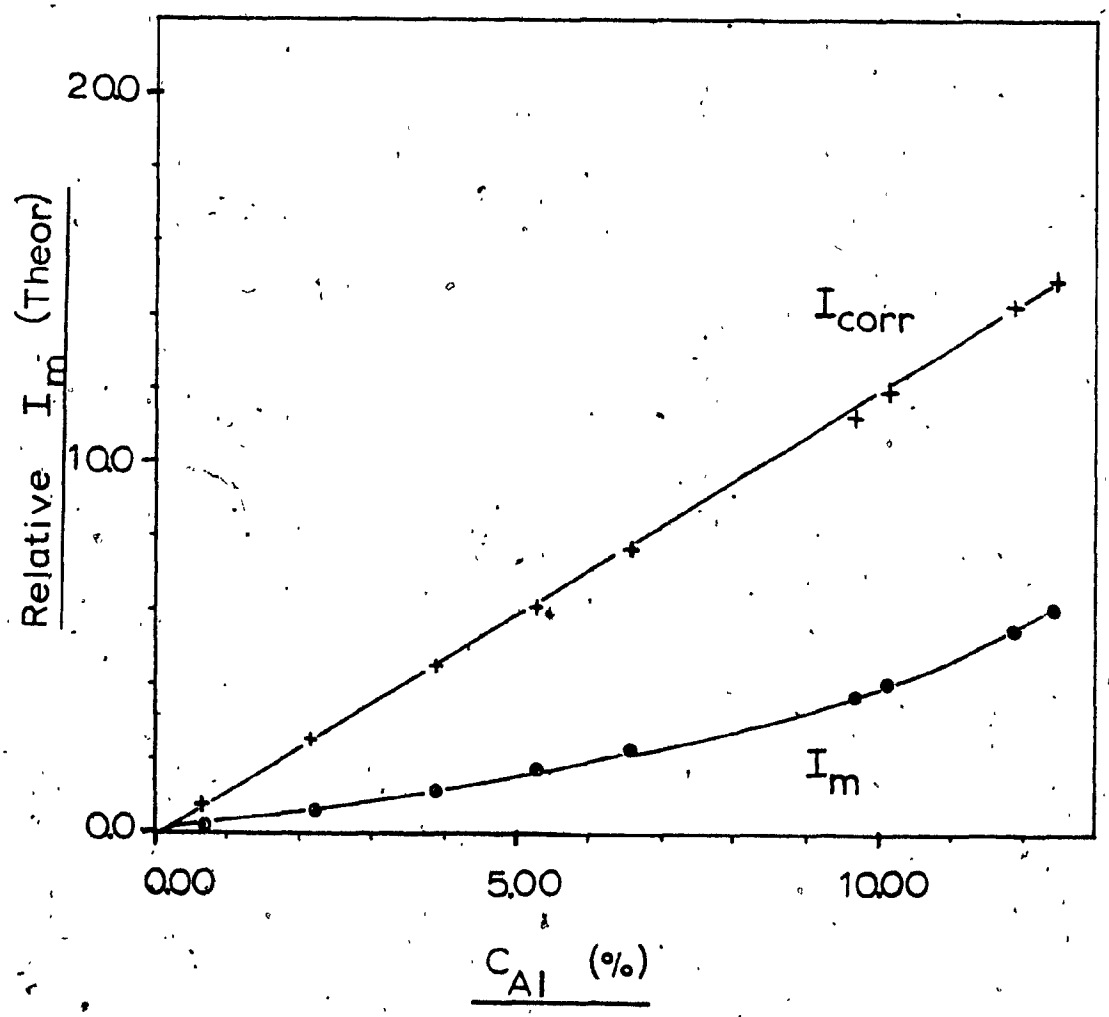

Figure 18

GRAPH OF I_{Fe} VERSUS C_{Fe} (Series TALS - solid)

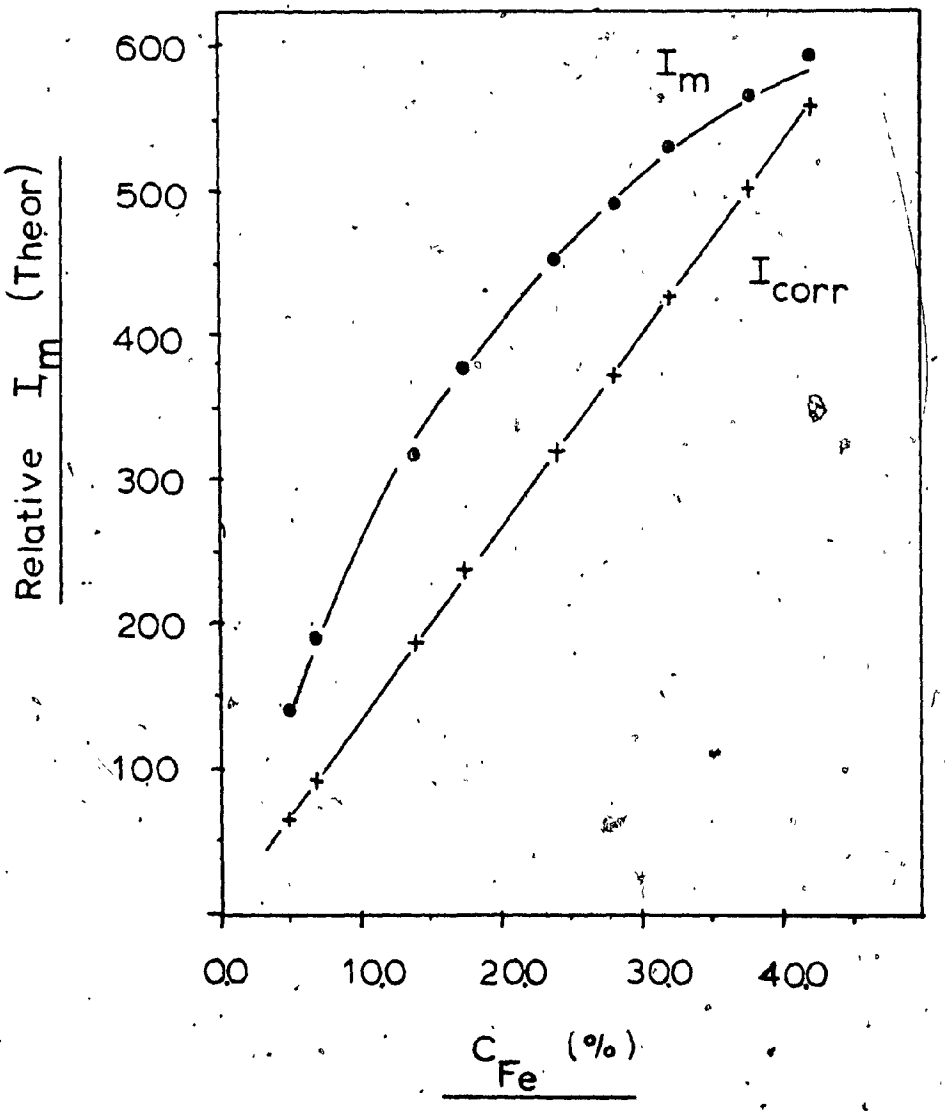

accurate results for most types of specimens over a large concentration range. Other advantages to this approach can be summarized by the following:

1. Experimentally determined α-correction coefficients derived from simple binary solutions can be successfully used in the analysis of complex multi-component systems.

2. Theoretically derived coefficients can be correlated to the experimental coefficients and can also be used.

3. Only one single standard is required in the computation of the chemical composition of solutions of unknown specimens.

4. The procedure yields simultaneously concentration values for all the elements of interest in the specimen.

5. Absorption-enhancement effects are minimized in aqueous or fused specimens.

6. Higher accuracy, as well as rapidity and flexibility show the usefulness of the empirical approach.

4. CONCLUSIONS

This investigation has revealed the following significant points:

1. Experimental coefficients are valid since they can be correlated to theoretical coefficients derived under similar experimental conditions.

2. The theoretical coefficients can be used for systems, (ie. of low Z), where α's are not easily obtained due to the low solution concentrations.

3. Matrix effects arising from elements with $Z < 11$

can be grouped into one coefficient and individual contributions need not be determined.

4. The aqueous solution as well as solid-solution techniques are comparable in yielding the same coefficients.

5. The Lachance-Traill approach adequately compensates for most absorption-enhancement effects which occur.

6. The Lachance-Traill approach yields high accuracy on the basis of a truely homogeneous sample. As such, geological specimens pressed from raw powders are not suitable for used in XRF analysis and should be fused prior to analysis.

7. The theoretical model developed allows direct comparison as to the inter-element effects which occur in complex systems and can be adequately used to obtain preliminary data for study of different effects which can arise.

8. The results indicate the validity of such an empirical approach in the analysis of a wide variety of specimens without the need of higher order correction terms.

5. SUGGESTIONS FOR FURTHER WORK

Further work should be conducted on the experimental analysis of various metal and geological specimens using different sample preparation techniques and fusion methods.

In many analyses only certain elements are required to be certified. An example of this is the analysis of bauxite ores for the Bayer process. Different ores are blended to obtain a particular overall concentration of various elements required by the process. The major components ana-

lyzed are aluminum, silicon, titanium and iron. Accordingly, in what manner could the modified approach described be applied in such cases where only a few elemental compositions are required?

This investigation has shown the usefulness of theoretically calculated XRF intensities for multi-component systems which could again serve a very significant part in these further studies preceeding experimental work. This shows only one aspect which could be extended to any number of different specimen types.

Different empirical methods could also be studied to show the further contributions of higher order coefficients and their particular advantages, if any, over the simpler techniques.

In this study, the use of wavelength dispersive XRF is emphasized. Nowadays, there is an ever increasing use of energy dispersive instruments which have the advantage of simultaneous multi-element analysis through the use of solid state detectors and multi-channel analyzers. With respect to this type of instrument, can the modified Lachance-Traill approach be used just as efficiently? It would appear to be highly desirable since the accumulated

intensities can easily be transferred to a micro-processor programmed to apply the modified Lachance-Traill approach. It is understood that due to the differing geometries in these instruments, a different set of matrix and inter-element correction coefficients may be required but could be theoretically evaluated using the proper equations for this type of system.

REFERENCES

1. Rasberry, S.D. and K.F.J. Heinrich, Anal. Chem. 46, 81 (1974).

2. Mitchell, B.J. and J.E. Kellam, Appl. Spectrosc. 22, 742 (1968).

3. Gillam, E. and H.T. Heal, Brit. J. Appl. Phys. 3, 353 (1952).

4. Sherman, J., Spectrochim. Acta 7, 283 (1955).

5. Sherman, J., Adv. X-Ray Anal. 1, 231 (1957).

6. Shiraiwa, T. and N. Fujino, Jap. J. Appl. Phys. 5, 886 (1966).

7. Shiraiwa, T. and N. Fujino, Bull. Chem. Soc. Jap. 40, 2289 (1967).

8. Müller, R.O., Spectrochim. Acta 18,123 (1962).

9. Bertin, E.P., "Principles and Practice of X-Ray Spectrometric Analysis", Plenum Press, New York (1975).

10. Müller, R.O., Spectrochim. Acta 18, 1515 (1962).

11. Pollai, G., M. Mantler and H. Ebel, Spectrochim. Acta 26B, 733 (1971).

12. Pollai, G. M. Mantler and H. Ebel, Spectrochim. Acta 26B, 747 (1971).

13. Pollai, G. and H. Ebel, Spectrochim. Acta 26B, 761 (1971).

14. Ebel, H., J. Derdan and G. Pollai, Spectrochim. Acta 26B, 237 (1971).

15. Tertian, R., Spectrochim. Acta 26B, 71 (1971).

16. Tertian, R., Spectrochim. Acta 27B, 159 (1972).

17. Müller, R.O., "Spectrochemical Analysis by XRF", Plenum Press, New York (1972).

18. Birks, L.S., "X-Ray Spectrochemical Analysis", Inter-Science Publication, New York and London (1959).

19. Criss, J.W. and L.S. Birks, Anal. Chem. 40, 1080 (1968).

20. Gilfrich, J.V. and L.S. Birks, Anal. Chem. 40, 1077 (1968).

21. Kalman, Z.H. and L. Heller, Anal. Chem. 34, 946 (1962).

22. Stephenson, D.A., Spectrochim. Acta 27B, 153 (1972).

23. Pluchery, M.M., Spectrochim. Acta 19, 533 (1963).

24. Pluchery, M.M., Spectrochim. Acta 24B,351 (1969).

25. Pluchery, M.M., Spectrochim. Acta 25B, 83 (1970).

26. Leroux, J., M. Mahmud and A.B.C. Davey, Cdn. Spectrosc. 12, 169 (1967).

27. Tertian, R. and R. Vié le Sage, X-Ray Spectrom. 5, 73 (1976).

28. Tertian, R., Spectrochim. Acta 27B, 155 (1972).

29. Jenkins, R., Adv. X-Ray Anal. 19, 1 (1975).

30. Jenkins, R., "Introduction to X-Ray Spectrometry", Heyden and Son, Ltd., London (1974).

31. Gould, R.W., Amer. Lab. 7, 12 (1974).

32. Mencik, Z., X-Ray Spectrom. 4, 108 (1975).

33. Criss, J.W., L.S. Birks and J.V. Gilfrich, Anal. Chem. 50, 33 (1978).

34. Gould, R.W. and S.R. Bates, X-Ray Spectrom. 1, 29 (1972).

35. Palme, C. and E. Jagoutz, Anal. Chem. 49, 717 (1977).

36. Flanagan, F.J., Geochim. Cosmochim. Acta 37, 1189 (1977).

37. Stephenson, D.A., Anal. Chem. 43, 1761 (1971).

38. Ciccarelli, M.F., Anal. Chem. 49, 345 (1976).

39. Laguitton, D. and M. Mantler, Adv. X-Ray Anal 20, 515 (1976).

40. Englund, E., Colloquium Spectroscopy Int. [Proc.] 18th, 3, 752 (1975).

41. Hawthorne, A.R. and R.P. Gardner, Anal. Chem. 48, 2130 (1976).

42. Gardner, R.P. and A.R. Hawthorne, X-Ray Spectrom. 4, 138 (1975).

43. Hawthorne, A.R. and R.P. Gardner, Anal. Chem. 47, 2290 (1975).

44. Liebhafsky, H.A., H.G. Pfeiffer, E.H. Winslow and P.D. Zemany, "X-Ray Absorption and Emission in Analytical Chemistry", John Wiley and Sons, New York (1960).

45. Beattie, M.J. and R.M. Brissey, Anal. Chem. 26, 980 (1954).

46. Sherman, J., ASTM Spec. Tech. Pub. 157, 27 (1954).

47. Burnam, H.D., J. Hower and L.C. Jones, Anal. Chem. 29, 1827 (1957).

48. Lachance, G.R. and R.J. Traill, Cdn. Spectrosc. 11, 43 (1966).

49. Marti, W., Spectrochim. Acta 18, 1499 (1962).

50. Lachance, G.R., Geological Survey of Canada, Paper 64-50 (1964).

51. Traill, R.J. and G.R. Lachance, Geological Survey of Canada, Paper 64-57 (1965).

52. Traill, R.J. and G.R. Lachance, Cdn. Spectrosc. 11, 63 (1966).

53. Claisse, F. and M. Quintin, Cdn. Spectrosc. 12, 129 (1967).

54. Rousseau, R. and F. Claisse, X-Ray Spectrom. 3, 31 (1974).

55. Lachance, G.R., Cdn. Spectrosc. 15, 64 (1970).

56. Andrews, E.A., 9th X-Ray Anal. Conf., Exeter, U.K. (1974).

57. Tertian, R., X-Ray Spectrom. 2, 95 (1973).

58. Tertian, R., X-Ray Spectrom. 4, 52 (1975).

59. Tertian, R., X-Ray Spectrom. 3, 302 (1974).

60. Tertian, R., Adv. X-Ray Anal. 19, 85 (1975).

61. Tertian, R., X-Ray Spectrom. 3, 102 (1974).

62. Heinrich, K.F.J. and S.D. Rasberry, Adv. X-Ray Anal. 17, 309 (1973).

63. Claisse, F. and T.P. Thinh, Anal. Chem. 51, 954 (1979).

64. Fréchette, G.? J.C. Hébert, T.P.Thinh, R. Rousseau and F. Claisse, Anal. Chem. 51, 957 (1979).

65. Alley, B.J. and R.H. Meyers, Anal. Chem. 37, 1685 (1965).

66. Mitchell, B.J. and F.N. Hopper, Appl. Spectrosc. 20, 172 (1966).

67. Lucas-Tooth, H.J. and B.J. Price, Metalurgia 64, 149 (1961).

68. Lucas-Tooth, H.J. and C. Pyne, Adv. X-Ray Anal. 8, 523 (1964).

69. Thiele, M., Siemens-Z. 44, 707 (1970).

70. Budesinsky, B.W., Anal. Chim. Acta 100, 87 (1975).

71. Budesinsky, B.W., Anal. Chim. Acta 104, 9 (1979).

72. Caldwell, V.E., X-ray Spectrom. 5, 31 (1976).

73. Backerud, L., Appl. Spectrosc. 21, 315 (1967).

74. Jenkins, R. and J.L. de Vries, "Practical X-Ray Spectrometry", Springer-Verlag, New York (1967).

75. Kilday, B.A. and R.E. Michaelis, Appl. Spectrosc. 16, 137 (1962).

76. Claisse, F., Quebec Dept. of Mines, Progress Report 327 (1956).

77. Claisse, F., Norelco Reporter 4, 95 (1957).

78. Claisse, F., Quebec Dept. of Mines, Progress Report 402 (1960).

79. Claisse, F., Cdn. Spectrosc. 12, 20 (1967).

80. Claisse, F. and C. Samson, Adv. X-Ray Anal. 6, 335 (1962).

81. Gunn, E.L., Adv. X-Ray Anal. 4, 382 (1961).

82. Madlem, K.W., Adv. X-Ray Anal. 9, 441 (1966).

83. Waterbury, G.R. and E.A. Hakkila, Anal. Chem. 37, 1773 (1965).

84. Zimmerman, J.B. and J.C. Ingles, Dept. of Energy, Mines and Resources, Ottawa, Canada, Report No. EMA 72-14 (1972).

85. Kang, C.C., E.W. Keel and E. Solomon, Anal. Chem. 32, 221 (1960).

86. Dwiggins, C.W., Jr., Anal. Chem. 36, 1577 (1964).

87. Nguyen, A.D., Doctoral Thesis, Dept. of Chemistry, Concordia University, Montreal, Quebec (1974).

88. Dick, J.G. and A.D. Nguyen, Cdn. Spectrosc. 19, 110 (1974).

89. Dick, J.G. and A.D. Nguyen, Cdn. Spectrosc. 19, 141 (1974).

90. Dick, J.G., C.C. Wan and R. DiFruscia, X-Ray Spectrom. 6, 212 (1977).

91. Wan, C.C., Masters Thesis, Dept. of Chemistry, Concordia University, Montreal, Quebec (1975).

92. DiFruscia, R., Undergraduate Thesis, Dept. of Chemistry, Concordia University, Montreal, Quebec (1975).

93. DiFruscia, R., J.G. Dick and C.C. Wan, X-Ray Spectrom. 7, 86 (1978).

94. Wan, C.C., Doctoral Thesis, Dept. of Chemistry, Concordia University, Montreal, Quebec (1980).

95. DiFruscia, R. and C.C. Wan, Unpublished data

96. Backerud, L., X-Ray Spectrom. 1, 3 (1972).

97. Alvarez, A.G. and J.L. de Vries, Proc. Swansea Conf. on X-Ray Analysis 16 (1966).

98. Patterson, S.H., U.S. Geological Survey Bulletin 1228 (1967).

99. Flanagan, F.J., Geochim. Cosmochim. Acta 33, 81 (1969).

100. Abbey, S., Geological Survey of Canada, Paper 77-34 (1977).

APPENDIX A

PROGRAM ALPHAMAT

PURPOSE: To determine matrix effect correction coefficients from elemental concentration and x-ray intensity data for binary solution systems.

METHOD: The α-correction coefficients are determined using Equation 18. The calculation is carried out for all possible combinations and an average coefficient is determined after statistical analysis is performed.

PROGRAM ALPHAMAT

```
00100 PROGRAM ALPHMAT(TAPE3,OUTPUT,TAPE4,TAPE5)
00110 DIMENSION MM(100),NN(100),ALPHA(500),CX(500),CI(10),CM(10),
00120+C(10),CIC(10),CIO(10),ZZP(500),DX(500)
00130 REWIND 3
00140 CALL GET(5HTAPE3,5HTAPE3,0,0)
00141 CALL GET(5HTAPE5,5HTAPE5,0,0)
00150C-----------------------------------------------------------------
00160C  ALPHA COEFFICIENTS FOR THE DETERMINATION OF MATRIX
00170C  EFFECTS ON THE ANALYSIS OF AQUEOUS MEDIA BY X-RAY
00180C  FLOURESCENCE SPECTROMETRY
00190C  ****'  APRIL,1975******
00200C     WRITTEN BY***** ROBERT DIPUSCIA *****
00210C-----------------------------------------------------------------
00211 IPW=INDEX=0
00220 7 READ(3,1)SX
00230 READ(3,9)NX
00240 READ(3,20)(C(I),I=1,NX)
00250 READ(3,20)(CM(I),I=1,NX)
00260 READ(3,20)(CI(I),I=1,NX)
00270 1 FORMAT(A2)
00280 9 FORMAT(I1)
00290 20 FORMAT(6F15.6)
00300 MX=NX-1
00310 I=0
00320 DO 100 M=1,MX
00330 NM=M+1
00340 DO 100 N=NM,NX
00350 I=I+1
00360 A = (CI(N)*C(M))-(CI(M)*C(N))
00370 B=CI(M)*C(N)*CM(M)
00380 D=CI(N)*C(M)*CM(N)
00390 ALPHA(I)=A/(B-D)
00400 MM(I)=M     $   NN(I)=N
00410 100 CONTINUE
00420 PRINT,* COEFFICIENTS CALCULATED *
00421 CALL XMEAN(ALPHA,I,STDE,XA)
00422 CALL REJECT(ALPHA,I,STDE,XA,CX,INDEX)
00423 IPW=IPW+1
00424 IF(IPW.EQ.3)89,99
00425 89 CALL REPLACE(5HTAPE5,5HTAPE5,0,0)
00426 REWIND 5
00427 READ(5,)(ZZP(IX),IX=1,INDEX)
00428 CALL XMEAN(ZZP,INDEX,STDEVA,XMEEN)
00429 INDE=INDEX     $ INDEX=0
00430 CALL REJECT(ZZP,INDE,STDEVA,XMEEN,DX,INDEX)
00431 PRINT 109,SX,INDEX,XMEEN,STDEVA
00432 109 FORMAT(//5X,*SERIES MATRIX OF *A2/5X*NO OF ACC DATA =*I4/
00433+5X*MEAN VALUE =*E13.9/5X*STD DEV +/-= * E16.5//)
00440 IPW=INDEX=0
00441 REWIND 5
00442 99 CONTINUE
00450 CALL RESULTS(CI,CM,XA,CIC,CIC,STD,XC,NX,C)
00460 CALL OUTPT(MM,NN,ALPHA,CX,STDE,XA,CI,CM,C,CIC,CIO,STD,XC,NX,I,SX)
00470 READ(3,9)ING
```

```
00480 IF (ING.EQ.0)6,7
00490 6 PRINT,*  EXIT FROM FILE  *
00500 PRINT,*  OUTPUT AVAILABLE FROM TAPE 4    *
00510 REWIND 4
00520 CALL SAVE(5HTAPE4,5HTAPE4,0,0,0)
00530 STOP
00540 END
00550C*****************************************************************
00560C                    MEAN AND STD DEV  SUBROUTINE
00570C*****************************************************************
00580 SUBROUTINE XMEAN (ALPHA ,N,STDE,XA)
00590 DIMENSION ALPHA(500)
00600 SUM=0.0
00610 DO 1100 K=1,N
00620 1100 SUM=SUM+ALPHA(K)
00630 FN=N
00640 XA=SUM/FN
00650 SUM=0.0
00660 DO 1101 L=1,N
00670 1101 SUM=SUM+(ALPHA(L)-XA)**2
00680 FK=N-1
00690 STDE=SQRT(SUM/FK)
00700 RETURN
00710 END
00720C*****************************************************************
00730C                        STATISTICAL REJECTION SUBROUTINE
00740C*****************************************************************
00750 SUBROUTINE REJECT(ALPHA,N,STDE,XA,CX,INDEX)
00760 DIMENSION CX(500),ALPHA(500)
00770 CCUNT=SUM=0.0
00780 DO 1000 II=1,N
00790 IF(ABS(ALPHA(II)-XA).GE.STDE)1001,1002
00800 1001 CX(II)=5H(.R.)
00810 GO TO 1000
00820 1002 CX(II)=5H
00830 SUM=SUM+ALPHA(II)
00840 CCUNT=CCUNT+1
00850 1000 CONTINUE
00860 XA=SUM/CCUNT
00870 COUNT=COUNT-1
00880 SUM=0.0
00890 DO 1004 L=1,N
00900 IF(CX(L).EQ.5H     )1005,1004
00910 1005 SUM=SUM+(ALPHA(L)-XA)**2
00911 WRITE(6,)ALPHA(L)
00912 INDEX=INDEX+1
00920 1004 CONTINUE
00930 STDE =SQRT(SUM/COUNT)
00940 RETURN
00950 END
00960C*****************************************************************
00970C                        CALCULATED RESULTS USING ALPHA
00980C*****************************************************************
00990 SUBROUTINE RESULTS (CI,CM,XA,CIC,CIO,STD,XO,NX,C)
```

```
01000 DIMENSION C(10),CI(10),CM(10),CIC(10),CIO(10)
01010 DO 1007 J=1,NX
01020 W=CI(J)*(1.+(XA*CM(J)))
01030 CIC(J)=AINT(W)
01040 Z=CIC(J)/C(J)
01050 1007 CIO(J)=AINT(Z)
01060 CALL XMEAN (CIO,NX,STD,XO)
01065 XO=AINT(XO)
01070 RETURN
01080 END
01090C*****************************************************************
01100C                        OUTPUT TO FILE RCUTINE
01110C*****************************************************************
01120 SUBROUTINE OUTPT(MM,NN,ALPHA,CX,STDE,XA,CI,CM,C,CIC,CIO,STD,XO,
01130+NX,I,SX)
01140 DIMENSION MM(100),NN(100),ALPHA(100),C(10),CX(100),CI(10),CM(10),
01150+CIC(10),CIO(10)
01160 WRITE(4,49)
01170 WRITE(4,50)SX
01180 WRITE(4,51)SX,SX
01190 WRITE(4,52)(K,C(K),CM(K),CI(K),CIC(K),CIO(K),K=1,NX)
01200 WRITE(4,53)XO,STD
01210 WRITE(4,54)
01220 WRITE(4,55)(MM(K),NN(K),ALPHA(K),CX(K),K=1,I)
01230 WRITE(4,56)XA,STDE
01235 WRITE(4,59)
01236 59 FORMAT(5/)
01240 WRITE(4,57)
01250 49 FORMAT(1H1)
01260 50 FORMAT(//45X,*EFFECT OF MATRIX ON * A2///)
01270 51 FORMAT(25X,*SOLT*3X*C(*A2*)*6X*CM*8X*I(*A2*KA)*5X*I(CORR)*
01271+7X*IO*//)
01280 52 FORMAT(26X,I1,4X,F7.5,4X,F7.5,3X,F8.1,5X,F7.1,4X,F8.1)
01290 53 FORMAT(//50X,*AVE IO =  *F9.1,* +/- *E12.5//)
01300 54 FORMAT(25X * DATA RESULTS -*//)
01310 55 FORMAT(25X,I1,*/*,I1,8X,F8.4,*...*8X,A5)
01320 56 FORMAT(//25X,*AVERAGE VALUE = * 3X,F13.9//25X* STD DEV *
01330+7X,*=* 3X*+/-  *E16.5)
01340 57 FORMAT (1H1)
01350 PRINT,*  OUTPUT TO FILE ESTABLISHED  *
01360 RETURN
01370 END
```

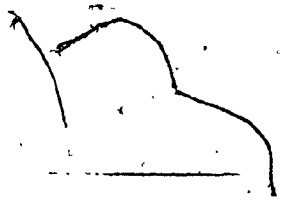

PROGRAM INTERM1

PURPOSE: To determine inter-element and "third-element" correction coefficients from elemental concentration and x-ray intensity data for binary and ternary solution systems.

METHOD: The α-correction coefficients are determined using Equations 19 and 20. The calculation is carried out for all possible combinations and an average coefficient is determined after statistical analysis is performed.

PROGRAM INTERM1

```
00100 PROGRAM INTERAL (TAPE3,OUTPUT,TAPE4,TAPE5)
00110 DIMENSION MM(100),NN(100),ALPHA(100),CX(100),CI(10),CM(10),
00120+C(10),CIC(10),CIO(10),C2(10),CIO(10),ZZP(100)
00130 REWIND 3
00140 CALL GET(5HTAPE3,5HTAPE3,0,0)
00141 CALL GET(5HTAPE5,5HTAPE5,0,0,0)
00150C-----------------------------------------------------------------
00160C  ALPHA COEFFICIENTS FOR THE DETERMINATION OF MATRIX
00170C  EFFECTS ON THE ANALYSIS OF AQUEOUS MEDIA BY X-RAY
00180C  FLOURESCENCE SPECTROMETRY
00190C  ****    APRIL,1975******
00200C      WRITTEN BY***** ROBERT DIFRUSCIA *****
00210C-----------------------------------------------------------------
00211 IPW=INDEX=0
00220 7 READ(3,1)SX,PX
00230 READ(3,9)NX
00235 READ(3,108)AM
00240 READ(3,20)(C(I),I=1,NX)
00245 READ(3,20)(C2(I),I=1,NX)
00250 READ(3,20)(CM(I),I=1,NX)
00260 READ(3,20)(CI(I),I=1,NX)
00267 PRINT,*FILE READ*
00270 1 FORMAT(2A2)
00280 9 FORMAT(1I1)
00290 20 FORMAT(6F15.6)
00295 108 FORMAT(F15.6)
00300 MX=NX-1
00310 I=0
00320 DO 100 M=1,MX
00330 NM=M+1
00340 DO 100 N=NM,NX
00350 I=I+1
00360 A=CI(N)*C(M)*(1.-(AM*CM(N)))
00370 B=CI(M)*C(N)*(1.-(AM*CM(M)))
00380 D=(CI(M)*C(N)*C2(M))-(CI(N)*C(M)*C2(N))
00390 ALPHA(I)=(A-B)/D
00400 MM(I)=M     $    NN(I)=N
00410 100 CONTINUE
00420 PRINT,* COEFFICIENTS CALCULATED *
00430 CALL XMEAN(ALPHA,I,STDE,XA)
00440 CALL REJECT(ALPHA,I,STDE,XA,CX,INDEX)
00441 IPW=IPW+1
00442 IF(IPW.EQ.3)89,99
00443 89 CALL REPLACE(5HTAPE5,5HTAPE5,0,0)
00444 REWIND 5
00445 READ(5,)(ZZP(I),I=1,INDEX)
00446 CALL XMEAN(ZZP,INDEX,STDEVA,XMEEN)
00447 INDE=INDEX
00448 CALL REJECT(ZZP,INDE,STDEVA,XMEEN,CX,INDEX)
00449 PRINT 109 ,PX,SX,INDE,XMEEN,STDEVA
00450 109 FORMAT(//5X,*SERIES OF EFFECT OF *A2* ON *A2/5X*NO OF ACC DATA*
00451+I4/5X*MEAN VALUE =*F13.9/5X*STD DEV  +/-= *E16.5//)
00452 IPW=INDEX=0
00453 REWIND 5
```

```
00454 99 CONTINUE
00459 CALL RESULTS(CI,CM,XA,CIC,CIO,STD,XO,NX,C,C2,AM,CID)
00460 CALL OUTPT(MM,NN,ALPHA,CX,STDE,XA,CI,CM,C,CIC,CIO,STD,XO,NX,I,SX,
00465+PX,CID,C2)
00470 READ(3,9)ING
00480 IF (ING.EQ.0)6,7
00490 6 PRINT,*  EXIT FROM FILE  *
00500 PRINT,*    OUTPUT AVAILABLE FROM TAPE 4     *
00510 REWIND 4
00520 CALL SAVE(5HTAPE4,5HTAPE4,0,0,0)
00530 STOP
00540 END
00550C*****************************************************************
00560C                    MEAN AND  STD DEV  SUBROUTINE
00570C*****************************************************************
00580 SUBROUTINE XMEAN (ALPHA ,N,STDE,XA)
00590 DIMENSION ALPHA(100)
00600 SUM=0.0
00610 DO 1100 K=1,N
00620 1100 SUM=SUM+ALPHA(K)
00630 FN=N
00640 XA=SUM/FN
00650 SUM=0.0
00660 DO 1101 L=1,N
00670 1101 SUM=SUM+(ALPHA(L)-XA)**2
00680 FK=N-1
00690 STDE=SQRT(SUM/FK)
00700 RETURN
00710 END
00720C*****************************************************************
00730C                    STATISTICAL REJECTION SUBROUTINE
00740C*****************************************************************
00750 SUBROUTINE REJECT(ALPHA,N,STDE,XA,CX,INDEX)
00760 DIMENSION CX(100),ALPHA(100)
00770 COUNT=SUM=0.0
00780 DO 1000 II=1,N
00790 IF(ABS(ALPHA(II)-XA).GE.STDE)1001,1002
00800 1001 CX(II)=5H(,R.)
00810 GO TO 1000
00820 1002 CX(II)=5H
00830 SUM=SUM+ALPHA(II)
00840 COUNT=COUNT+1
00850 1000 CONTINUE
00860 XA=SUM/COUNT
00870 COUNT=COUNT-1
00880 SUM=0.0
00890 DO 1004 L=1,N
00900 IF(CX(L).EQ.5H     )1005,1004
00910 1005 SUM=SUM+(ALPHA(L)-XA)**2
00911 WRITE(5,)ALPHA(L)
00912 INDEX=INDEX+1
00920 1004 CONTINUE
00930 STDE =SQRT(SUM/COUNT)
00940 RETURN
```

```
00950 END
00960C*****************************************************************
00970C                    CALCULATED RESULTS USING ALPHA
00980C*****************************************************************
00990 SUBROUTINE RESULTS(CI,CM,XA,CIC,CIO,STD,XO,NX,C,C2,AM,CID)
01000 DIMENSION C(10),CI(10),CM(10),CIC(10),CIO(10),C2(10),CID(10)
01010 DO 1007 J=1,NX
01020 W=CI(J)*(1.+(AM*CM(J))+(XA*C2(J)))
01030 CIC(J)=AINT(W)
01031 Z2=CI(J)*(1.+(AM*CM(J)))
01032 CID(J)=AINT(Z2)
01040 Z=CIC(J)/C(J)
01050 1007 CIO(J)=AINT(Z)
01060 CALL XMEAN (CIO,NX,STD,XO)
01065 XO=AINT(XO)
01070 RETURN
01080 END
01090C*****************************************************************
01100C                    OUTPUT TO FILE ROUTINE
01110C*****************************************************************
01120 SUBROUTINE OUTPT(MM,NN,ALPHA,C,CX,CI,CM,CIC,CIO,STD,XO,
01130+NX,I,SX,PX,CID,C2)
01140 DIMENSION MM(100),NN(100),ALPHA(100),C(10),CX(100),CI(10),CM(10),
01150+CIC(10),CIO(10),CID(10),C2(10)
01160 WRITE(4,49)
01170 WRITE(4,50)PX,SX
01180 WRITE(4,51)SX,PX,SX
01190 WRITE(4,52)(K,C(K),C2(K),CM(K),CI(K),K=1,NX)
01191 WRITE(4,60)
01192 60 FORMAT(//)
01193 WRITE(4,58)PX,SX
01195 WRITE(4,59)(K,CID(K),CIC(K),CIO(K),K=1,NX)
01200 WRITE(4,53)XO,STD
01210 WRITE(4,54)
01220 WRITE(4,55)(MM(K),NN(K),ALPHA(K),CX(K),K=1,I)
01230 WRITE(4,56)XA,STDE
01240 WRITE(4,57)
01250 49 FORMAT(1H1,3(/))
01260 50 FORMAT(50X,*EFFECT OF *A2* ON *A2//)
01271 51 FORMAT(25X*SOLT*4X*C(*A2*)*6X*C'(*A2*)*8X*CM*6X*I(*A2*KA)*/)
01280 52 FORMAT(26X,I1,4X,F7.5,4X,F7.5,4X,F7.5,3X,F8.1)
01285 58 FORMAT(25X,*SOLT*5X*I(CORR M)*7X*I(CORR M + *A2*)*7X*IO(*
01286+ A2* KA)*/)
01287 59 FORMAT(26X,I1,7X,F7.1,10X,F7.1,11X,F8.1)
01290 53 FORMAT(/55X,*AVE IO = *F9.1,* +/- *E12.5///)
01300 54 FORMAT(25X* DATA RESULTS -*/)
01310 55 FORMAT(25X,I1,*/*,I1,8X,F8.4,*...*8X,A5)
01320 56 FORMAT(/25X,* AVERAGE VALUE = *3X,F13.9/25X* STD.DEV. *
01330+7X,*=*3X*+/-  *E16.5.6(/))
01340 57 FORMAT (1H1)
01360 RETURN
01370 END
```

APPENDIX B

PROGRAM THEORET and MUV

PURPOSE: To determine theoretical x-ray intensities for binary solution systems using elemental concentrations and appropriate instrumental parameters.

METHOD: Intensities are calculated using Equation 4 which is a simplified form of the fundamental XRF Equations 1 and 2. The algorithm uses the method of Criss and Birks (19).

PROGRAM THEORET

```
00100 PROGRAM THEORET(INPUT,OUTPUT,TAPE1,TAPE2,TAPE3)
00110 DIMENSION XL(500),UA(500),UB(500),UM(500),XIDL(500),XYDL(150),UX(50)
00111+,UXT(20),U1(20),U2(20),U3(20),XXK(20)
00120 CALL GET(5HTAPE1,5HTAPE1,0,0)
00130 REWIND 1
00131 CALL GET(5HTAPE3,5HTAPE3,0,0)
00132 REWIND 3
00133 66 REWIND 1
00144 PRINT,*READ IN MATRIX MASS ABSORPTION FOR K ALPHA RADI*
00145 READ,CXT
00150 READ(3,)N1,NT
00151 IF(N1.GT.136)80,81
00152 80 NP=136
00153 X=2.99    $  XYZ=2.49
00154 DO 154 I=137,N1
00155 X=X+0.02
00156 XL(I)=X
00157 UM(I)=COEFF(2.9857,3.1989,XL,I)
00158 XYZ=XYZ-0.07
00159 XIDL(I)=XYZ
00165 154 CONTINUE
00166 GO TO 82
00167 81 NP=N1
00170 82 READ(1,1)(XL(I),XIDL(I),XYDL(I),UM(I),I=1,NP)
00180 1 FORMAT(2X,F5.3,2X,2(F6.2,2X),F6.2)
00190 N2=N1+1
00200 IF(NT.EQ.1)2,4
00210 2 DO 3 I=1,NP
00220 3 XIDL(I)=XYDL(I)
00230 4 READ(3,)A,B,C,D,E,F,ED,FD
00240 CALL XMASS(N1,N2,XL,A,B,C,D,E,F,ED,FD,UA)
00260 6 READ(3,45)APXC
00270 WRITE(2,45)APXC
00280 45 FORMAT(A4)
00300 READ(3,)N2,A,B,C,D,E,F,ED,FD
00310 CALL XMASS(N1,N2,XL,A,B,C,D,E,F,ED,FD,UB)
00330 READ(3,)AX,CX,CA,JK
00335 IF(N2.EQ.1500)GO TO 340
00350 READ(3,)NXT
00380 READ(3,)(XXK(I),I=1,NXT)
00400 READ(3,)(U1(I),U2(I),U3(I),I=1,NXT)
00410 340 DO 200 II=1,10
00420 CA=II*0.1
00430 CM=0.0   $  CB=1.-CA
00440 IF(N2.EQ.1500)GO TO 370
00450 DO 9 J=1,NXT
00470 UXT(J)=(U1(J)*CA)+(U2(J)*CB)+(U3(J)*CM)
00475 9 CONTINUE
00480 370 XP=XXP=XXS=0.0
00490 XK=(AX*CA)+(CX*CB)+(CXT*CM)
00500 XB=1.414
00520 DO 100 I=1,N1
```

```
00530 A=XIDL(I)*UA(I)
00540 B=(UA(I)*CA)+(UB(I)*CB)+(UM(I)*CM)
00550 CL=A/(B+XK)
00560 XP=XP+CL
00570 CD=1./UA(I)
00580 XXP=0.0
00590 IF(N2.EQ.1500)100,201
00600 201 IF(XL(I).GT.XL(N2))100,202
00610 202 DO 99 J=1,NXT
00611 XY=XXK(J)/(2.*XB)
00620 C=UXT(J)
00630 YA=1.+((B*XB)/C)
00640 YB=1.+((XK*XB)/C)
00650 YP=((1./B)*ALOG(YA))+((1./XK)*ALOG(YB))
00660 XXP=XXP+(U1(J)*UB(I)*YP*XY)
00670 99 CONTINUE
00680 XXS=XXS+(XXP*CL*CD)
00690 100 CONTINUE
00700 XXP=XXS*CB
00710 TOT=XP+XXP
00720 ZP1=(XP/TOT)*100.
00730 ZP2=(XXP/TOT)*100.
00740 WRITE(2,20)CA,CB,CM,XP,XXP,TOT,ZP1,ZP2
00750 20 FORMAT(2X,3(F6.4,4X),3(F10.2,4X),5X,2(F6.2,2X))
00760 200 CONTINUE
00761 PRINT,*OUTPUT TO FILE*
00770 IF(JK.EQ.0)5,6
00780 5 READ(3,)JL
00781 IF(JL.EQ.0)7,66
00782 7 CALL SAVE(5HTAPE2,5HTAPE2,0,0,0)
00783 PRINT,*OUTPUT AVAILABLE TAPE2*
00790 STOP
00800 END
00810 SUBROUTINE XMASS(N1,N2,XL,A,B,C,D,E,F,ED,FD,UX)
00820 DIMENSION XL(500),UX(500)
00830 DO 101 I=1,N1
00840 IF(XL(I).LT.1.00)102,103
00850 102 UX(I)=A+(B*XL(I))+(C*(XL(I)**2))+(D*(XL(I)**3))
00855 GO TO 101
00860 103 IF(I.GT.N2)104,105
00870 104 E=ED
00880  F=FD
00890 105 XX=E*ALOG(XL(I))
00900 UX(I)=F*EXP(XX)
00910 101 CONTINUE
00920 RETURN
00930 END
00940 FUNCTION COEFF(A,C,XL,I)
00950 DIMENSION XL(1)
00960 XX=A*ALOG(XL(I))
00970 COEFF=C*EXP(XX)
00980 RETURN
00990 END
```

```
 78/05/04. 17.14.24.
PROGRAM   MUV

00100 PROGRAM THEORY(INPUT,OUTPUT,TAPE1,TAPE6,TAPE2,TAPE3)
00110 DIMENSION XL(200),U(200,20),N2(20),UM(20),IJ(20),C(20),
00120+XXK(20),US(15,20),NP1(20),NL(20),XIDL(200),XYDL(200),
00130+UXT(20),XXS(20),XXY(20),APXC(20)
00131+,EDLIM(30)
00140 CALL GET (5HTAPE1,5HTAPE1,0,0)
00150 CALL GET(5HTAPE6,5HTAPE6,0,0)
00160 CALL GET(5HTAPE3,5HTAPE3,0,0)
00170 REWIND 3
00180 REWIND 1
00185 REWIND 6
00190 READ(3,)N1,NT,N,NTT
00191 READ(6,10)((U(I,J),J=1,19),I=1,N1)
00192 READ(1,20)(XL(I),XIDL(I),XYDL(I),I=1,N1)
00210 READ(3,)(N2(I),I=1,N)
00220 66 CONTINUE
00230 10 FORMAT(5X,9F8.2,/10F8.2)
00250 READ(3,11)AX,BXC
00260 11 FORMAT(2A2)
00265 WRITE(2,11)AX,BXC
00280 20 FORMAT(2X,F5.3,2X,2(F6.2,2X))
00290 READ(3,)NP,NQ
00300 READ(3,)(IJ(J),J=1,N)
00305 READ(3,)(UM(J),J=1,N)
00310 READ(3,)NXT
00315 IF(NXT.EQ.0)GO TO 49
00320 READ(3,)(XXK(I),I=1,NXT)
00330 READ(3,)((US(I,J),J=1,N),I=1,NXT)
00340 READ(3,)(NP1(I),I=1,N)
00350 READ(3,)(NL(I),I=1,N)
00351 DO 1137 IL=1,N
00352 IF (NP1(IL).EQ.3)1138,1137
00353 1138 READ(3,)NXZ
00354 READ(3,)(EDLIM(I),I=1,NXZ)
00355 1137 CONTINUE
00360 49 IF(N1.GT.136)80,81
00370 80 CONTINUE
00380 X=2.99    $ XYZ=2.49
00390 DO 154 I=137,N1
00400 X=X+0.02
00410 XL(I)=X
00420 XYZ=XYZ-0.07
00430 XIDL(I)=XYZ
00440 154 CONTINUE
00450 81 IF(NT.EQ.1)2,4
00460 2 DO 3 I=1,N1
00470 3 XIDL(I)=XYDL(I)
00480 4 DO 200 IIP=1,NTT
00490 C(1)=0.01   $ C(2)=IIP*0.01
00494 C(3)=1.-C(1)-C(2)
```

```
00495 IF(NXT.EQ.0)GO TO 59
00500 DO 130 I=1,NXT
00510 SUM=0.0
00520 DO 135 J=1,N
00530 135 SUM=SUM+(US(I,J)*C(J))
00540 UXT(I)=SUM
00550 130 CONTINUE
00560 59 DO 136 I=1,N
00570 136 XXS(I)=0.0
00580 XP=XXP=0.0
00590 SUM=0.0
00600 DO 140 I=1,N
00610 140 SUM=SUM+(UM(I)*C(I))
00620 XK=SUM
00625 XB=1.414
00630 DO 100 I=1,N1
00640 A=XIDL(I)*U(I,NP)
00650 SUM=0.0
00660 DO 150 J=1,N
00665 IA=IJ(J)
00670 150 SUM=SUM+(U(I,IA)*C(J))
00680 B=SUM
00690 CL=A/(B+XK)
00700 XP=XP+CL
00710 CD=1./U(I,NP)
00720 XXP=0.0
00730 INIT=1
00731 IF(NXT.EQ.0)GO TO 100
00740 DO 160 II=1,N
00750 IF(NP1(II).EQ.2)30,40
00760 30 XXS(II)=0.0
00770 GO TO 160
00775 40 IF(NP1(II).EQ.3)411,412
00776 411 NLL=NXZ
00778 CALL LAMBDA(INIT,NLL,EDLIM,XL,XXK,XB,UXT,B,IJ,
00779+XXP,U,I,XK,US,NP1,NQ,II)
00780 GO TO 169
00784 412 NN2=N2(II)
00785 IF(XL(I).GT.XL(NN2))GO TO 160
00787 NLL=NL(II)
00788 XXP=0.0
00790 DO 170 JJ=INIT,NLL
00800 XY=XXK(JJ)/(2.*XB)
00810 CO=UXT(JJ)
00820 YA=1.+((B*XB)/CO)
00830 YB=1.+((XK*XB)/CO)
00840 YP=((1./B)*ALOG(YA))+((1./XK)*ALOG(YB))
00845 IB=IJ(II)
00850 XXP=XXP+(US(JJ,NQ)*U(I,IB)*YP*XY)
00860 170 CONTINUE
00865 169 INIT=NL(II)+1
00870 XXS(II)=XXS(II)+(XXP*CL*CD)
00880 160 CONTINUE
00890 100 CONTINUE
```

```
00900 TINTER=0.0
00910 DO 180 I=1,N
00920 180 TINTER=TINTER+(XXS(I)*C(I))
00930 TOT=XP+TINTER
00940 ZP1=(XP/TOT)*100.0
00950 DO 190 I=1,N
00960 190 XXY(I)=((XXS(I)*C(I))/TOT)*100.00
00965 WRITE(2,208)(C(I),I=1,N),XP,TINTER,TOT,ZP1,XXY(2)
00970 208 FORMAT(2X,3(F6.4,4X),3(F10.2,4X),5X,2(F6.2,2X))
01200 200 CONTINUE
01210 PRINT,*OUTPUT TO FILE ESTABLISHED*
01220 READ(3,)JL
01230 IF(JL.EQ.0)7,66
01240 7 CALL SAVE(5HTAPE2,5HTAPE2,0,0,0)
01250 PRINT,*OUTPUT AVAILABLE ON TAPE2*
01260 STOP
01270 END
01280 SUBROUTINE LAMBDA(INIT,NLL,EDLIM,XL,XXK,XB,UXT,B,IJ,
01281+XXP,U,I,XK,US,NP1,NQ,II)
01290 DIMENSION UXT(20),XXK(20),XL(200),IJ(20),U(200,20),EDLIM(30)
01295+,US(15,20),NP1(20
01300 IQ=0
01310 XXP=0.0
01320 DO 170 JJ=INIT,NLL
01330 IQ=IQ+1
01340 NN2=EDLIM(IQ)
01350 IF(XL(I).GT.XL(NN2))GO TO 170
01360 XY=XXK(JJ)/(2.*XB)
01370 CO=UXT(JJ)
01380 YA=1.+((B*XB)/CO)
01390 YB=1.+((XK*XB)/CO)
01400 YP=((1./B)*ALOG(YA))+((1./XK)*ALOG(YB))
01410 IB=IJ(II)
01420 XXP=XXP+(US(JJ,NQ)*U(I,IB)*YP*XY)
01430 170 CONTINUE
01440 RETURN
01450 END
```

PROGRAM COMPU

PURPOSE: To determine matrix and inter-element correction coefficients from elemental concentration and x-ray intensity data provided by the output tape from program MUV.

METHOD: The -correction coefficients are determined using Equation 19. The calculation is carried out for all possible combinations and an average coefficient is determined after statistical analysis is performed.

```
 78/06/12. 09.17.24.  1
PROGRAM   COMPU

00100 PROGRAM COMPU(INPUT,OUTPUT,TAPE2,TAPE4)
00110 DIMENSION ALPHA(100),CX(100),MM(100),NN(100),CA(20),CB(20),CM(20),XI(20
00120 CALL GET(5HTAPE2,5HTAPE2,0,0)
00130 REWIND 2
00135 PRINT,*READ IN THE MATRIX COEFF*
00140 READ,XALPHA
00145 PRINT,*TYPE IN THE TERMINATOR*
00146 READ 57,DT
00147 57 FORMAT(A2)
00150 NX=11
00160 6 READ(2,9)SX,FX
00170 9 FORMAT(2A2)
00180 READ(2,20)(CA(I),CB(I),CM(I),XP,XXP,XI(I),Z1,Z2,I=1,NX)
00190 20 FORMAT(2X,3(F6.4,4X),3(F10.2,4X),5X,2(F6.2,2X))
00200 NX=NX-1
00210 I=0
00220 DO 100 M=1,NX
00230 NM=M+1
00240 DO 100 N=NM,NX
00250 I=I+1
00260 A=XI(M)-XI(N)
00270 B=XALPHA*((XI(M)*CM(M))-(XI(N)*CM(N)))
00280 C=(XI(N)*CB(N))-(XI(M)*CB(M))
00290 ALPHA(I)=(A+B)/C
00300 MM(I)=M
00310 NN(I)=N
00320 100 CONTINUE
00330 PRINT,*COEFF CALCULATED*
00340 CALL XMEAN(ALPHA,I,STDE,XA)
00350 CALL REJECT(ALPHA,I,STDE,XA,CX,INDEX)
00360 PRINT 109,PX,SX,INDEX,XA,STDE
00370 109 FORMAT(/2X*SERIES OF EFFECT OF *A2* ON *A2,6X*NO OF DATA *I4,5X,
00371+*MEAN VALUE = *F13.9,5X* +/- *E16.5/)
00390 INDEX=0.0
00410 50 FORMAT(//45X*EFFECT OF *A2* ON *A2///)
00430 54 FORMAT(25X*DATA RESULTS *//)
00460 55 FORMAT(10X,2(I2*/*I2,8X,F8.4,*...*8X,A5,15X))
00480 56 FORMAT(//10X*MEAN VALUE = *F13.9,5X,*+/-*5X,E16.5//)
00490 IF(PX.EQ.DT)5,6
00500 5 CONTINUE
00510 STOP
00520 END
00530 SUBROUTINE XMEAN(ALPHA,N,STDE,XA)
00540 DIMENSION ALPHA(100)
00550 SUM=0.0
00560 DO 1100 K=1,N
00570 1100 SUM=SUM+ALPHA(K)
00580 FN=N
00590 XA=SUM/FN
00600 SUM=0.0
```

```
00610 DO 1101 L=1,N
00620 1101 SUM=SUM+(ALPHA(L)-XA)**2
00630 FK=N-1
00640 STDE=SQRT(SUM/FK)
00650 RETURN
00660 END
00670 SUBROUTINE REJECT(ALPHA,N,STDE,XA,CX,INDEX)
00680 DIMENSION CX(100),ALPHA(100)
00690 COUNT=SUM=0.0
00700 DO 1000 II=1,N
00710 IF(ABS(ALPHA(II)-XA).GE.STDE)1001,1002
00720 1001 CX(II)=5H(.R.)
00730 GO TO 1000
00740 1002 CX(II)=5H
00750 SUM=SUM+ALPHA(II)
00760 COUNT=COUNT+1
00770 1000 CONTINUE
00780 XA=SUM/COUNT
00790 COUNT=COUNT-1
00800 SUM=0.0
00810 DO 1004 L=1,N
00820 IF(CX(L).EQ.5H     )1005,1004
00830 1005 SUM=SUM+(ALPHA(L)-XA)**2
00840 INDEX=INDEX+1
00850 1004 CONTINUE
00855 STDE=SQRT(SUM/COUNT)
00860 RETURN
00870 END
```

APPENDIX C

PARAMETERS FOR FUNDAMENTAL PARAMETERS APPROACH :

Fluorescent Yields :

Bambynek, W., B. Crasemann, R.W. Fink, H.U. Freund, H. Mark, C.D. Swift, R.E. Price and P.V. Rao, Rev. Mod. Phys. 44, 716 (1972).

Absorption-Edge Jump Ratios :

Birks, L.S., "X-Ray Spectrochemical Analysis", Interscience Publication, New York and London (1959).

Bertin, E.P., "Principles and Practice of X-Ray Spectrometric Analysis", Plenum Press, New York (1975).

Mass Absorption Coefficient Data :

Robinson, J.W., ed., "CRC Handbook of Spectroscopy", Vol. 1, CRC Press, Div. of Chemical Rubber Co., Cleveland, O. (1974).

Principle Emission Lines of X-Ray Spectra :

Zangaro, P.W., "Table of Principle Emission Lines of X-Ray Spectra", Application Laboratory, North American Philips Company, Inc., Mount Vernon, New York .

APPENDIX D

TABLE D-1

INTENSITY RATIOS FOR ALLOYS 2 AND 8 - SOLID SPECIMEN*

Alloy No.	Sn	Pb	Fe	Ni	Zn	Cu
2-1	15.84	27.30	614.14	308.16	37.09	1.21
2-2	12.89	27.94	481.38	325.30	24.28	1.25
2-3	10.96	27.77	510.60	339.21	20.60	1.28
2-5	11.21	25.78	470.69	335.45	21.81	1.28
2-9	13.91	18.39	564.43	214.59	33.17	1.27
2-10	13.94	17.02	593.51	210.30	34.09	1.27
8-1	13.03	180.72	4357.00	30000.00	56.92	1.14
8-3	9.50	181.27	2711.00	26000.00	25.24	1.21
8-8	11.66	58.08	3697.00	1242.00	43.91	1.17
8-13	10.24	45.94	4122.00	647.30	33.24	1.20

* Intensity ratio expressed as the ratio of calculated I^o to the measured net I (I^o/I).

TABLE D-2

INTENSITY RATIOS FOR ALLOYS 2 AND 8 - AQUEOUS SPECIMEN*

Alloy No.	Cu	Sn	Pb	Fe	Ni	Zn	Cl**
2-1	7.50	43.95	71.11	7550.40	2730.80	221.51	17.96
2-2	8.06	37.06	73.42	6536.90	2898.00	150.59	15.54
2-3	7.83	31.79	74.81	6625.90	2753.50	120.18	17.06
2-5	7.69	30.02	59.71	6049.70	2701.10	124.79	17.70
2-9	7.04	35.38	41.38	6283.80	1640.30	177.37	40.55
2-10	6.80	35.48	38.22	6493.30	1558.00	172.12	59.69
8-1	8.32	47.07	549.62	68750.00	30000.00	385.14	9.84
8-3	8.18	32.10	510.64	57895.00	36818.00	159.09	11.69
8-8	7.99	39.44	174.76	62857.00	10125.00	271.84	12.55
8-13	8.48	34.21	112.85	64706.00	6183.00	219.26	11.11

* Intensity ratio expressed as the ratio of calculated I^o to the measured net I (I^o/I).

** Chloride concentrations determined by potentiometric titration.

TABLE D-3

INTENSITY RATIOS FOR SERIES J - SOLID SPECIMEN*

Alloy No.	Sn	Pb	Fe	Ni	Zn	Cu
J-1	15.365	27.74	642.89	376.77	34.24	1.21
J-2	11.06	27.80	554.45	327.02	21.51	1.28
J-3	11.47	21.99	523.39	321.76	22.86	1.31
J-4	11.88	18.11	462.21	443.40	23.48	1.34
J-5	14.35	18.49	481.31	235.99	30.48	1.29
J-6	12.11	17.24	542.47	288.18	26.70	1.34
J-7	27.46	14.06	688.21	533.37	13.73	1.35
J-8	11.66	196.85	4338.98	15656.01	51.36	1.12
J-9	11.38	62.39	3279.53	1206.77	41.90	1.17
J-10	9.69	37.74	1876.01	743.46	34.39	1.24

* Intensity ratio expressed as the ratio of calculated I^o to the measured net I (I^o/I).

TABLE D-4

INTENSITY RATIOS FOR SERIES J - AQUEOUS SPECIMEN*

Alloy No.	Cu	Sn	Pb	Fe	Ni	Zn	Cl**
J-1	7.51	43.73	73.69	9203.14	3089.41	207.28	17.62
J-2	7.89	31.45	75.24	7632.72	2639.70	128.90	16.92
J-3	***	***	***	***	***	***	***
J-4	6.97	29.97	43.77	5084.81	2950.43	119.12	59.64
J-5	7.08	37.13	45.76	5722.99	1663.18	162.43	35.56
J-6	6.85	30.17	41.18	5829.54	1874.05	132.94	79.63
J-7	***	***	***	***	***	***	***
J-8	8.24	39.07	590.48	80514.30	157093.02	369.99	9.96
J-9	7.96	35.64	178.52	53371.20	11019.58	279.70	12.25
J-10	8.44	29.75	110.99	29232.40	6658.45	228.94	11.22

* Intensity ratio expressed as the ratio of calculated I^o to the measured net I (I^o/I).

** Chloride concentrations determined by potentiometric titration.

*** Data unavailable for sample.

TABLE D-5

INTENSITY RATIOS FOR SERIES K - SOLID SPECIMEN*

Alloy No.	Mn	Fe	Ni	Zn
K-1	32.70	37.78	126.86	2.79
K-2	24.96	56.85	240.21	2.66
K-3	24.70	64.31	392.30	2.78
K-4	16.92	165.74	171.76	2.75
K-5	52.48	30.38	1122.93	2.82
K-6	32.41	65.39	49.06	2.83
K-7	18.83	35.46	95.36	2.96
K-8	244.20	768.34	3257.83	3.14
K-9	487.04	510.97	2163.40	3.09
K-10	99.47	335.71	1670.65	3.20

Alloy No.	Sn	Pb	Al	Cu
K-1	48.23	547.04	1266.13	1.66
K-2	622.09	230.36	2565.36	1.63
K-3	93.09	141.89	4337.02	1.63
K-4	219.82	109.42	9075.14	1.68
K-5	42.00	317.55	934.52	1.63
K-6	207.96	573.82	388.71	1.60
K-7	619.71	144.33	689.81	1.66
K-8	60.38	75.83	442.63	1.45
K-9	82.88	66.45	692.85	1.45
K-10	234.90	46.41	1083.50	1.47

* Intensity ratio expressed as the ratio of calculated I^o to the measured net I (I^o/I).

TABLE D-6

INTENSITY RATIOS FOR SERIES K - AQUEOUS SPECIMEN*

Alloy No.	Mn	Fe	Ni	Cu
K-1	717.09	788.67	1473.90	12.89
K-2	608.68	1322.32	3099.52	13.70
K-3	627.18	1560.31	5275.19	14.47
K-4	388.04	3627.65	2090.63	13.50
K-5	1251.17	690.18	14191.87	13.75
K-6	878.01	1694.28	695.52	15.00
K-7	524.31	942.93	1355.04	15.87
K-8	5463.11	16424.38	39679.30	11.80
K-9	11089.85	11119.05	26791.34	11.94
K-10	2353.05	7593.50	21298.90	12.59

Alloy No.	Zn	Sn	Pb	Al	Cl**
K-1	19.40	137.25	1574.13	23214.29	9.49
K-2	20.07	1835.07	687.47	37142.86	7.80
K-3	22.12	282.11	447.75	68421.05	6.64
K-4	19.84	627.23	320.74	130000.00	8.40
K-5	21.44	124.95	975.34	17808.22	7.53
K-6	23.28	662.41	1862.93	5882.35	6.27
K-7	25.09	2004.95	487.16	9848.48	5.56
K-8	23.20	167.96	221.94	7926.83	9.10
K-9	23.06	230.34	195.14	11711.71	8.73
K-10	24.85	379.25	141.47	17105.26	7.54

* Intensity ratio expressed as the ratio of calculated I^o to the measured net I (I^o/I).

** Chloride concentrations determined by potentiometric titration.

TABLE D-7

INTENSITY RATIOS FOR SERIES ALS - SOLID SPECIMEN*

Rock No.	Mg	Al	Si	Ca	Ti	Mn	Fe
ALS-2	210.53	51.57	31.65	20.63	4.13	835.25	2.69
ALS-4	183.67	68.16	80.47	52.33	2.75	677.02	2.18
ALS-5	194.59	127.74	42.53	27.57	3.46	759.58	2.47
ALS-6	264.71	34.98	21.67	15.20	6.62	1129.53	3.70
ALS-7	238.41	40.50	25.32	17.47	5.04	981.98	3.19
ALS-8	375.00	24.60	15.43	10.71	28.60	1895.65	8.08
ALS-10	333.33	29.54	18.30	12.63	8.88	1267.44	4.55
ALS-11	165.90	366.49	335.54	240.50	2.45	654.65	2.00
ALS-12	400.00	23.91	14.98	10.60	28.92	1626.87	9.00

* Intensity ratio expressed as the ratio of calculated I^o to the measured net I (I^o/I).

TABLE D-8

INTENSITY RATIOS FOR SERIES ALS - FUSED SPECIMEN*

Rock No.	Al	Si	Ca	Ti	Mn	Fe
ALS-2	301.02	119.24	61.92	10.05	1502.16	4.59
ALS-4	719.51	333.33	165.40	7.27	1261.82	3.78
ALS-5	414.33	180.33	15.61	8.82	1427.98	4.24
ALS-6	192.31	72.93	42.15	15.80	2065.48	6.33
ALS-7	260.14	100.08	53.82	12.41	1761.42	5.37
ALS-8	140.74	51.54	29.87	68.19	4337.50	16.18
ALS-10	175.39	64.02	35.98	21.50	2532.85	7.97
ALS-11	1475.00	1306.93	761.90	6.53	1192.44	3.47
ALS-12	126.39	46.30	27.46	69.99	3652.63	17.84

* Intensity ratio expressed as the ratio of calculated I^o to the measured net I (I^o/I).

TABLE D-9

INTENSITY RATIOS FOR SERIES TALS - SOLID SPECIMEN*

Rock No.	Mg	Al	Si	Ca	Ti	Cr	Mn	Fe
TALS-2	208.33	69.87	31.92	21.74	4.00	1173.86	825.23	2.73
TALS-4	276.91	188.56	91.45	55.16	2.81	1165.95	717.48	2.36
TALS-5	221.06	99.67	47.40	30.82	3.39	1214.53	749.57	2.52
TALS-6	206.35	32.00	17.34	14.35	6.91	2385.95	1070.02	3.54
TALS-7	216.22	51.89	23.54	17.59	4.91	1661.76	930.92	2.95
TALS-8	191.43	20.90	10.72	10.09	26.14	7991.37	1723.27	7.07
TALS-10	269.54	28.16	14.02	11.81	9.07	3129.07	1377.66	4.22
TALS-11	298.73	658.34	453.12	173.72	2.49	1000.85	707.59	2.25
TALS-12	215.58	19.04	10.03	9.62	30.59	nil	1645.76	9.59

* Intensity ratio expressed as the ratio of calculated I^o to the measured net I (I^o/I).

TABLE D-10

INTENSITY RATIOS FOR SERIES TALS - FUSED SPECIMEN*

Rock No.	Mg	Al	Si	Ca	Ti	Cr	Mn	Fe
TALS-2	1827.73	569.99	226.87	114.18	16.45	3516.66	2154.28	6.71
TALS-4	2142.86	1375.14	616.13	300.34	11.77	3259.67	1726.55	5.34
TALS-5	1831.58	771.60	328.93	165.39	14.16	3553.24	1896.13	6.01
TALS-6	2132.35	305.55	129.89	71.60	27.65	7703.26	3087.64	9.74
TALS-7	2013.89	448.99	171.79	90.63	20.03	5152.84	2533.44	7.58
TALS-8	2443.82	243.99	88.56	48.62	102.02	28590.31	5808.89	23.19
TALS-10	2979.45	288.62	109.53	58.11	35.68	10317.97	4092.20	12.15
TALS-11	2202.53	4578.75	2992.13	966.37	10.53	2734.36	1656.74	4.93
TALS-12	2871.29	231.78	84.17	45.90	117.69	nil	5599.83	31.96

* Intensity ratio expressed as the ratio of calculated I^o to the measured net I (I^o/I).

TABLE D-11

INTENSITY RATIOS FOR SERIES BXT - SOLID SPECIMEN*

Ore No.	Mg	Al	Si	Ca	Ti
B-61	1224.19	9.77	163.05	104.05	29.72
B-62	875.53	8.89	202.33	66.66	28.59
B-63	1624.27	11.34	2037.79	1105.33	24.27
B-64	1435.99	10.66	145.44	51.03	38.80
B-65	1765.96	7.62	137.85	1244.05	28.24
B-66	2009.69	6.48	1390.42	6415.09	23.95
B-67	2953.74	10.86	22.98	6071.43	71.50
B-68	2064.68	13.27	468.65	5546.49	30.89
B-69	3656.39	7.75	135.09	2074.44	28.91
B-70	4462.37	16.33	48.87	5782.31	41.88

Ore No.	Cr	Mn	Fe	P	K
B-61	677.69	4928.30	2.66	9487.18	790.18
B-62	1653.59	424.32	3.13	7034.22	138.02
B-63	467.22	398.05	2.76	1388.89	208.12
B-64	1422.51	103.93	3.82	78.03	45.22
B-65	2576.89	5099.57	7.35	8043.48	345.20
B-66	789.25	4782.13	33.72	4057.02	630.26
B-67	4756.19	4475.67	5.88	6491.23	10420.71
B-68	810.04	2742.55	2.19	3008.13	328.14
B-69	2545.28	5095.59	6.48	8043.48	9757.58
B-70	1539.82	5219.82	2.17	14919.35	442.79

* Intensity ratio expressed as the ratio of calculated I^o to the measured net I (I^o/I).

TABLE D-12

INTENSITY RATIOS FOR SERIES BXT - FUSED SPECIMEN*

Ore No.	Mg	Al	Si	Ca	Ti
B-61	5723.68	43.35	454.27	261.77	72.22
B-62	4243.90	40.64	561.09	166.09	67.74
B-63	6258.99	41.81	5083.61	2823.05	54.60
B-64	6126.76	43.33	3877.55	111.51	81.07
B-65	8207.55	32.85	346.40	2877.52	62.99
B-66	9157.89	27.96	3355.41	14411.76	52.00
B-67	14262.30	49.04	66.15	14533.90	163.17
B-68	7767.86	48.13	1194.97	14000.00	71.34
B-69	16415.09	33.21	340.04	4777.16	64.86
B-70	17400.00	61.88	134.80	14115.23	98.29

Ore No.	Cr	Mn	Fe	P	K
B-61	1551.81	10356.86	5.18	25000.00	2025.00
B-62	3693.44	864.44	6.11	18686.87	351.52
B-63	991.80	745.86	5.05	3382.08	490.83
B-64	2860.27	192.59	6.89	192.33	102.67
B-65	5559.81	9804.80	14.59	19072.16	805.37
B-66	1612.94	9631.27	67.36	9487.18	1427.31
B-67	10874.27	9666.91	12.03	15546.22	23478.26
B-68	1776.39	5266.13	4.01	7429.72	786.41
B-69	5522.20	9797.45	12.85	19072.16	23142.86
B-70	3535.46	10456.37	4.05	37755.10	1074.27

* Intensity ratio expressed as the ratio of calculated I^o to the measured net I (I^o/I).

TABLE D-13

INTENSITY RATIOS FOR SERIES DX - SOLID SPECIMEN*

Ore No.	Mg	Al	Si	Ca	Ti
DX-1	1010.96	19.53	8.03	101.67	206.22
DX-2	79.15	29.52	9.67	9.12	208.85
DX-3	58.50	43.91	9.88	6.84	26.56
DX-4	13606.56	19.35	25.71	6613.23	18.31
DX-5	83.67	38.44	10.32	9.92	97.44
DX-6	2311.98	14.63	15.68	7096.77	23.33
DX-7	2686.08	6.62	1706.76	11913.36	17.97
DX-8	180.63	23.96	7.47	132.91	96.29
DX-9	40.20	43.83	9.72	7.66	168.52
DX-10	51875.00	7.23	529.12	354.23	65.36

Ore No.	Mn	Fe	P	K
DX-1	238.60	25.13	10769.23	13.77
DX-2	1386.98	5.82	70000.00	479.52
DX-3	164.30	7.31	10340.91	778,91
DX-4	5631.69	2.53	60666.67	1058.17
DX-5	352.23	4.61	4516.13	189.28
DX-6	5323.89	4.26	4678.66	8256.41
DX-7	4259.80	69.81	1467.74	7076.92
DX-8	131.60	12.09	140000.00	29.14
DX-9	6848.96	7.15	5741.32	211.45
DX-10	3974.01	10.67	55151.52	14061.14

* Intensity ratio expressed as the ratio of calculated I^o to the measured net I (I^o/I).

TABLE D-14

INTENSITY RATIOS FOR SERIES DX - FUSED SPECIMEN*

Ore No.	Mg	Al	Si	Ca	Ti
DX-1	5918.37	109.83	32.25	221.70	431.65
DX-2	462.27	151.94	38.88	22.63	444.17
DX-3	342.25	220.52	40.89	17.10	54.36
DX-4	58000.00	77.70	77.91	16201.92	42.82
DX-5	448.45	183.35	40.15	24.32	206.58
DX-6	11600.00	70.34	52.09	17552.08	55.12
DX-7	11917.81	28.02	4097.04	26746.03	38.36
DX-8	1084.79	132.65	30.75	309.34	215.20
DX-9	243.97	218.04	39.80	19.01	350.49
DX-10	21750.00	28.79	1245.90	785.73	139.10

Ore No.	Mn	Fe	P	K
DX-1	488.30	51.22	26911.76	32.71
DX-2	2776.72	11.44	183000.00	1214.29
DX-3	309.74	13.61	28593.75	2014.97
DX-4	10965.86	4.72	152500.00	2577.81
DX-5	690.11	8.83	11883.12	474.86
DX-6	11095.20	8.59	11883.12	20314.47
DX-7	8399.23	137.63	4216.59	15380.95
DX-8	318.08	29.04	366000.00	71.44
DX-9	13549.38	13.96	15508.47	542.40
DX-10	7972.16	21.19	122000.00	30761.90

* Intensity ratio expressed as the ratio of calculated I^o to the measured net I (I^o/I).

TABLE D-15

INTENSITY RATIOS FOR SERIES APD - SOLID SPECIMEN*

Rock No.	Mg	Al	Si	Ca	Ti
APD-1	50000.00	51.37	7.29	9.14	312.99
APD-2	50000.00	70.75	5.83	10.00	309.22
APD-3	53125.00	34.91	9.88	9.82	270.89
APD-4	50000.00	29.27	7.06	25.33	151.87
APD-5	47222.22	48.83	5.19	88.90	288.07
APD-6	47222.22	42.52	5.40	401.73	212.41
APD-7	50000.00	27.56	7.84	63.54	136.59

Rock No.	Cr	Mn	Fe	P	K
APD-1	8136.45	93.00	23.59	28.69	9047.62
APD-2	803.69	121.04	22.57	45.18	18044.69
APD-3	683.47	29.21	24.09	25.60	8706.20
APD-4	142.14	354.35	25.80	48.27	8997.21
APD-5	4533.61	329.62	38.85	56.14	18248.59
APD-6	3152.23	350.34	37.46	57.42	6082.86
APD-7	6354.22	392.44	23.27	35.87	4418.60

* Intensity ratio expressed as the ratio of calculated I^0 to the measured net I (I^0/I).

TABLE D-16

INTENSITY RATIOS FOR SERIES APD - FUSED SPECIMEN*

Rock No.	Mg	Al	Si	Ca	Ti
APD-1	303333.3	291.67	34.78	21.61	634.21
APD-2	303333.3	413.52	29.13	23.92	639.03
APD-3	303333.3	182.74	42.08	22.85	545.17
APD-4	303333.3	166.29	31.28	60.33	332.52
APD-5	303333.3	293.36	25.68	213.31	657.23
APD-6	303333.3	252.15	26.02	962.09	489.73
APD-7	303333.3	151.26	33.51	149.50	303.58

Rock No.	Cr	Mn	Fe	P	K
APD-1	16311.79	184.77	46.65	79.76	21533.33
APD-2	1641.37	245.15	45.39	121.27	43066.67
APD-3	1353.17	57.02	46.77	70.72	20314.46
APD-4	305.84	754.61	54.16	125.00	21111.11
APD-5	10133.86	737.33	86.79	142.75	42500.00
APD-6	7130.19	791.61	84.23	145.09	14292.04
APD-7	13868.53	851.48	50.06	92.90	10221.52

* Intensity ratio expressed as the ratio of calculated I^o to the measured net I (I^o/I).

TABLE D-17

INTENSITY RATIOS FOR SERIES XY-1 - SOLID SPECIMEN*

Rock No.	Mg	Al	Si	Ca	Ti
MRG-1	43.79	63.32	13.13	5.37	34.03
SY-2	184.59	33.12	7.16	11.37	812.24
SY-3	189.08	34.23	7.19	10.92	810.00
AGV-1	318.60	22.74	7.59	17.28	104.36
BCR-1	157.02	32.51	8.61	11.84	50.14
DTS-1	9.24	2390.44	14.06	475.91	8247.66
G-2	594.35	23.30	6.02	45.74	213.36
GSP-1	487.80	24.44	6.33	47.24	167.31
PCC-1	10.80	878.48	12.99	135.59	8209.30
W-1	81.30	30.97	9.35	7.57	113.64

Rock No.	Cr	Mn	Fe	P	K
MRG-1	1625.05	490.99	4.85	8632.08	451.25
SY-2	86333.33	214.83	11.19	1491.44	19.56
SY-3	85761.59	206.26	10.93	1173.83	20.68
AGV-1	16248.43	645.64	9.50	1314.66	30.19
BCR-1	16796.37	360.46	5.37	2013.20	51.60
DTS-1	94.21	455.94	6.18	63103.45	8661.20
G-2	76176.47	1490.44	22.79	5027.47	20.17
GSP-1	16434.01	409.78	14.77	970.82	15.48
PCC-1	136.92	412.67	6.30	122000.00	8191.21
W-1	4344.18	436.82	6.05	4632.91	136.70

* Intensity ratio expressed as the ratio of calculated I^o to the measured net I (I^o/I).

TABLE D-18

INTENSITY RATIOS FOR SERIES XY-1 - FUSED SPECIMEN*

Rock No.	Mg	Al	Si	Ca	Ti
MRG-1	241.80	283.06	52.05	13.53	67.74
SY-2	1147.76	182.54	31.71	25.98	1626.95
SY-3	1163.10	186.90	31.71	24.98	1620.26
AGV-1	2027.97	130.11	32.78	41.05	222.71
BCR-1	924.55	169.49	36.39	29.05	106.94
DTS-1	65.07	9328.36	53.28	1283.71	21385.54
G-2	4027.78	143.05	27.63	105.18	460.14
GSP-1	3246.27	146.77	28.81	106.66	354.75
PCC-1	71.21	3424.66	48.83	357.11	20520.23
W-1	486.03	157.83	38.44	18.58	232.50

Rock No.	Cr	Mn	Fe	P	K
MRG-1	3141.96	898.71	8.67	24285.71	1193.64
SY-2	168441.56	419.11	21.55	3928.57	48.43
SY-3	170657.89	400.87	20.98	3085.81	51.11
AGV-1	34131.58	1320.07	19.11	3450.18	75.34
BCR-1	34959.57	712.57	10.36	5404.62	131.61
DTS-1	238.72	1096.38	14.25	170000.00	23237.41
G-2	160123.46	3147.12	47.70	12896.55	49.28
GSP-1	34221.64	843.33	30.07	2500.00	37.82
PCC-1	337.38	968.08	14.26	374000.00	21390.73
W-1	8739.89	844.97	11.47	12550.34	347.87

* Intensity ratio expressed as the ratio of calculated I^o to the measured net I (I^o/I).

TABLE D-19

INTENSITY RATIOS FOR SERIES XY-2 - SOLID SPECIMEN*

Rock No.	Mg	Al	Si	Ca	Ti
I-1	396.28	24.03	5.28	114.62	2079.91
I-3	139.49	35.40	9.88	9.96	43.63
M-2	208.55	16.85	10.52	55.62	158.11
M-3	409.71	21.73	8.21	6.91	148.83
302/1	577.33	59.41	33.49	16.54	175.04
DTN	10000.00	5.23	18.39	1989.05	65.82
UB-N	14.09	200.85	13.36	59.35	675.70
NIM-S	963.14	19.89	6.73	181.71	3361.82
NBS-97a	288.26	8.81	12.83	688.28	45.79
NBS-99a	21891.89	16.28	6.71	43.29	10892.31

Rock No.	Cr	Mn	Fe	P	K
I-1	759.52	1908.96	101.71	34716.98	21.87
I-3	86.97	334.80	4.85	1579.40	59.79
M-2	84.39	263.41	7.70	1309.61	11.44
M-3	92.16	250.25	15.95	1742.42	121.98
302/1	621.23	238.00	1.65	267.83	132.75
DTN	1764.71	5297.47	79.90	7829.79	763.72
UB-N	176.41	409.47	6.10	20444.44	3878.79
NIM-S	19563.25	7377.98	52.33	5786.16	6.27
NBS-97a	2166.81	2425.83	113.16	1789.88	169.59
NBS-99a	2571.77	2853.38	892.76	33454.54	17.62

* Intensity ratio expressed as the ratio of calculated I^o to the measured net I (I^o/I).

TABLE D-20

INTENSITY RATIOS FOR SERIES XY-2 - FUSED SPECIMEN*

Rock No.	Mg	Al	Si	Ca	Ti
I-1	2797.43	155.82	25.17	260.74	4544.29
I-3	762.49	174.57	39.73	24.02	90.53
M-2	1270.07	92.88	41.05	122.00	328.81
M-3	2500.00	122.12	34.21	16.28	291.60
302/1	2142.86	209.25	105.43	40.82	389.57
DTN	79090.91	37.46	61.40	4970.33	157.14
UB-N	81.51	767.33	47.58	148.76	1604.71
NIM-S	6850.39	130.27	31.37	368.58	6654.14
NBS-97a	1820.08	50.44	43.19	1610.58	102.54
NBS-99a	145000.00	103.29	29.10	96.26	22838.71

Rock No.	Cr	Mn	Fe	P	K
I-1	1632.21	4203.64	221.34	85454.55	52.56
I-3	173.28	641.72	8.99	4253.39	150.44
M-2	171.10	523.62	14.89	3443.22	27.97
M-3	176.36	479.96	30.06	4596.58	300.44
302/1	1355.16	448.80	2.91	722.52	331.76
DTN	4050.99	12308.41	184.21	20434.78	1893.32
UB-N	410.11	916.62	13.27	53714.29	9556.21
NIM-S	37631.58	14085.56	102.64	15284.55	15.25
NBS-97a	4649.57	5280.67	245.16	4382.28	397.10
NBS-99a	5320.38	6027.46	1881.30	85454.55	42.16

* Intensity ratio expressed as the ratio of calculated I^o to the measured net I (I^o/I).

APPENDIX E

PROGRAM MULTHE

PURPOSE: To calculate theoretical XRF intensities for complex multi-component systems of less than 15 elements.

METHOD: The intensities are calculated using Equation 4.

PROGRAM MULTHE

```
00100 PROGRAM THEORY(INPUT,OUTPUT,TAPE1,TAPE6,TAPE2,TAPE3)
00110 DIMENSION XL(200),U(200,20),N2(20),UM(20),IJ(20),C(20),
00120+XXK(30),US(30,20),NP1(30),NL(30),XIDL(200),XYDL(200),
00130+UXT(30),XXS(20),XXY(20),APXC(20)
00131+,EDLIM(30)
00140 CALL GET (5HTAPE1,5HTAPE1,0,0)
00150 CALL GET(5HTAPE6,5HTAPE6,0,0)
00160 CALL GET(5HTAPE3,5HTAPE3,0,0)
00170 REWIND 3
00180 66 REWIND 1
00190 REWIND 6
00200 READ(3,)N1,NT,N,NTT
00210 READ(3,)(N2(I),I=1,N)
00220 READ(6,10)((U(I,J),J=1,19),I=1,N1)
00230 10 FORMAT(5X,9F8.2,/10F8.2)
00240 PRINT,*READ IN THE ELEMENTS*
00250 READ 11,(APXC(I),I=1,N)
00260 11 FORMAT(18A2)
00270 READ(1,20)(XL(I),XIDL(I),XYDL(I),I=1,N1)
00280 20 FORMAT(2X,F5.3,2X,2(F6.2,2X))
00290 READ(3,)NP,NQ
00300 READ(3,)(IJ(J),J=1,N)
00305 READ(3,)(UM(J),J=1,N)
00310 READ(3,)NXT
00315 IF(NXT.EQ.0)GO TO 49
00320 READ(3,)(XXK(I),I=1,NXT)
00330 READ(3,)((US(I,J),J=1,N),I=1,NXT)
00340 READ(3,)(NP1(I),I=1,N)
00350 READ(3,)(NL(I),I=1,N)
00351 DO 1137 IL=1,N
00352 IF(NP1(IL).EQ.3)1138,1137
00353 1138 READ(3,)NXZ
00354 READ(3,)(EDLIM(I),I=1,NXZ)
00355 1137 CONTINUE
00360 49 IF(N1.GT.136)80,81
00370 80 CONTINUE
00380 X=2.99    $ XYZ=2.49
00390 DO 154 I=137,N1
00400 X=X+0.02
00410 XL(I)=X
00420 XYZ=XYZ-0.07
00430 XIDL(I)=XYZ
00440 154 CONTINUE
00450 81 IF(NT.EQ.1)2,4
00460 2 DO 3 I=1,N1
00470 3 XIDL(I)=XYDL(I)
00480 4 DO 200 IIP=1,NTT
00490 READ(3,)(C(J),J=1,N)
00495 IF(NXT.EQ.0)GO TO 59
00500 DO 130 I=1,NXT
00510 SUM=0.0
00520 DO 135 J=1,N
00530 135 SUM=SUM+(US(I,J)*C(J))
00540 UXT(I)=SUM
```

```
00550 130 CONTINUE
00560 59 DO 136 I=1,N
00570 136 XXS(I)=0.0
00580 XP=XXP=0.0
00590 SUM=0.0
00600 DO 140 I=1,N
00610 140 SUM=SUM+(UM(I)*C(I))
00620 XK=SUM
00625 XB=1.414
00630 DO 100 I=1,N1
00640 A=XIDL(I)*U(I,NP)
00650 SUM=0.0
00660 DO 150 J=1,N
00665 IA=IJ(J)
00670 150 SUM=SUM+(U(I,IA)*C(J))
00680 B=SUM
00690 CL=A/(B+XK)
00700 XP=XP+CL
00710 CD=1./U(I,NP)
00720 XXP=0.0
00730 INIT=1
00731 IF(NXT.EQ.0)GO TO 100
00740 DO 160 II=1,N
00750 IF(NP1(II).EQ.2)30,40
00760 30 XXS(II)=0.0
00770 GO TO 160
00775 40 IF(NP1(II).EQ.3)411,412
00776 411 NLL=NXZ
00778 CALL LAMBDA(INIT,NLL,EDLIM,XL,XXK,XB,UXT,B,IJ,
00779+XXP,U,I,XK,US,NP1,NQ,II)
00780 GO TO 169
00784 412 NN2=N2(II)
00785 IF(XL(I).GT.XL(NN2))GO TO 160
00787 NLL=NL(II)
00788 XXP=0.0
00790 DO 170 JJ=INIT,NLL
00800 XY=XXK(JJ)/(2.*XB)
00810 CO=UXT(JJ)
00820 YA=1.+((B*XB)/CO)
00830 YB=1.+((XK*XB)/CO)
00840 YP=((1./B)*ALOG(YA))+((1./XK)*ALOG(YB))
00845 IB=IJ(II)
00850 XXP=XXP+(US(JJ,NQ)*U(I,IB)*YP*XY)
00860 170 CONTINUE
00865 169 INIT=NL(II)+1
00870 XXS(II)=XXS(II)+(XXP*CL*CD)
00880 160 CONTINUE
00890 100 CONTINUE
00900 TINTER=0.0
00910 DO 180 I=1,N
00920 180 TINTER=TINTER+(XXS(I)*C(I))
00930 TOT=XP+TINTER
00940 ZP1=(XP/TOT)*100.0
00950 DO 190 I=1,N
```

```
00960 190 XXY(I)=((XXS(I)*C(I))/TOT)*100.00
00965 WRITE(2,31)IIP
00966 31 FORMAT(5X,*   SERIES OF CONCENTRATIONS  *,I4//)
00970 WRITE(2,21)NQ
00980 21 FORMAT(5X,*ANALYTE NUMBER IS *I4//)
00990 DO 195 I=1,N
01000 WRITE(2,22)I,APXC(I),C(I)
01010 22 FORMAT(5X,I3,5X,*CONCENTRATION OF *A2,2X,*IS *E15.6)
01020 195 CONTINUE
01030 WRITE(2,23)
01040 23 FORMAT(5X,*THE INTENSITY DISTRIBUTIONS ARE  *//)
01045 XP=XP*C(NQ)
01050 WRITE(2,24)XP,ZP1
01060 24 FORMAT(5X,*FROM PURE ABSORPTION = *F10.4,5X,*PER*,
01070+ *CENT = *F7.2//)
01075 IF(NXT.EQ.0)GO TO 69
01080 WRITE(2,25)
01090 25 FORMAT(5X,*FROM ENHANCEMENT = *//)
01100 DO 196 I=1,N
01110 XYY=XXS(I)*C(I)*C(NQ)
01120 WRITE(2,26)I,XYY,XXY(I)
01130 26 FORMAT(5X,I4,5X,* I = *F10.4,5X,*PERCENT = *F7.2)
01140 196 CONTINUE
01150 69 WRITE(2,27)
01160 27 FORMAT(//)
01170 TTOT=TOT*C(NQ)
01180 WRITE(2,29)TTOT
01190 29 FORMAT(5X,*NET INTENSITY OF ANALYTE IS  *F10.4//)
01200 200 CONTINUE
01210 PRINT,*OUTPUT TO FILE ESTABLISHED*
01220 READ(3,)JL
01230 IF(JL.EQ.0)7,66
01240 7 CALL SAVE(5HTAPE2,5HTAPE2,0,0,0)
01250 PRINT,*OUTPUT AVAILABLE ON TAPE2*
01260 STOP
01270 END
01280 SUBROUTINE LAMBDA(INIT,NLL,EDLIM,XL,XXK,XB,UXT,B,IJ,
01290+XXP,U,I,XK,US,NP1,NQ,II)
01300 DIMENSION UXT(30),XXK(30),XL(200),IJ(20),U(200,20),EDLIM(30)
01310+,US(30,20),NP1(30)
01320 IQ=0.0
01330 XXP=0.0
01340 DO 170 JJ=INIT,NLL
01350 IQ=IQ+1
01360 NN2=EDLIM(IQ)
01370 IF(XL(I).GT.XL(NN2))GO TO 170
01380 XY=XXK(JJ)/(2.*XB)
01390 CO=UXT(JJ)
01400 YA=1.+((B*XB)/CO)
01410 YB=1.+((XK*XB)/CO)
01420 YP=((1./B)*ALOG(YA))+((1./XK)*ALOG(YB))
01430 IB=IJ(II)
01440 XXP=XXP+(US(JJ,NQ)*U(I,B)*YP*XY)
01450 170 CONTINUE
01460 RETURN
01470 END
```

PROGRAM DGAUSS*

PURPOSE: To determine elemental concentrations from XRF intensities of multi-component systems using the modified Lachance-Traill approach.

METHOD: The program uses the Gauss-Jordan reduction with a maximum pivot strategy to solve a set of simultaneous linear algebraic equations in the form of Equation 17. The program is performed in double precision arithmetic.

* reference: Carnahan, B., H.A. Luther and J.O. Wilkes, "Applied Numerical Methods", John Wiley & Sons, Inc., New York (1969).

PROGRAM DGAUSS

```
00100 PROGRAM GAURDF(INPUT,OUTPUT,TAPE12)
00110 DOUBLE X,A,EPS,DETER
00120 DIMENSION X(50),A(51,51),AB(51,51)
00124 CALL GET(6HTAPE12,6HTAPE12,0,0)
00125 READ(12,)N
00128 NN=N+1
00129 READ(12,)((AB(I,J),J=1,NN),I=1,N)
00130 1 READ(12,)N,INDIC,EPA
00131 EPS=DBLE(EPA)
00132 IF(N.EQ.100) GO TO 53
00135 READ(12,)(AB(I,I),I=1,N)
00136 EPS=DBLE(EPA)
00140 PRINT 200,N,INDIC,EPS
00150 MAX=N
00160 IF(INDIC.GE.0)MAX=N+1
00171 DO 55 I=1,N
00172 DO 55 J=1,MAX
00173 55 A(I,J)=DBLE(AB(I,J))
00180 PRINT 201,((A(I,J),J=1,MAX),I=1,N)
00190 DETER=SIMUL(N,A,X,EPS,INDIC,51)
00200 IF(INDIC.GE.0)GO TO 8
00210 PRINT 202,DETER
00220 PRINT 201,((A(I,J),J=1,N),I=1,N)
00230 GO TO 1
00240 8 PRINT 203,DETER,N,(X(I),I=1,N)
00250 IF(INDIC.NE.0)GO TO 1
00260 9 PRINT 204
00270 PRINT 211,((A(I,J),J=1,N),I=1,N)
00280 GO TO 1
00290 200 FORMAT(10H N      = ,I4/10H INDIC  = ,I4/10H EPS    = ,
00300+ D10.1/23H THE STARTING MATRIX IS /1H  ,/)
00320 202 FORMAT(10H DETER  = ,D12.6/22H THE INVERSE MATRIX IS //)
00330 203 FORMAT(10H DETER  = D12.6/24H THE SOLUTIONS X(1)...X(,
00334+ I2,5H) ARE //(1H ,
00335+ 7D15.6))
00336 211 FORMAT(2X,6D15.6)
00337 201 FORMAT(2X,7D15.6)
00340 204 FORMAT(22H THE INVERSE MATRIX IS //)
00350 53 STOP
00360 END
00370 DOUBLE FUNCTION SIMUL(N,A,X,EPS,INDIC,NRC)
00380 DOUBLE X,Y,A,EPS,DETER,PIVOT,AIJCK
00390 DIMENSION IROW(50),JCOL(50),JORD(50),Y(50),A(NRC,NRC),X(N)
00400 MAX=N
00410 IF(INDIC.GE.0)MAX=N+1
00420 IF(N.LE.50)GO TO 5
00430 PRINT 200
00440 SIMUL=0.0
00450 RETURN
00460 5 DETER=1.0
00470 DO 18 K=1,N
```

```
00480 KM1=K-1
00490 PIVOT=0.0
00500 DO 11 I=1,N
00510 DO 11 J=1,N
00520 IF(K.EQ.1)GO TO 9
00530 DO 8 ISCAN=1,KM1
00540 DO 8 JSCAN=1,KM1
00550 IF(I.EQ.IROW(ISCAN))GO TO 11
00560 IF(J.EQ.JCOL(JSCAN))GO TO 11
00570 8 CONTINUE
00580 9 XMP=DABS(A(I,J))-DABS(PIVOT)
00581 IF(XMP.LE.0)GO TO 11
00590 PIVOT=A(I,J)
00600 IROW(K)=I
00610 JCOL(K)=J
00620 11 CONTINUE
00630 XMP=DABS(PIVOT)-EPS
00631 IF(XMP.GT.0.0)GO TO 13
00640 SIMUL=0.0
00650 RETURN
00660 13 IROWK=IROW(K)
00670 JCOLK=JCOL(K)
00680 DETER=DETER*PIVOT
00690 DO 14 J=1,MAX
00700 14 A(IROWK,J)=A(IROWK,J)/PIVOT
00710 A(IROWK,JCOLK)=1./PIVOT
00720 DO 18 I=1,N
00730 AIJCK=A(I,JCOLK)
00740 IF(I.EQ.IROWK)GO TO 18
00750 A(I,JCOLK)=-AIJCK/PIVOT
00760 DO 17 J=1,MAX
00770 17 IF(J.NE.JCOLK)A(I,J)=A(I,J)-AIJCK*A(IROWK,J)
00780 18 CONTINUE
00790 DO 20 I=1,N
00800 IROWI=IROW(I)
00810 JCOLI=JCOL(I)
00820 JORD(IROWI)=JCOLI
00830 20 IF(INDIC.GE.0)X(JCOLI)=A(IROWI,MAX)
00840 INTCH=0
00850 NM1=N-1
00860 DO 22 I=1,NM1
00870 IP1=I+1
00880 DO 22 J=IP1,N
00890 IF(JORD(J).GE.JORD(I))GO TO 22
00900 JTEMP=JORD(J)
00910 JORD(J)=JORD(I)
00920 JORD(I)=JTEMP
00930 INTCH=INTCH+1
00940 22 CONTINUE
00950 IF(INTCH/2*2.NE.INTCH)DETER=-DETER
00960 IF(INDIC.LE.0)GO TO 26
00970 SIMUL=DETER
```

```
00980 RETURN
00990 26 DO 28 J=1,N
01000 DO 27 I=1,N
01010 IROWI=IROW(I)
01020 JCOLI=JCOL(I)
01030 27 Y(JCOLI)=A(IROWI,J)
01040 DO 28 I=1,N
01050 28 A(I,J)=Y(I)
01060 DO 30 I=1,N
01070 DO 29 J=1,N
01080 IROWJ=IROW(J)
01090 JCOLJ=JCOL(J)
01100 29 Y(IROWJ)=A(I,JCOLJ)
01110 DO 30 J=1,N
01120 30 A(I,J)=Y(J)
01130 SIMUL=DETER
01140 RETURN
01150 200 FORMAT(10HON TOO BIG )
01160 END
```

APPENDIX F

TABLE F-1

CALCULATED I^o FOR INTENSITY RATIOS

SOLID SPECIMEN

Series	Cu	Sn	Pb	Fe	Ni	Zn	Mn	Al
Alloy 2	239000	118000	72000	530000	999980	671000		
Alloy88	214000	118000	60000	510000	780000	250000		
J	1344	410	831	1280	1420	1300		
K	1302	454	803	1192	1467	1310	1146	157

AQUEOUS SPECIMEN

Series	Cu	Sn	Pb	Fe	Ni	Zn	Mn	Al	Cl
Alloy 2	264000	110000	79000	974000	994000	826000			191000
Alloy 8	246000	1300000	72000	4400000	810000	280000			190000
J	1323	441	806	1409	1351	1283			254
K	1319	405	791	1401	1361	1278	1333	130	

N.B. Alloy 2 & 8 represent experimental data results in terms of cps.
Series J & K represent theoretical data simulations in terms of relative intensities.

TABLE F-2

CALCULATED I^{o} FOR INTENSITY RATIOS

SOLID SPECIMEN***

Series	Mg	Al	Si	Ca	Ti	Cr	Mn	Fe	P	K
TALS	80	116	144	322	343	1297	1299	1340		
BXT	83	119	151	340	354	1307	1306	1343	185	322
DX	83	119	149	330	354		1315	1353	182	322
APD	85	124	151	326	353	1288	1309	1352	187	323
XY-1	80	120	145	326	353	1295	1294	1336	183	317
XY-2	81	118	146	327	354	1299	1300	1342	184	320

FUSED SPECIMEN***

Series	Mg	Al	Si	Ca	Ti	Cr	Mn	Fe	P	K
TALS	87	125	152	342	353	1298	1307	1376		
BXT	87	124	152	343	356	1306	1306	1367	185	324
DX	87	124	152	337	354		1317	1380	182	322
APD	91	126	153	335	353	1287	1314	1379	186	323
XY-1	87	125	152	338	355	1297	1307	1368	187	323
XY-2	87	124	152	335	354	1287	1317	1382	188	323

EXPERIMENTAL SAMPLES

Series	Al	Si	Ca	Ti	Mn	Fe	Mg
ALS*	134000	152000	329000	228900	218000	146900	36000
ALS**	147500	132000	1136000	562000	347000	212000	

* Solid specimen.
** Fused specimen.
***Theoretical simulation data.